Physiological Role of Fatty Acid Desaturation in *Agrobacterium*-induced *Arabidopsis* Crown Galls

Dissertation zur Erlangung

des naturwissenschaftlichen Doktorgrades

der Julius-Maximilians Universität Würzburg

vorgelegt von

Diplom Biologe Jörn Klinkenberg

aus Aachen

Würzburg 2011

Eingereicht am: .....

Mitglieder der Promotionskommission:

Vorsitzender: Prof. Dr. Wolfgang Rössler

Gutacher: Prof. Dr. Rainer Hedrich

Gutachter: Prof. med Dr. Dr. Martin J. Müller

Tag des Promotionskolloqiums: .....

Doktorurkunde ausgehändigt am: .....

Eidesstattliche Erklärung

Hiermit erkläre ich, dass ich die vorliegende Dissertation in allen Teilen selbst angefertigt und keine anderen als die von mir angegebenen Quellen und Hilfsmittel verwendet habe. Ich habe die Dissertation weder in gleicher noch in ähnlicher Form in anderen Prüfungsverfahren vorgelegt.

Ich habe bislang noch keine weiteren akademischen Grade erworben oder zu erwerben versucht.

Würzburg, den

.....

Jörn Klinkenberg

Ich danke:

Dr. Rosalia Deeken für die spannende und interessante Aufgabenstellung, die sorgfältige Betreuung meiner Arbeit, sowie für zahlreiche Hilfestellungen, sowohl bei der Gestaltung der Experimente, der Ergebnis-Diskussion als auch bei der Erstellung der Dissertation

Professor Dr. Rainer Hedrich und Professor Dr. Martin J. Müller für die Anregungen zur Bearbeitung und Weiterentwicklung des Themas, sowie für die Unterstützung meiner Arbeit

Dr. Markus Krischke und Dr. Nadja Stingl für die Zusammenarbeit bei den zahlreichen Lipid-Analysen

Professor Dr. Werner Kaiser und Stefan Rümer für die Hilfe bei der Durchführung der Hypoxie Experimente

Professor Dr. Dietmar Geiger und Chil-Woo Lee für die Hilfestellung bei Klonierungen

Professor Dr. Thomas Müller und Tae-Kyung für die Hilfe bei Proteinextraktion und Western-blots

Sophie Lamberts, Stefanie Saupe und Gunnar Hartmann für die Unterstützung im Labor

Joachim Rothenhöfer für die Pflanzenanzucht und dem Personal des Sequenzier-Labors, aber auch allen Mitarbeitern des Julius-von-Sachs Institutes

Professor Dr. Detlev Weigel (MPMI Tübingen, Deutschland) für den Vektor pSR300

GABI-Kat, (MPI für Pflanzenzüchtungsforschung, Köln, Deutschland), "Genomic Analysis Laboratory" des "SALK Institute for Biological Studies" (La Jolla, CA, USA), dem "European *Arabidopsis* Stock Center" (University of Nottingham, UK) für die Bereitstellung der T-DNA Insertionslinien

Professor Lois Banta, Professor Dan Lynch und dem Graduiertenkolleg 1342 für die Ermöglichung des Aufenthaltes am Williams College, MA, USA

Martin, Chil-Woo, Björn und Sadek für die Korrektur der Dissertation

meinen Eltern für die Unterstützung

dem Graduiertenkolleg 1342 und dem SFB 587 für die finanzielle Unterstützung

Veit ec at ec hecc vindga meiði a
netr allar nío,
geiri vndaþr oc gefinn Oðni…

Contents

1. Introduction

Tumors at the crown of plants (crown gall) are feared in agriculture because they cause a reduction in crop yield (Kennedy, 1980). In 1853 the development of crown galls was documented for the first time (Fabre and Dunal, 1853). A few years later, in 1907 *Agrobacterium tumefaciens*, a soil borne gram negative bacterium of the *Rhizobiaceae* family was found to be the causative agent of the crown gall disease (Smith and Townsend, 1907; Smith et al., 1911). Agrobacteria have a broad host range infecting many dicotyledonous plant families. Crown gall development is initiated upon recognition of chemical signals by *Agrobacterium tumefaciens* released from wounded areas of the plant (Braun, 1952). For successful pathogenesis the Ti-Plasmid (tumor inducing plasmid) of *Agrobacterium* is essential (Zaenen et al., 1974). This plasmid enables the bacterium to transfer a DNA fragment, the transfer DNA (T-DNA) into the host genome. The T-DNA transfer is mediated by the activity of virulence (*vir*) genes, which are also located on the Ti plasmid (Tzfira and Citovsky, 2006). Expression of the T-DNA encoded genes (oncogenes), involved in synthesis of the phytohormones, cytokinin and auxin, causes reprogramming and leads to re-differentiation of transformed plant cells. Uncontrolled cellular proliferation of transformed host cells finally results in development of a tumor (Klee et al., 1984; Lichtenstein et al., 1984). A second class of T-DNA encoded genes, enables the transformed plant cell to produce the amino acid derivatives, opines, which serve as carbon and nitrogen source for agrobacteria (Dessaux et al., 1993).

1.1 Crown gall microenvironment

The development of crown galls is characterized by fundamental changes in metabolism and morphology. A unique crown gall microenvironment with hypoxic conditions, oxidative and drought stress is established.

1.1.1 Drought stress

The proliferating tumor penetrates the outermost cell layers of the plant and lacks an intact epidermis covered by a cuticle. This hydrophobic aliphatic wax polymer provides a protective barrier in all aerial plant organs against water loss. The ruptured surface of the tumor promotes loss of water (Schurr et al., 1996) and requires adaptation to drought stress conditions which is mediated by abscisic acid (ABA; Efetova et al., 2007). ABA induces the development of a protective suberized periderm-like layer on the surface of *Arabidopsis*

crown galls which is important for tumor development. Impairment of ABA mediated drought stress protection limits *Arabidopsis* crown gall growth (Efetova et al., 2007). In plants suberin is deposited in roots, such as cell walls of the endodermis and hypodermis and the periderm of stems during secondary growth (Schreiber, 2010). ABA induces further drought stress adaptations in crown galls (Efetova et al., 2007). Osmoprotectants are accumulated which reduce the osmotic potential of cells and result in elevated water uptake. Drought stress-responsive genes, such as aquaporines, are transcriptionally up-regulated.

1.1.2 Hypoxia and oxidative stress

In plant tumor cells the number of chloroplasts is reduced and the ultrastructure of thylacoid membranes is altered, resulting in the heterotrophic metabolism of the tumor (Gee et al., 1967; Deeken et al., 2006). Thus, the tumor depends on nutrients, provided by the host plant through translocation of metabolites via the vascular tissue and therefore represents a metabolic sink tissue (Aloni et al., 1995; Pradel et al., 1999; Wächter et al., 2003). The reduced photosynthetic capacity and the diffusional limitation of oxygen in the compact crown gall leads to hypoxia (Deeken et al., 2006). As consequence, the production of ATP in the crown gall is mainly powered by glycolysis and fermentation to produce ATP (Deeken et al., 2006). Other compact organs like animal and human tumors are known to suffer from hypoxia which results in enhanced glycolysis and fermentation (Warburg, 1930; Aisenberg, 1961; Pedersen, 1978; Yotdna et al., 2010).

An apparent contradiction to the oxygen depletion in the crown gall is that reactive oxygen species (ROS) are still formed (Lee et al., 2009). The different ROS are either produced chemically due to incomplete reduction of oxygen as inevitable byproduct of the aerobic metabolism in mitochondria and chloroplasts, or by enzymes, such as nicotinamide adenine dinucleotide phosphate-oxidase (NADPH-oxidase) in the plasma membrane. The superoxide anion (O_2^-) is converted by superoxide dismutase (SOD) activity into hydrogen peroxide (H_2O_2). H_2O_2 is further processed into the ROS hydroxyl radical ($HO\cdot$). In addition, singlet oxygen is generated by photosensitisation of chlorophyll molecules. ROS have a detrimental effect on the cell, because they are highly reactive and cause damage of proteins, DNA and lipids (Baier and Dietz, 2005; Rhoads et al., 2006). ROS production is known to occur under hypoxic conditions in plants, but is abolished under anoxic conditions due to the lack of oxygen (Blokhina et al., 2003; Blokhina and Fagerstedt, 2010). The phenomenon of oxidative stress under oxygen deprivation is also indicated by changes in the metabolism: ethane emission, lipid peroxidation, non-fermentative acetaldehyde formation and activation of

antioxidant systems (Blokhina and Fagerstedt, 2010). In crown galls genes, encoding gluthation-S-transferases, peroxidases and superoxid dismutases are transcriptionally up-regulated, indicating that antioxidant systems are activated to cope with increased oxidative stress conditions (Jia et al., 1996; Lee et al., 2009). However, constitutive activation of ROS scavenging enzymes in transgenic plants results in smaller tumors (Jia et al., 1996), suggesting that ROS and oxidative stress promote the development of plant tumors. A positive effect of oxidative stress on dedifferentiation and transformation of healthy into cancerous cells is also known about animal tumors (Klaunig and Kamendulis, 2004).

1.2 Lipids are affected by hypoxia, oxidative and drought stress

Oxygen deprivation, oxidative and drought stress have a negative impact on unsaturated fatty acids (FAs) of membrane lipids and therefore affect fluidity and integrity of membranes (Blokhina et al., 2003; Upchurch, 2008). It is essential for stress challenged plants to adjust membrane fluidity. This is achieved by increasing the levels of unsaturated fatty acids to generate an environment that protects the function of integral membrane proteins, such as the photosynthetic machinery (Upchurch, 2008).

Lipid biosynthesis is energy dependent, thus de novo synthesis of membrane lipids and unsaturated FAs can hardly occur under oxygen deprivation (Brown and Beevers, 1987). Lipid degradation processes are initiated, such as the release of free FAs from the membrane lipids, as a result of low oxygen levels (Rawyler et al., 1999). Hypoxia is associated with the production of ROS and therefore with oxidative stress (1.1.2). Most susceptible to oxidative stress are unsaturated FAs. ROS singlet oxygen and hydroxyl radicals (HO·) react with the methylene group of unsaturated FAs to form conjugated dienes that upon reaction with oxygen are converted to lipid peroxy radicals. Peroxy radicals propagate further lipid peroxidation as part of a radical chain reaction, reacting again with a methylene group and forming additional conjugated dienes (Blokhina et al., 1999; Blokhina et al., 2003). Lipid peroxidation associated with oxygen deprivation can also be catalyzed by lipoxygenase activity (Pavelic et al., 2000). A derivative of enzymatic PUFA peroxidation is 12-oxo-phytodienoic acid (OPDA), esterified with plastidial galactolipids. Since these compounds were at first detected in *Arabidopsis* they are referred to as arabidopsides (Hisamatsu et al., 2003, 2005; Andersson et al., 2006). Their formation is known to be induced upon wounding.

Membrane damage by lipid peroxidation occurs under hypoxia or water logging conditions (Yan et al., 1996; Santosa et al., 2007). The apparent and severe damage of tissues, however, occurs only after re-aeration of oxygen deprived organs, a phenomenon which is described as

O_2-paradoxon (Hendry and Crawford, 1994). ROS production is known to peak after re-oxygenation which is associated with a markedly enhanced lipid peroxidation (Hunter et al., 1983 Albrecht et al., 1994). The products of lipid peroxidation restructure the membrane, altering the physical properties and form a less ordered and more hydrophilic membrane (Blokhina and Fagerstedt, 2010) with detrimental consequences for the cell. Thus, survival is achieved by the ability of the plant to preserve the levels of unsaturated FAs and lipid composition during and after oxygen deprivation (Blokhina et al., 2003).

Drought stress causes inhibition of lipid biosynthesis (Monteiro de Paula et al., 1993). Furthermore, degradative processes, such as lipolysis and peroxidation of unsaturated FAs are initiated (Monteiro de Paula et al., 1993; Ferrai-Iliou et al., 1993; Matos et al., 2001). The content of 18:3 poly unsaturated FAs (PUFAs) declines in membranes of non-tolerant plants under drought stress (Dakhma et al., 1995; Upchurch, 2008). An increase in 18:3 levels by overexpression of the omega-3 desaturases *FAD3* and *FAD7* has shown to enhance tolerance to drought stress in tobacco (Zhang et al., 2005). Thus, tolerance to drought stress is dependent on the inherent levels of PUFAs and the ability to maintain FA desaturation activity (Berberich et al., 1998; Mikami and Murata, 2003; Torres-Franklin et al., 2009).

1.3 Acyl lipid metabolism of plants

Acyl lipids are essential constituents of all plant cells and due to their hydrophobic nature almost all are components of membranes. Acyl lipids contain FAs, defined as monocarboxylic acids with an unbranched aliphatic tail. The FA biosynthesis pathway is a primary metabolic pathway, which is essential for growth. Unlike in other eukaryotes, in plants de novo synthesis of FAs occurs in the plastid. Synthesis is performed by the FA synthase (FAS), a multisubunit complex, consisting of monofunctional enzymes. Acetyl-coenzyme A (acetyl-coA), is provided by the oxidative decarboxylation of pyruvate and used as the starting unit. Acetyl-coA is elongated by two carbon units from malonyl-ACP in each cycle to give 16:0 palmitic acid. The growing acyl chain is bound to an acyl carrier protein (ACP) during synthesis. Some of the palmitic acid molecules are bound to ACP and released as 16:0-ACP from the FAS machinery. However, most of 16:0-ACP is elongated by the ketoacyl-ACP synthase II (KASII) to generate 18:0 stearic acid which is also bound to ACP and released as 18:0-ACP (Li-Beisson et al., 2010).

1.3.1 S-ACP-desaturases

Desaturase enzymes catalyze energy-demanding dehydrogenation reactions of methylene groups that result in the introduction of double bonds into FAs. This reaction requires molecular oxygen which is activated by the active di-iron cluster of the desaturase enzyme and reduced completely to water. Two electrons are required for the formation of each double bond. Ferredoxin serves as electron donor for FA desaturation in plastids. The introduction of the first double bond is at the delta 9 position of stearic acid (18:0) and carried out by the stearoyl-acyl carrier protein delta-9-desaturases (SAD) family in the stroma of plastids (figure 1; Shanklin and Cahoon, 1998). *SAD* genes exhibit a tissue-specific expression profile and the encoding enzymes regulate the monounsaturated FA (MUFA) pools in plants (Kachroo et al., 2007). The enzymatic function of several plant SADs has been demonstrated (Shanklin and Somerville 1991; Thompson et al., 1991; Cahoon et al., 1996; Cahoon et al., 1998; Whittle et al., 2005). This was done by in vitro assays with the purified SAD, measuring the ferredoxin-dependent release of $^{3}H_20$ from stearoyl CoA and gas chromatographic identification of the product 18:1 FA. These biochemical assays have shown that in *Arabidopsis* five out of seven members of the *SAD* gene family (*SAD1, 3, 4, 5* and *SSI2*) are capable of desaturating 18:0 and are contributing to the 18:1 pool (Kachroo et al., 2007).

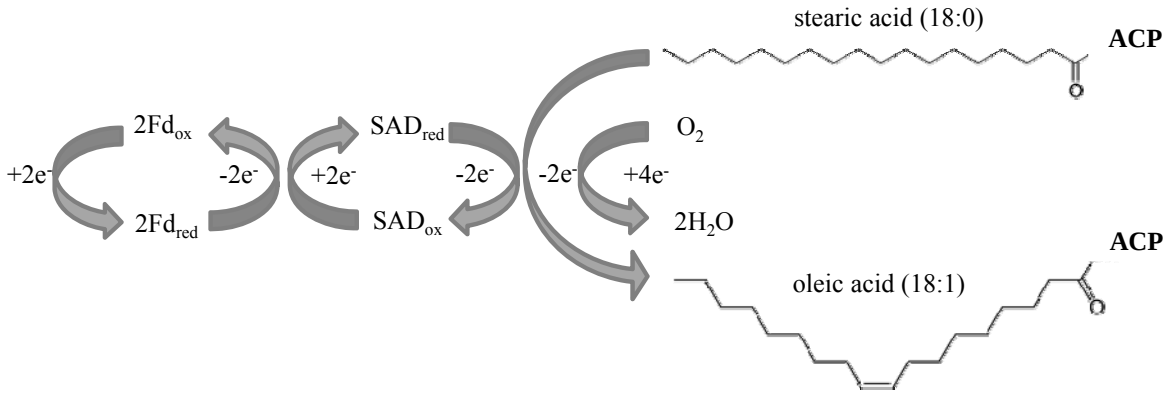

Figure 1. Electron transport chain of stearoyl-acyl carrier protein delta-9-desaturase (SAD). During photosynthesis, the ferredoxin (Fd) is directly reduced by photosystem I. ACP, acyl carrier protein; ox, oxidized; red, reduced.

1.3.2 Membrane bound desaturases

Mono unsaturated fatty acids (MUFAs) are further desaturated to PUFAs by two sets of membrane-bound FA desaturases (FADs). The biochemistry of FADs and SADs is considered to be similar (Shanklin et al., 2009). Nevertheless, the integral membrane desaturases have

evolved independently of the soluble SADs (Shanklin et al., 2009). They contain a histidine motif which is associated with the di-iron site other than the di-iron binding amino acid motif of SADs ((D/E) $X_2H)_2$) and is necessary for desaturation (Shanklin and Cahoon, 1998). FADs are either located in plastids or the ER (Ohlrogge and Browse, 1995). In plastids the omega-6-desaturase, FAD6 is providing dienoic fatty acids. The omega-3-desaturases, FAD7 and FAD8 are converting glycosyldiacylglycerol dienoic into trienoic FAs (Iba et al., 1993; McConn et al., 1994; Falcone et al., 1994; Los and Murata, 1998). In the ER, conversion of the phospholipid unsaturated 18:1 FA to 18:2 FA and of 18:2 FA to 18:3 FA is carried out by the omega-6-desaturase, FAD2 and omega-3-desaturase, FAD3, respectively (Browse et al., 1993; Okuley et al., 1994; Los and Murata, 1998).

1.3.3 The prokaryotic and eukaryotic pathway of glycerolipid synthesis

MUFAs together with saturated FAs are transferred to glycerol by the activity of acyltransferases to form lysophosphatidic acid (LPA) and phosphatidic acid (PA) in the plastid and the eukaryotic reticulum (ER). PA is the precursor for polar glycerolipid synthesis. Glycerolipids are composed of two FAs, the glycerol backbone and a polar head group. Glycerolpid synthesis can either take place in the prokaryotic pathway of the plastid or in the eukaryotic pathway of the ER (figure 2). Galacto-, phospho- and sulfolipids of photosynthetic membranes (phosphatidylglycerol, PG; monogalactosyldiacylglycerol, MGDG; digalacto-syldiacylglycerol, DGDG; and sulphoquinovosyldiacylglycerol, SQDG) are synthesized by the prokaryotic pathway in the inner envelope of plastids. The PA-pool, produced in the inner envelope of the plastids, can be used for synthesis of cytidine diphosphate diacylglycerol (CDP-DAG) which, together with glycerol-3-phosphate (G3P) is required for PG synthesis. The remaining PA pool is dephosphorylated to the diacylglycerol (DAG) backbone by the PA-phosphatase. Galactose moieties from UDP-Galactose are transferred to DAG by galactosyltransferase activity to form the galactolipids MGDG and DGDG, the major lipid components of plastidial membranes. DAG serves also as precursor for SQDG synthesis.

In the ER the phospholipids of extrachloroplastidic membranes (phosphatidylcholine, PC, phosphatidylinositol, PI; phosphatidylethanolamine, PE; phosphatidylserine, PS) are produced via the eukaryotic pathway using FAs imported from the plastids. PA, synthesized in the ER, is converted to CDP-DAG, from which PI is produced. The remaining PA pool is dephosphorylated to the DAG backbone. DAGs are combined with CDP-choline and CDP-ethanolamine to produce PC and PE, respectively. The latter two represent the major lipids of extrachloroplastidial membranes (Li-Beisson et al., 2010). Both lipid biosynthesis pathways

are interconnected (figure 2). Lipids from the eukaryotic pathway can serve as precursor for lipid biosynthesis in chloroplasts and are responsible for the major galactolipid synthesis in many plant species. In *Arabidopsis* both pathways contribute equally to the pools of MGDG, DGDG and SQDG (Browse and Sommerville, 1991). This plant species, also named as 16:3 plant, contains substantial amounts of 16:3 FAs bound in the galactolipid pool. The origin of the DAG moiety in MGDG, DGDG and SQDG glycerolipids can be distinguished by the fact that glycerolipids from the prokaryotic pathway contain C16 FA at the sn-2 position of the glycerol, whereas ER derived lipids exclusively contain C18 FA at this position (Li-Beisson et al., 2010).

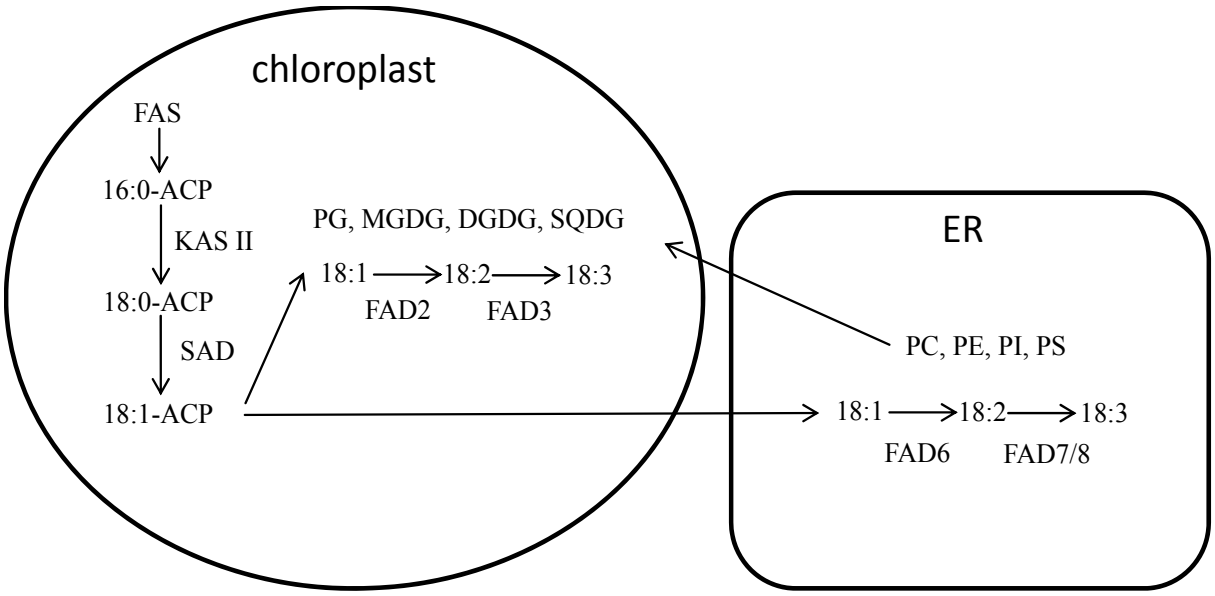

Figure 2. Simplified model of the *Arabidopsis* acyl lipid metabolism including desaturation and glycerolipid synthesis via the prokaryotic and eukaryotic pathway. The first desaturated FA, 18:1, is the result of stearoyl acyl carrier protein desaturase (SAD) activity. The desaturated FAs 18:1, 18:2 and 18:3 are components of glycerolipids of the plastid and ER.. ACP, acyl carrier protein; FAS, fatty acid synthase; KAS II ketoacyl-ACP synthase II; SAD, stearoyl-acyl carrier protein delta-9-desaturase; PG, phosphatidylglycerol; MGDG, monogalactosyldiacylglycerol; DGDG, digalactosyldiacylglycerol, SQDG, sulphoquinovosyldiacylglycerol, PC, phosphatidylcholine; PI, phosphatidylinositol; PE, phosphatidylethanolamine; PS, phosphatidylserine.

1.4 Objectives of this study

This study focuses on the role of desaturated lipids in *Arabidopsis* crown gall developments induced by *Agrobacterium tumefaciens*. The significance of lipid desaturation is well known for the establishment of animal tumors (Igal, 2010), but still unknown in plant tumors. These studies were conducted in particular, with regard to the stress conditions that are associated with plant tumor development. Plant tumors are known to form a unique microenvironment which results in hypoxic, oxidative and drought stress. These stress factors are known to affect FA desaturation and distribution within organisms.

One of the first objectives of this study therefore was to determine the lipid pattern of the crown gall in order to understand the protective role of lipids in stress situations as experienced by the tumor. A detailed analysis of the unsaturated FA pool was performed by using high pressure liquid chromatography (HPLC) coupled with mass spectrometry (MS). A correlation of the observed lipid pattern with the existing gene expression data set of plant tumors (Deeken et al., 2006) was expected to uncover the candidate genes, important for shaping the lipid metabolism of crown galls. The gene expression pattern was particularly dominated by two desaturases, FAD3 a membrane bound FAD and SAD6, a putative soluble SAD, both involved in the production of unsaturated FAs. The enzymatic function of the SAD6 protein, however, has never been demonstrated before and thus was elucidated by complementation of mutants deficient in the well-known *SAD SSI2* by *SAD6*. Furthermore, the impact of SAD6 on the lipid pattern was studied analyzing *SAD6* overexpressing mutants. Tumor growth assays with *Arabidopsis* mutants were carried out in order to demonstrate the role the candidate desaturase genes on tumor development. Subjecting the mutants to stress conditions known to occur in tumors during their growth should elucidate the physiological role of desaturases and unsaturated FAs in the crown gall. Identification of factors for transcriptional regulation of the candidate genes were intended to further contribute to the understanding of the physiological role of unsaturated FAs and desaturases in the tumor microenvironment.

In summary, this study contributes to the understanding of how plant tumors cope with abiotic stress conditions and what is role of lipids in stress adaptation.

2. Material and methods

2.1 Growth of bacteria

2.1.1 Growth of *Agrobacterium tumefaciens*

Agrobacterium tumefaciens strains (table 1) were stored in 50% (v/v) of glycerol in YEP-medium (2.1.2) at -80 °C. *Agrobacterium tumefaciens* strains from stocks stored in of glycerol and YEP-medium 50% (v/v) at -80 °C were plated on YEP Agar (2.1.2), containing the appropriate antibiotic (table 1 and 2.5, table 4) and incubated at 28 °C for 48 h to obtain single colonies. Plates were stored at 4 °C no longer as 1 month. Single colonies were transferred into 50 ml AB induction medium (2.1.2) and incubated at 220 rpm in a rotary shaker at 28 °C for overnight.

Table 1. *Agrobacterium tumefaciens* strains

***Agrobacterium* tumefaciens Strain**	**Virulence**	**Antibiotics**	**Reference**
C58 nocc, number 584	Oncogenic	None	Hamilton and Fall, 1971; Max Planck Institute for Plant Breeding, Cologne, Germany
GV3101	Non oncogenic, derivative of *Agrobacterium* tumefaciens C58, contains plasmid pMP90	Rifampicin (10 µg/ml), Gentamycin (25 g/ml); in addition: dependent on harbored plasmid (8.2.4)	Koncz and Schell, 1986

2.1.2 Media for *Agrobacterium tumefaciens*

Components of YEP (Tryptone, 0.5% (m/v); Yeast extract, 0.5% (m/v); Sucrose, 0.5% (m/v); $MgSO_4$, 50 mM; for solid Agar: 1.5% Agar(m/v)) were solubilized in purified water and autoclaved at 120 °C for 30 min. Antibiotics (2.5, table 4) were added later at 60 °C. For solid media, Agar was added to the liquid culture before autoclaving.

Components of 20x AB salt solution (NH_4Cl, 20 g/l; $MgSO_4 \cdot 7H_2O$, 0.6 g/l; KCl, 3 g/l; $CaCl_2$, 0.2 g/l; $FeSO_4 \cdot 7H_20$, 15 mg/l) and phosphate solution (K_2HPO_4, 60 g/l; NaH_2PO_4, 20 g/l) were solubilized in purified water and autoclaved at 120 °C for 30 min. 50 ml of 20x AB salt solution, 2.4 ml of phosphate solution and 10 ml of 20% (m/v) glucose solution were added to

937.6 ml AB buffer (3.9 g/l MES, pH=5.5 with KOH). In the end 100 µl of filter sterilized 10% (m/v) thiamine solution were added.

2.1.3 Growth of *Escherichia coli*

Escherichia coli strains (table 2), stored in LB-medium with 20% (v/v) glycerol (2.1.4) at -80 °C were transferred as single colony from a selective Agar plate, or directly from the glycerol stock into 3 ml LB medium (2.1.4) with the respective antibiotic (table 2; 2.5, table 4) and incubated overnight at 37 °C in rotary shaker at 220 rpm.

Table 2. *Escherichia coli* strains

***Escherichia coli* strain**	**Genotype**	**Antibiotic**	**Reference**
DH5 alpha	F- Φ80*lac*ZΔM15 Δ(*lac*ZYA-*arg*F) U169 *rec*A1 *end*A1 *hsd*R17 (rK-, mK+) *pho*A *sup*E44 λ- *thi*-1 *gyr*A96 *rel*A1	Dependent on the resistance gene of the vector (8.2.4)	Hanahan, 1985
One Shot® Top10	F- *mcr*A Δ(*mrr-hsd*RMS-*mcr*BC) Φ80*lac*ZΔM15 Δ*lac*X74 *rec*A1 *ara*D139 Δ(*ara leu*) 7697 *gal*U *gal*K *rps*L (StrR) *end*A1 *nup*G	Dependent on the resistance gene of the vector (8.2.4)	Invitrogen, Carlsbad, USA
MRF´	Δ(*mcrA*)*183* Δ(*mcrCB-hsdSMR-mrr*)*173 endA1 supE44 thi-1 recA1* gyrA96 relA1 lac *[F'* proAB lacI^{q}Z*Δ*M15 *Tn*10 *(Tet^{r})]*	Dependent on the resistance gene of the vector (8.2.4)	Bullock et al., 1987

2.1.4 Media for *Escherichia coli*

Components of SOB (Tryptone, 2%; Yeast extract, 0.5%; NaCl, 8.6 mM; $MgSO_4$, 20 mM), SOC (Glucose, 20 mM; in SOB) and LB medium (Tryptone, 1% (m/v); Yeast extract, 0.5% (m/v); NaCl, 171 mM; for solid Agar plates: 1.5% Agar (m/v)) were solubilized in purified water and autoclaved at 120 °C for 30 min. Antibiotics (2.5, table 4) were added later at 60 °C. For solid media, Agar was added to the liquid medium before autoclaving.

2.2 Manipulation of bacteria

2.2.1 Chemical competent *Escherichia coli*

Overnight cultures (2.1.3) were added to 100 ml SOB medium (2.1.4) and cultivated at 37 °C in a rotary shaker at 220 rpm. At an OD_{600} of 0.4-0.5 the bacterial suspension was transferred

into 50 ml tubes, cooled on ice for 15 min and centrifuged at 2,500 rcf and 4 °C for 15 min. The pellet was re-suspended in 15 ml of sterile and ice cold TFB1 buffer (K-Acetat, 30 mM; RbCl, 100 mM; $CaCl_2$, 10 mM; $MnCl_2 \cdot 4H_2O$, 50 mM; 12% Glycerol; pH=5.8 (with acetic acid)) and stored for 30 min on ice. Following a second centrifugation step for 10 min at 2,500 rcf at 4 °C the pellet was re-suspended in 2 ml of ice cold TFB2 buffer (Na-MOPS, 10 mM; RbCl, 10 mM; $CaCl_2$, 75 mM; 12% Glycerol; pH=6.8 (with NaOH)). Aliquots of 50 µl were frozen in liquid nitrogen and stored at -80 °C. Components of TFB1 and TFB2 buffer were solubilized in purified water and sterile filtrated.

2.2.2 Transformation of *Escherichia coli*

At least 100 ng of plasmids were transformed into *Escherichia coli* strains using the heat shock method. Therefore competent *Escherichia coli* strains (2.2.1) were incubated at 42 °C for 45 s in a water bath followed by 10 min on ice. After transformation *Escherichia coli* strains were regenerated in 450 µl of SOC medium (2.1.4) at 37 °C and 300 rpm in a rotary shaker for 1 h. Finally transformed bacterial suspensions (10-100 µl) were distributed on selective Agar plates (2.1.4) and incubated at 37 °C for overnight.

2.2.3 Transformation of *Agrobacterium tumefaciens* by electroporation

Overnight cultures (0.5 ml) of *Agrobacterium tumefaciens* strain GV3101 (2.1.1) were centrifuged at 2,500 rcf for 1 min. Pellets were washed five times with purified water and re-suspended in 50 µl of purified water. The suspensions were transferred into 2 mm electroporation cuvettes after addition of 50-200 ng of plasmid. The electroporation cuvettes were placed in an electroporator (Elektroporator 2510, Eppendorf, Hamburg, Germany) and bacterial suspensions were exposed to a capacity of 25 µF, electrical resistance of 400 Ω and a voltage of 2,500 V for 5 to 6 ms. Immediately after electroporation 500 µl of YEP medium (2.1.2) was added and the transformed cells regenerated at 28 °C for one hour. An aliquot of 100 µl was plated onto selective media.

2.3 Cultivation of Plants

2.3.1 Cultivation of *Arabidopsis thaliana* on soil

Arabidopsis seeds of the genotype Wassilewskija (Ws-2) and Columbia (Col-0, Heynh.) were germinated on soil (Einheitserde Type P, Gebr. Hagera GmbH, Sinntal-Jossa, Germany) and separated into single pots as with two primary leaves. Plants were cultivated in growth

chambers or the greenhouse under short-day conditions with approximately 120 µmol·m^{-2}·s^{-1} of fluorescent white light (TL70, Philips, Eindhoven, The Netherlands and Osram 25 W, Osram, Munich) at 22 °C (8 h) and 16 °C during the dark period (16 h) at a relative humidity of 45-55%. *Arabidopsis* plants, for the use of stable transformation (2.4.3), were cultivated under long-day conditions with 16 h of light.

2.3.2 Sterile cultivation of *Arabidopsis thaliana*

Selection of transgenic plants was performed on solid MS medium (Murashige und Skoog (Sigma Aldrich, St. Louis, USA); Sucrose, 1% (m/v); Agar 1% (m/v); pH=5.7 (with KOH)), containing the respective antibiotic (8.2.4 and 2.5, table 4). For sterilization the seeds were incubated in 100% ethanol for 20 min. After removal of ethanol, the seeds were sterilized in 5% NaClO solution with 0.2% Triton X-100 for 5 min. The sterilization solution was removed by five washing steps with sterilized water and the seeds were dried on Whatman paper (GE Healthcare, Chalfont St Giles, UK) under sterile conditions before distribution on MS Agar plates. Plates were sealed with parafilm (Pechiney Plastic Packaging Company, Chicago, USA) and incubated under long day conditions with 120 µmol·m^{-2}·s^{-1} of fluorescent white light (TL70, Philips, Eindhoven, the Netherlands and Osram 25 W, Osram, Munich) at 22 °C (16 h) and 16 °C during the dark period (8 h).

2.3.3 *Arabidopsis* mutants

Seeds of *Arabidopsis* mutants (table 3) were obtained from T-DNA insertion collections Nottingham *Arabidopsis* Stock Centre, (NASC, http://*arabidopsis*.info/) and GABI-Kat (http://www.gabi-kat.de/). T-DNA insertion collections provide tools for reverse genetics to study gene function. Depending on the type, position and direction of the T-DNA insertion, the result is a knock down, knock out or overexpression of a gene (Krysan et al., 1999). GABI-Kat and the Salk Institute have determined the T-DNA insertion sites by sequencing the flanking sequences of the T-DNA using a T-DNA specific primer. Based on this information primers can be designed that are specific for the genomic DNA flanking the T-DNA insertion site (left and right genomic primer; 8.2.3, supplemental table 1). This primer pair only gives a PCR product (2.6.8) with the genomic DNA from wild type plants, or from heterozygous plants with one T-DNA in one allele. The right genomic primer together with the T-DNA specific left border primer results in a PCR product with genomic DNA from plants that are homozygous or heterozygous for the T-DNA insertion, but not with DNA from wild type plants.

Thus, heterozygous T-DNA insertion lines are identified by two PCR products: One product derives from amplification with the left and right genomic primer, the other with the left border and right genomic primer. Homozygous T-DNA insertion plants are identified by a PCR product for the PCR using the right genomic primer and the left border primer. Using this screening method the genotype of single plants of the segregating T2 generation, provided by GABI-Kat and the Salk Institute were determined in order to harvest the seeds only from homozygous non-segregating T-DNA-insertion lines of the T3 generation. The site of T-DNA insertion was confirmed by sequencing of the purified PCR product (2.6.4 and 2.6.7). Based on sequencing the gene models including the T-DNA insertions were generated (8.1). In addition to the *Arabidopsis* mutants obtained from T-DNA insertion collections *Arabidopsis* mutants were generated in this study (table 3).

Table 3. *Arabidopsis* mutants

***Arabidopsis* mutant**	**Gene locus**	**Accession numbers**	**Genetic background**	**Reference**
fad3-2	At2g29980	N8036	Col-0	James et al., 1990; Browse et al., 1993
fad7-1/ fad8-1	At3g11170, At5g05580	N8034	Col-0	McConn et al., 1994; Gibson et al., 1994
Salk70018	At1g43800	N70018/ Salk70018	Col-0	SALK Institute La Jolla, CA, USA
SAD6-OE	At1g43800	none/gk30d04	Col-0	Gabi-Kat, University Bielefeld, Germany
SAD6-OE-RNAi		Generated in this study	Col-0, gk30d04 homozygous	Generated in this study using binary plasmid pCambia2300-SAD6$_{AmiRNAi}$ (2.8, 2.4.3 and 8.2.4, supplemental figure 5)
ssi2-2	At2g43710	N539852/ Salk039682	Col-0	SALK Institute La Jolla, CA, USA
ssi2-2-35S$_{PRO}$:SAD6		Generated in this study	Col-0, salk039862 homozygous	Generated in this study using binary vector pCAmbia3300-SAD6$_{CDS}$ (2.8, 2.4.3 and 8.2.4, supplemental figure 10)
SAD6$_{PRO}$:GUS		Generated in this study	WS-2	Generated in this study using pMDC164-SAD6$_{pro}$ (2.8, 2.4.3 and 8.2.4, supplemental figure 7)

2.3.4 *Nicotiana benthamiana* cultivation on soil

Nicotiana benthamiana, supplied by K. Oparka (Scottish Crop Research Institute, Dundee, UK) was grown on soil (Einheitserde Type T, Gebr. Hagera GmbH, Sinntal-Jossa, Germany) and cultivated in a green house with a day and night interval of 16 h (26 °C) to 8 h (22 °C) and a photon flux density of 600 $\mu mol \cdot m^{-2} \cdot s^{-1}$ light.

2.4 Manipulation of plants

2.4.1 Tumor induction and preparation

Tumor development was induced by inoculating the nopaline-utilizing *Agrobacterium tumefaciens* strain C58 nocc (nopaline catabolism construction) number 584 (Max Planck Institute for Plant Breeding, Cologne, Germany). Agrobacteria were grown overnight in AB medium (2.1.2) and a suspension with an OD_{600} of 0.8-1.0 was injected at the base of *Arabidopsis* inflorescence stalks over a distance of 1 cm using a syringe. Tumor tissue was separated from the inflorescence stalk tissue with a scalpel 21 d after inoculation. Mock-injected inflorescence stalk segments of the same age served as reference tissues.

2.4.2 Application of hypoxia and waterlogging stress

Arabidopsis plants were placed in a desiccator and flushed with a mixture of 2 ml/min air and 80 ml/min nitrogen (Messer Griesheim, Darmstadt, Germany) containing 0.5% oxygen for 24 h. Air flow controllers (FC-260, Tylan General, Eching, Germany) were used to adjust the gas flows. Control plants were flushed with 82 ml/min air. Waterlogging stress was applied in a water-filled basin by flooding the roots but not shoots of *Arabidopsis* plants grown in pots filled with soil for 24 h. Pots with control plants were placed in a basin without water for the same time.

2.4.3 Stable transformation of *Arabidopsis thaliana*

Stable transformation of *Arabidopsis* was carried out by applying the floral dipping technique as described by Clough and Bent (1998). In order to increase the number of flowers the primary inflorescence stalk of *Arabidopsis* plants was removed immediately after emerging to induce the development of secondary inflorescences. *Agrobacterium tumefaciens* strain GV3101, carrying the binary plasmid of interest (8.2.4, supplemental figures 5 to 7 and 10), grown in 50 ml of YEP overnight (2.1.1 and 2.1.2) was spinned down at 2,500 rcf for 10 min. The bacterial pellet was re-suspended in 25 ml of transformation buffer (Sucrose, 5% (m/v);

Silwett-L77 (OSi Specialties inc., Danbury, USA), 0.05% (v/v), in purified water). *Arabidopsis* plants with young flowers and all siliques removed were dipped into transformation buffer. The plants were covered in plastic bags for 24 h after floral dipping and then cultivated under long day conditions in the greenhouse to set seeds (2.3.1). Transformants of the harvested T1 seeds were selected on solid media or on soil depending on respective resistance gene.

2.4.4 Transient expression by Agroinfiltration

The agroinfiltration method (Romeis et al., 2001) was applied to study transient gene expression in *Nicotiana benthamiana* leaves, transformed with a recombinant binary plasmid (8.2.4, supplemental figure 9). *Agrobacterium* strain GV3101, harboring 19K was co-infiltrated in order to suppress posttranscriptional gene silencing (Liu et al., 2002). A 50 ml YEP overnight culture of *Agrobacterium tumefaciens* strain GV3101, with the appropriate binary vector (8.2.4, supplemental figure 9) and with the 19K plasmid were centrifuged at 2,500 rcf for 10 min. Each pellet was re-suspended in 5 ml of agromix buffer (MES, pH=5.8), 10 mM; $MgCl_2$, 10 mM; Acetosyringone, 150 µM; in purified water) and incubated for 2 h in the dark at 120 rpm in a rotary shaker. Bacterial suspensions with an OD_{600} of 1.0 were combined, such that 20% agrobacteria with 19 K and 80% with the respective gene of interest for transient were infiltrated by pressing the tip of a syringe without needle onto the lower leaf surface of 3-4 week old, well watered, *Nicotiana benthamiana* plants. Plant material was harvested for protein extraction three d after infiltration (2.9.1).

2.5 Antibiotics

Table 4. List of antibiotics

Antibiotic	Stock Solution	*Escherichia coli*	*Agrobacterium tumefaciens*	Plant
Ampicillin	50 mg/ml in sterile H_2O	50 µg/ml		
Kanamycin	50 mg/ml in sterile H_2O	50 µg/ml	100 µg/ml	100 µg/ml
Gentamicin	25 mg/ml in sterile H_2O		25 µg/ml	
Rifampicin	10 mg/ml in DMSO		10 µg/ml	
Spectinomycin	100 mg/ml in sterile H_2O	100 µg/ml	100 µg/ml	
Hygromycin	40 mg/ml in sterile H_2O			100 µg/ml

2.6. DNA methods

2.6.1 Plasmid extraction from *Escherichia coli*

Plasmid extraction was performed by alkaline lysis (Birnboim and Doly, 1979). An overnight culture (1 ml, 2.1.3) was centrifuged at 10,000 rcf for 30 s. The supernatant was discarded except for 50 µl in which the bacterial pellet was re-suspended. The bacteria were lysed in 300 µl TENS buffer (SDS, 10% (m/v); NaOH, 0.1 M; RNAse, 200 µg/ml; dissolved in TE (Tris-HCl, 10 mM, pH=7.5)) at room temperature. The alkaline lysate was neutralized by the addition of 150 µl of 3 M sodium acetate (pH=5.2), which resulted in renaturation of the plasmid DNA, but not the chromosomal DNA and precipitation of SDS and proteins. Precipitated cell debris, chromosomal DNA, SDS and proteins were removed by centrifugation at 10,000 rcf for 10 min. The supernatant was transferred into a 1.5 ml reaction tube. The plasmid DNA was precipitated after addition of 600 µl of isopropanol and centrifugation at 10,000 rcf for 5 min. The supernatant was discarded and the precipitate washed in 500 µl 70% ethanol. The dry plasmid DNA was dissolved in 50 µl of Tris-HCl (10 mM, pH=7.5) and stored at -4 °C. DNA concentration was determined spectrophotometrically (2.6.3). Plasmid DNA (500-1,000 ng) was used for restriction analysis (2.6.5).

2.6.2 Genomic DNA extraction from *Arabidopsis thaliana*

Genomic DNA extraction was performed based on a protocol from Kasajima et al., (2004). An 200 µl aliquot of extraction buffer (Tris-HCl (pH=7.5), 20 mM; NaCl, 25 mM; EDTA, 2.5 mM; SDS, 0.05%) was added to 5 mg of plant material in a 1.5 ml reaction tube. Plant material was homogenized in a ball mill at room temperature (MM2000, Retsch, Haan, Germany). Cell debris was precipitated min at 10,000 rcf in 10 min and 0.5 µl of the supernatant were used in 50 µl of PCR reaction mix.

2.6.3 Quantifitation of nucleic acids

Quantification of DNA was performed by applying UV-photo-spectrometry (Gene Quant, Pharmacia, Uppsala, Sweden) at 230 nm, 260 nm and 280 nm. The samples were 1:70 diluted and filled into a quartz cuvette (1 cm ∅). Absorbance was measured spectrophotometrically.

Nucleic acid concentration of samples was determined as following:

$$\text{Concentration of the sample [µg/µl]} = \frac{E_{260nm} \cdot F \cdot dilution\ factor}{1{,}000}$$

DNA extinction factor F = 50 µg/µl

The ratio of the absorption at 260 nm to 280 nm and 260 nm to 230 nm, allowed the estimation of the purity of DNA preparation. Values below 1.8-2.0 indicated an increased contamination with proteins (absorption maxima at 280 nm) and carbohydrates (absorption maxima at 230 nm).

2.6.4 DNA purification

DNA fragments, separated by Agarose gel electrophoresis, were excised with a scalpel under UV light and purified by a silica column-based method. The QIAquick Gel Extraction Kit protocol (Quiagen, Hilden, Germany) was used according to the manufacture´s protocol. The DNA was eluted with 30-50 µl of 10 mM Tris-HCl (pH=8.5) and stored at 4 °C until use.
PCR products were directly purified according to the protocol of MinElute PCR Purification Kit (Quiagen). The DNA was eluted in 10 µl of 10 mM Tris-HCl (pH=8.5) and stored at 4 °C until use.

2.6.5 Restriction enzyme digestion of DNA

In this study, type II restriction enzymes were used that cut the DNA within their recognition sequence and create either blunt or sticky ends. Recombinant plasmids were analyzed by digestion with restriction enzymes to verify the successful insertion and the orientation of the fragment of interest. In general 1 µg of DNA was digested with 1 unit of the respective endonuclease in the buffer system suggested by the supplier (Fermentas, St. Leon-Rot, Germany) for one hour at 37 °C. The digested DNA was analyzed by Agarose gel electrophoresis (2.6.6).

2.6.6 Agarose gel electrophoresis.

DNA samples in buffer (Bromophenol blue, 0.05% (w/v); Xylen cyanol, 0.05% (w/v); EDTA (pH=8.3), 20 mM, Glycerol, 10% (w/v); in purified water) were separated in Agarose gels applying an electric field of 80-100 V. The electrophoresis buffer used was 1x TBE (Tris-HCl (pH=8.3), 0.1 M; Boric acid, 0.90 M; EDTA, 1 mM; in purified water). DNA fragments shorter than 500 bp were separated in 3% Agarose gel, longer fragments (500-1,500 bp) in a 1% Agarose gel. DNA fragments were stained by addition of 0.001% ethidium bromide. Size fractionated DNA bands were documented when excited with UV light of 260-360 nm applying an Image Master (VDS, Pharmacia, Uppsala, Sweden). As a size standard either Lambda PstI (Gibco/Invitrogen, Carlsbad, USA) or 100 bp marker (Biocat, Heidelberg, Germany) were used.

2.6.7 DNA sequencing and sequence analysis

All sequencing reactions were based on the dideoxy chain termination method according to Sanger (Sanger et al., 1977) and were performed with the LICOR 4200 sequencer (LICOR, MWG Biotech, Ebersberg, Germany) or the 3100 Avant Genetic Analyzer (Applied Biosystems, Darmstadt, Germany). DNA sequences determined by Licor 4200 were analyzed using the program Base ImageIR (LICOR). Sequences obtained from the 3100 Avant were analyzed by using the DNA Sequencing Analysis Software V5.1 (Applied Biosystems) and ABI Prism 3100 Avant Genetic Analyzer Data Collection Software V2.0 (Applied Biosystems).

2.6.8 Polymerase Chain Reaction (PCR)

A typical PCR mix (table 5) was prepared on ice in 0.5 ml reaction tubes by combining a nucleoside triphosphate (dNTPs) mix, a heat stable polymerase and 25-50 ng of template

DNA. The reaction mix was placed in thermal cycler (Mastercycler personal, Eppendorf, Hamburg, Germany or Primus 96 Plus, MWG Biotech, Ebersberg, Germany). The heat-stable TAQ-Polymerase from *Thermus aquaticus* produced PCR fragments with a 3´ adenylate overhang (tables 5 and 6) for TA-TOPO cloning (2.8.2). The recombinant Phusion Cx Polymerase from *Pyrococcus furiosus*, incorporates dUTP, has 3´-5´ exonuclease activity, and produces blunt end PCR-fragments (tables 7 and 8), suitable for uracil excision based cloning (2.8.5) or directional TOPO cloning (2.8.3). All PCR products were analysed by gel Agarose gel electrophoresis (2.6.6).

Table 5. Standard TAQ-PCR-reaction mixture (50 µl)

Component	**Concentration/Amount**
Taq-Polymerase (Biotherm, Genecraft, Cologone, Germany)	1 unit
dNTP	0.2 mM
sense primer	0.5 µM
anti sense primer	0.5 µM
$MgCl_2$	1 mM
TAQ-reaction-buffer (Biotherm, Genecraft, Cologne, Germany; $(NH_4)_2SO_4$, 16 mM; Tris-HCl, 67 mM (pH=8.8); $MgCl_2$, 1.5 mM; Tween 20, 0.01%)	1 fold

Table 6. Standard TAQ-PCR program

Step	**Time**	**Temperature (°C)**
1. Initial Denaturation:	3 min	95
2. Denaturation	30 s	95
3. Annealing	30 s	Primer dependent (8.2.3, supplemental tables 1 to 5)
4. Elongation	45 s/kb of template DNA sequence	72
Step 2 to 4 were repeated 35 times		
5.Dinal extension	5 min	72

Table 7. Standard Phusion Cx-PCR-reaction mixture (50 µl)

Component	**Concentration/Amount**
Phusion Cx Polymerase	1 unit
mM dNTP	0.2 mM
sense primer	0.5 µM
anti sense primer	0.5 µM
Phusion® HF (Finnzymes Oy, Finnland, 1.5 mM $MgCl_2$)	1 fold

Table 8. Standard Phusion Cx-PCR program

Step	**Time**	**Temperature (°C)**
1. initial denaturation:	30 s	98
2. denaturation	10 s	98
3. annealing	10 s	Primer dependent (8.2.3, supplemental tables 1 to 5)
4. elongation	15 s/kb of template DNA sequence	72
Step 2 to 4 were repeated 35 times		
5.final extension	5 min	72

2.6.9 Quantitative real time RT-PCR

Quantitative real time RT-PCR allows the relative quantification of cDNAs, synthesized from transcripts (2.7.1 and 2.7.2). This method relies on the detection and quantification of a fluorescent reporter, the signal of which increases directly proportional with the amount of PCR product. For each sample the threshold cycle is determined which is the amplification cycle at which the PCR product increases exponentially and which is dependent on the amount of input cDNA. The threshold cycle of a sample is then compared with the threshold cycle of an external standard. As external standard serves a PCR product of the cDNA of interest of which the concentration is known and a calibration curve is prepared. The concentration of cDNA in an unknown sample is calculated by comparing the unknown to a set of standard samples of known concentration.

In order to equalize the amount of input cDNA for different samples the constitutively expressed housekeeping genes, *actin2* and *actin8* (*ACT2/8*) were determined in each sample as internal standard.

Components of the quantitative real time RT-PCR were mixed and pipetted into glass capillaries (Roche, Basel, Switzerland). The capillaries were placed in the Lightcycler 3.1 (Roche, Basel, Switzerland) and the PCR was performed according to the protocol (tables 9 to 11). The specificity of PCR products was confirmed by determining the temperature at which the PCR product is melting (melting point).

Table 9. Primer-Mix (400 µl)

Component	**PM6**	**PM12**	**PM18**
Sense primer (50 µM)	6 µl	12 µl	18 µl
Antisense primer (50 µM)	6 µl	12 µl	18 µl
Purified water	388 µl	376 µl	364 µl

Table 10. Quantitative real time RT-PCR reaction mixture (20 µl)

Component	Volume
ABSOLUTE™ QPCR SYBR® GREEN MIXES (Thermo Fisher Scientific, Waltham, USA)	10 µl
Primer-Mix (PM)	8 µl
cDNA diluted 20 fold in purified water	2 µl

Table 11. Quantitative real time RT-PCR program (20 µl)

Step	Time	Temperature (°C)
1. Initialisation	15 min	95
2. Denaturation	15 s	98
3. Annealing	20 s	Primer dependent (8.2.3, supplemental tables 2)
4. Elongation	20 s	72
5. Detection	5 s	79
Step 2 to 5 were repeated 35 times		

2.6.9.1 Calibration curve for the external standard

Fragments, going to be quantitatified by real time RT-PCR in samples, were used as external standards. Therefore, PCR products were purified (2.6.4) and the concentration was determined spectrophotometrically (2.6.3). A set of standards of known concentration was prepared by a 10-fold serial dilution from 20 fg to 20 atg of the purified PCR-product to create a calibration curve. Specificity of the PCR-products was confirmed by melting point analysis and Agarose gel electrophoresis (2.6.6).

2.6.9.2 Calculation of transcript numbers

Quantification of the fluorescence intensity data was carried out with the Lightcycler software (Roche, Basel, Germany). The software calculates the amount of input cDNA according to the known amount of DNA of the calibration curve. Therefore the fluorescence intensity (log10) vs. cycle number of log-linear range of the PCR was calculated for both, the internal standard *ACT2/8* and the cDNA of interest. For normalization of the input cDNA the number of transcript molecules of interest was determined in relation to 10,000 *ACT2/8* transcripts for each sample according to Szyroki et al., (2001). Assuming that 4.778 fg of *ACT2/8* correspond to 10,000 *ACT2/8* molecules the number of *ACT2/8* transcripts x could be calculated as follows:

$$x = \frac{m\,(x)}{4.778\ fg} \cdot 10{,}000$$

m (x), measured *ACT2/8* cDNA amount [fg]

The normalized number of cDNA molecules of interest y was calculated as follows:

$$y = ((\frac{m\,(y)\ \cdot\ 435\ bp}{4{,}778\ fg\ \cdot\ length\,(y)} \cdot 10{,}000) \div x) \cdot 10{,}000$$

m (y), measured y cDNA amount [fg]

length (y), amplicon size [bp]

2.7 RNA methods

2.7.1 Poly-A-mRNA isolation

Poly-A-mRNA was isolated by the oligonucleotide Poly-dTTP (25) bound to polystyrene beads (Dynabeads Oligo-(dT) 25, Dynabeads/Invitrogen, Carlsbad, USA). The plant tissue was frozen in liquid nitrogen and homogenized in a ball mill (MM2000, Retsch, Haan, Germany). For 50 mg of tissue sample 1 ml lysis buffer was added. The lysate was centrifuged for 30 s at 10,000 rcf. The supernatant was incubated for 30 min with 20 µl of Dynabeads at room temperature in an overhead shaker. The washing steps were performed according to the manufacturer´s protocol. In order to exclude contaminations with DNA, mRNA was eluted from the Dynabeads by incubation at 65 °C for 2 min. In a second step the eluted mRNA was again bound to the Dynabeads for 20 min at room temperature in an overhead shaker. After two washes with washing buffer without lithium dodecyl sulfate, the mRNA was eluted from the magnetic beads with 16 µl RNase-free H_2O at 65 °C for 2 min. The eluated mRNA was directly used for reverse transcription (2.7.2).

2.7.2 Reverse transcription (RT)

For the reverse transcription of mRNA oligo (dT) primers were used. In a 0.5 ml reaction tube 13.2 µl of mRNA eluate (2.7.1) and 0.5 µl oligo dT primer (100 µM) were incubated at 70 °C for two min. After two min on ice and short spin down, 4 µl 5x RT buffer (Promega, Madison, WI, USA), 1 µl dNTPs (10 mM dATP, dGTP, dTTP and dCTP), 0.5 µl of RNase inhibitor (Promega, Madison, WI, USA) and 0.8 µl reverse transcriptase (Promega, Madison, USA) were added to the reaction mixture. The cDNA synthesis was carried out at 42 °C for one hour. The cDNA was either used for amplification by PCR (2.6.8) or stored at -20 °C.

2.8 Cloning Strategies

Recombinant plasmids in this study were generated by ligating PCR fragments into an entry vector using the TOPO cloning technique (2.8.2 and 2.8.3). The insert was then transferred from the entry clone into the destination vector using the Gateway recombination method (2.8.4). PCR fragments were also directly inserted into the destination vector using the uracil-excision based cloning technique (2.8.5).

2.8.1 Micro-RNA constructs

MicroRNAs (miRNAs) are endogenous single stranded RNAs (19-24 nucleotides) that have a negative regulatory function on gene expression by inducing transcript-degradation. A single miRNA is processed by the double strand specific dicer enzyme from the miRNA precursor, a long non-coding RNA with a fold-back structure. These miRNAs target mRNAs with high sequence homology by the RNA induced silencing complex (RISC). In this study a miRNA precursor was engineered according to Schwab et al., (2006) based on the *Arabidopsis* stem-loop forming precursor microRNA-319a, which was in the vector pRS300 (MPMI, Tübingen, Germany; 8.2.4, supplemental figure 4). Three fragments of the miRNA319a precursor with the SAD6-specific sequence (5´-TAATGTTCGAATAGCATCGGC-3´) forming the stem were PCR-amplified by applying site-specific mutagenesis according to Schwab et al., (2006) using standard Phusion Cx-PCR conditions (2.6.8, tables 7 and 8) and mismatch primers (8.2.3, supplemental figure 4). The three purified (2.6.4) overlapping PCR fragments were fused in an overlapping PCR using the Phusion Cx under standard conditions (2.6.8, tables 7 and 8) with primers, suitable for uracil-excision based cloning (8.2.3, supplemental table 3). The purified PCR product (2.6.4), containing the modified miRNA precursor was then transferred into the binary vector pCambia2300 (Cambia, Brisbane, Australia) using a uracil-excision based cloning strategy (2.8.5 and 8.2.4, supplemental figure 5).

2.8.2 TA TOPO cloning

For TA-TOPO cloning the DNA-fragments were PCR-amplified using Taq Polymerase without proofreading activity (2.6.8, tables 7 and 8; 8.2.3, supplemental figure 3). Taq enzymes produces 3´ dATP overhangs at the PCR-products. This overhang anneals with the complementary 3´ dTTP overhangs of the linearized cloning vector pCR8/GW/TOPO (Invitrogen, Carlsbad, CA, USA). The PCR products are ligated in both orientations into the vector. The PCR product was purified (2.6.4) before addition to the TOPO cloning reaction mixture. The reaction mixture (table 12) was incubated at room temperature for 5-30 min. The

recombinant plasmid was subsequently transformed into the E. coli strains One Shot Top10 or MRF´ (2.2.1). After restriction digestion (2.6.5) and sequence analysis (2.6.7) the insertions were transferred from the entry clone into the binary destination vector pMDC164 to be inserted 5´-upstream of the ß-glucuronidase (GUS) coding sequence using LR Gateway recombination (2.8.4).

Table 12. Composition of reaction mixture for TA-TOPO Cloning

Component	**Amount/Volumne**
Salt solution (1.2 M NaCl, 0.06 M $MgCl_2$)	0.5 µl
PCR product	10-30 ng
TOPO® pENTR vector (5-10 ng/µl)	0.5 µl
Adjusted to 3 µl with purified water	

2.8.3 Directional TOPO cloning

For directional cloning the vector pcDNA3.1-D-V5/His-TOPO (Invitrogen, Carlsbad, USA) was applied. For directional cloning the 5´ end of the sense primer contained the sequence 5´-CACC-3´ (8.2.3, supplemental table 3). This sequence hybridizes to the 5´overhang 3´-GTGG-5´ in the linearized cloning vector pcDNA3.1-D-V5/His-TOPO (Invitrogen, Carlsbad, CA, USA) thereby stabilizing the inserted PCR product in the correct orientation. Translational fusion of coding sequences with the V5 epitope and HIS6-tag were generated by PCR, using the phusion Cx polymerase (2.6.8, tables 7 and 8) and primers, omitting the stop codon of the coding sequence (8.2.3, supplemental table 3). The PCR product was purified (2.6.4) before addition to the TOPO cloning reaction mixture. The reaction mixture (table 13) was incubated at room temperature for 5-30 min. The recombinant plasmid (8.2.4, supplemental figure 8) was subsequently transformed into the E. coli strains One Shot Top10 or MRF´ (2.2.1). After restriction digestion (2.6.5) and sequence analysis (2.6.7) the uracil excision-based cloning strategy was applied (2.8.5) in order to transfer the translational fusion into the binary vector pCambia2300 (Cambia, Brisbane, Australia).

Table 13. Composition of reaction mixture for directional-TOPO Cloning

Component	**Amount/Volume**
Salt solution (1.2 M NaCl, 0.06 M $MgCl_2$)	0.5 µl
PCR product	10-30 ng
TOPO® pENTR vector (5-10 ng/µl)	0.5 µl
adjusted to 3 µl with purified water	

2.8.4 Gateway LR reaction

Gateway technology is derived from the recombination procedure performed by λ phage during the lysogenic and lytic cycle in E. coli. For application of the Gateway recombination reactions, the PCR-products were transferred into the entry vector pCR8/GW/TOPO (2.8.2) where they were flanked by attL1 and attL2 sites. The attL sites undergo a recombination reaction, catalyzed by the Gateway LR Clonase Enzyme Mix (Invitrogen, Carlsbad, USA) with the attR sites of the destination vector pMDC164. When applying the vector pMDC164 an expression clone was generated by recombination, in which a promoter fragment was inserted 5′-upstream of the ß-glucuronidase (GUS; 8.2.4, supplemental figure 7). The LR Gateway recombination reaction mixture (table 14) was incubated at room temperature for 1 h. The reaction was stopped upon addition of 1 µl of proteinase K (2 µg/µl), followed by a 10 min incubation at 37 °C. The recombined binary vector pMDC164 was subsequently transformed into E. coli strain DH5 alpha (2.2.1). The recombinant binary vector was transformed into *Agrobacterium* strain GV3101 by electroporation (2.2.3) after verification by restriction enzyme digestion (2.6.5) and sequence analysis (2.6.7). The clones were finally used for *Agrobacterium*-mediated stable transformation of *Arabidopsis thaliana* (ecotype Ws-2; 2.3) to study tissue-specific promoter activity (2.10).

Table 14. Composition of the reaction mixture for LR Gateway recombination

Component	**Amount/Volume**
Destination vector	30-50 ng
Entry vector	30-50 ng
LR clonase™ (Invitrogen, Carlsbad, USA)	2 µl
5 fold LR clonase reaction buffer (Invitrogen, Carlsbad, USA)	2 µl
Adjusted to 10 µl with purified water	

2.8.5 Uracil excision-based cloning

The uracil excision-based cloning procedure was performed as described by Nour-Eldin et al., (2006). The binary vectors pCambia2300 and pCambia3300 (Cambia, Brisbane, Australia), harboring the cassette 5′-GCTGAGGGAAAGTCTAGAGGATCCTCTAGATGTCTCCT-CAGC-3′ downstream of the 35S promoter were used in this work. A total of 5 µg of the respective plasmid DNA of the vectors was digested with 40 units of the PacI restriction enzyme in 200 µl (New England Biolabs, Ipswich, USA) at 37 °C overnight. The following day additional 20 units of PacI were added together with 20 units of Nt.BbvCI (New England

Biolabs) and the reaction mixture was incubated at 37 °C for 2 h. This procedure generated a linearized vector with 3´ overhangs and was finally purified (2.6.4). The coding sequences and miRNA precursor fragment were PCR-amplified by phusion Cx polymerase (2.6.8, tables 7 and 8) using forward and reverse primers that contained the sequences 5´-GGCTTAAU-3´ and 5´-GGTTTAAU-3´ (8.2.3, supplemental tables 3 and 4). The PCR products were mixed either with the linearized vectors pCambia2300 or pCambia3300, in a molar ratio of 10:1 and incubated at 37 °C for 20 min with one unit of USER enzyme mix (uracil-specific excision reagent; New England Biolabs). This step was followed by a 20 minute-incubation at room temperature. The resulting recombinant plasmids, harboring the respective insert under control of the 35S promoter, were transformed into the E. coli strains One Shot Top10 or MRF´ (2.2.1). After verification of the recombinant plasmids by restriction enzyme digestion (2.6.5) and sequence analysis (2.6.7) the binary plasmids were transformed into the *Agrobacterium* strain GV3101 using electroporation (2.2.3). Agrobacteria, harboring the plasmids, were used for transient transformation of *Nicotiana benthamiana* leaves applying the agroinfiltration technique and for stable transformation of *Arabidopsis* by floral dipping (2.4.3 and 2.4.4).

2.9 Protein methods

2.9.1 Extraction of total and chloroplast proteins from *Nicotiana benthamiana* leaves

Proteins in this study were extracted from chloroplasts and tissue areas of transiently transformed and non-transformed *N. benthamiana* leaves. Chloroplasts were isolated with minor modifications according to Pineda et al., 2010. For this purpose 100 mg of plant material in 400 µl of semi-frozen isolation buffer (Sorbitol, 0.33 M; HEPES (pH=7.5), 50 mM; serum bovine albumin, 0.1%; EDTA, 2 mM; $MgCl_2$, 1 mM) was homogenized using a pre-cooled glass homogenizer. The homogenate was filtered through a 50 µm nylon mesh and centrifuged at 7,000 rcf and 4 °C for 1 min through a 330 µl Percoll layer (40% in isolation buffer), at the bottom of a 1.5 ml reaction tube. After the quality of the pelleted chloroplasts was verified by applying phase contrast microscopy, the chloroplasts were shock frozen in liquid nitrogen. The freeze-fractured chloroplasts were re-suspended in an equal volume of protein extraction buffer (Glycerol, 10%; DTT, 10 mM; EDTA, 5 mM, HEPES (pH=7.2), 100 mM; protease inhibitor cocktail (Complete Mini EGTA-free, Roche, Basel, Switzerland)) and centrifuged at 15,000 rcf at 4 °C for 10 min.

For protein extraction from leaf tissue, 100 mg of plant material were homogenized in liquid nitrogen for 1 minute using a ball mill (MM300, Retsch, Haan, Germany) at a frequency of

30 hz. The homogenized tissue was re-suspended in 500 µl of protein extraction buffer and centrifuged at 15,000 rcf at 4 °C for 10 min. The concentration of the soluble protein fraction was subsequently determined (2.9.2).

2.9.2 Determination of the protein concentration

The protein concentration was determined based on the method of Bradford (1976) by using the Roti-Quant nano kit (Roth, Karlsruhe, Germany) according to the manufacturer´s protocol. First of all a serial dilution was prepared (0, 20, 30, 40, 50, 60, 80, 100 µg BSA/ml) from a 100 µg/ml stock solution of serum bovine albumin (BSA). Next, the protein samples of unknown concentration and of the serial dilution with known concentration were diluted 1:20 (10 µl of protein sample and 190 µl purified water). A microtiter plate with 200 µl Roti-Nanoquant solution and 50 µl of the diluted protein samples per well were incubated at room temperature for 5 min. The optical density of the reaction mixture was measured at 450 nm (OD_{450}) and 590 nm (OD_{590}) using a microplate reader (Dynex MRX TC Revelation, Dynex Technologies, Denkendorf, Germany). The ratio of OD_{590}/OD_{450} was plotted for each of the standard samples with BSA against their concentration in order to create the calibration curve. Finally, the unknown protein concentration of each sample was calculated by comparing them to the set of standard samples with known concentrations as follows:

$$\text{Protein concentration [µg/ml]} = \left(\frac{OD_{590}}{OD_{450}}_{1} - Y\,axis\,intersection_{2}\right) \div slope_{2}$$

1, optical density of the sample with unknown protein concentration

2, Y-axis intersection and slope of the calibration curve

2.9.3 Protein size fractionation by SDS-polyacrylamide gel electrophoresis (SDS-PAGE)

The size fractionation of proteins was performed by SDS-PAGE (Laemmli, 1970). The ready-to-use SDS-PAGE with an gradient of 8-16% (Precise, Thermo Fisher Scientific, Waltham, USA) was loaded with 10 µg of chloroplast and leaf tissue proteins from the soluble protein fraction (2.9.1 and 2.9.2), of transformed and not transformed *N. benthamiana* leaves. A pre-stained protein ladder (PageRule-Plus, Thermo Fisher Scientific, Waltham, USA) was used to monitor protein separation during electrophoresis and the size of the separated proteins. Prior to protein loading SDS sample buffer (end concentration: Tris-HCl (pH=6.8), 12 mM; Glycerol, 5%; SDS, 0.4%; Bromophenol blue, 0.02%; DTT, 0.04 M; dissolved in purified water) was added to the protein samples, followed by denaturation at 95 °C for 5 min. Electrophoresis was performed vertically in an electrophoresis chamber (SE250, Hoefer Inc.,

Holliston, USA) with Tris-HEPES SDS as electrophoresis buffer (Tris, 100 mM; Hepes, 100 mM; SDS, 3 mM; dissolved in water) at 20 mA and 100 V for 45 min. After electrophoresis the gel was stained with Coomassie. The SDS-PAGE was placed in Coomassie staining solution (Brilliant Blue-R-250 (Merck, Darmstadt, Germany), 0.1% (m/v); Methanol, 45% (v/v); Acetic Acid, 10% (v/v); in water) for 15 min followed by washing in destaining solution (Methanol, 10% (v/v); Acetic acid, 10% (v/v); in water) at room temperature for 30 min in order to verify the protein bands.

2.9.4 Western blot

The western blot included the electrotransfer of the size fractionated proteins from the gel to a membrane (2.9.4.1) followed by immunodetection of tagged proteins (2.9.4.2).

2.9.4.1 Electrotransfer of proteins on a membrane

After electrophoresis (2.9.3) the proteins were electrotransferred (western blot) to a PVDF membrane (Hybond-P, GE Healthcare, Chalfont St Giles, UK). The dry membrane was activated in methanol for 15 sec, followed by a two-minute washing step in water. The gel, membrane and whatman papers (GE Healthcare) were equilibrated in transfer buffer (Tris, 25 mM; Glycin, 192 mM; Methanol, 15% (v/v); in water) and finally piled up between anode and cathode with 6 whatman papers (figure 3).

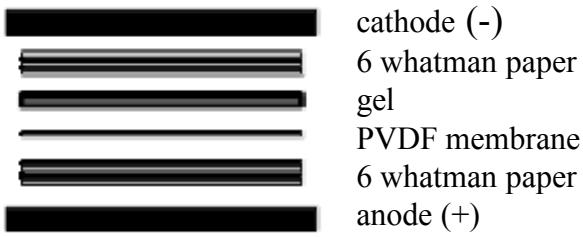

Figure 3. Arrangement of whatman paper, gel and membrane during electrotransfer.

Proteins were transferred from the gel to the membrane at 50 mA in 1 h. In order to verify the efficiency of the protein transfer the membranes were stained using Ponceau S solution (Ponceau S (Merck, Darmstadt, Germany), 0.5%; Acetic acid, 1%) for 1-5 min. After destaining in purified water the membrane was used for immunodetection (2.9.4.2).

2.9.4.2 Immunodetection

The PVDF membrane was blocked by incubation in TBS buffer (150 mM NaCl, 50 mM Tris, pH=7.8) containing 3% low-fat milk powder at room temperature for 0.5 h. After three

washing steps for five min in TBS buffer, membranes were incubated with mouse anti-V5 monoclonal antibodies (1:5,000 dilution, catalog number: R960-25, Invitrogen, Carlsbad, USA) in TBST (NaCl, 150 mM; Tris (pH=7.8), 50 mM; Tween 20, 0.05%) at room temperature for 1 h. Blots were washed three times in TBST for 5 min and incubated with the goat anti-mouse secondary antibody conjugated to a horseradish peroxidase (1:20,000 dilution, Pierce, Rockford, USA) at room temperature for 1 h. Excessive amount of secondary antibody was removed by three washings in TBST buffer each for 5 min. Peroxidase activity was detected by using luminol as substrate (super signal chemiluminescent, Pierce, Rockford, USA) and exposure to X-ray films (Kodak-Biomax Light, Rochester, USA).

2.10 Histochemical GUS assay

β-Glucuronidase (GUS) activity was assayed in *A. thaliana* (ecotype Ws-2) homozygous for the T-DNA containing GUS under control of a gene-specific promoter. GUS expressing plant tissue was vacuum infiltrated (100 mbar, 10 min) with GUS staining buffer (Na_2HPO_4 adjusted with NaH_2PO_4 to pH=7.0, 150 mM; EDTA, 10 mM; Potassium ferricyanide, 0.05 mM; Potassium ferrocyanide, 0.05 mM; Triton X-100, 0.1% (v/v); 2-bromo-4-chloro-3-indolyl glucuronide (Duchefa, Haarlem, the Netherlands), 1 mM; in water) and incubated at 37 °C in the dark for 0.5 h. Chlorophyll was removed by incubation in 70% ethanol at 4 °C for several days. Three independent transgenic plant lines were analyzed. GUS-staining was inspected and documented with a digital microscope (Keyence VHX-100, Keyence, Osaka, Japan) and a fluorescence stereomicroscope (Leica MZ FLIII, Leica, Solms, Germany) equipped with a CCD camera (Spot Insight Color 3.2.0, Diagnostic instruments, Sterling Heights, USA).

2.11 Determination of chloroplast number

The number of chloroplasts was compared in protoplasts from mesophyll cells of young chlorotic leaves of SAD6-OE and green leaves of Col-0, both, of similar size (1-1.5 cm long and 0.5-0.8 cm wide). Chloroplasts were counted by using a transmission light microscope focusing up and down through protoplasts of 50 µm in diameter (Biozero, Keyence, Japan). Mesophyll protoplasts were generated by placing the abaxial site of leaves after removal of the epidermis by mechanical abrasion with sandpaper onto a cell wall digesting enzyme solution. Leaves were incubated in digesting enzyme solution (Cellulase Onozuka R-10 (Serva, Heidelberg, Germany), 0.5% (w/v); Pectolyase Y23 (Seishin Corp., Tokyo, Japan), 0.05% (w/v); Macerozyme R10 (Serva, Heidelberg, Germany), 0.5% (w/v); Bovine serum

albumin (Sigma Aldrich, St. Louis, USA), 1% (w/v); $CaCl_2$, 1 mM; HEPES/Tris (pH=7.4), 10 mM) for 45 min at 23 °C and 80 rpm on a rotary shaker. The enzyme solution was adjusted to an osmolality of 400 mosmol·kg^{-1} with sorbitol. Released protoplasts were filtered through a 50 µm nylon mesh and washed with 400 mM sorbitol and 1 mM $CaCl_2$. After centrifugation at 60 rpm at 4 °C for 6 min protoplasts were stored on ice while aliquots were used for chloroplast counting.

2.12 Determination of chlorophyll content

Chlorophyll a and b was extracted from 25 mg leaf tissue homogenized in liquid nitrogen with 1 ml 80% (v/v) acetone. After centrifugation (2 min, 16,000 rcf) the supernatant was 80 fold diluted and the optical density (OD) was measured at 647 and 664 nm using a photospectrometer (Eppendorf, Hamburg, Germany). The total chlorophyll concentration was calculated according Strain et al., 1971 as follows:

Chlorophyll (a and b) concentration [µg/g fresh weight] =

$$((11.78 \cdot OD_{664} - 2.29 \cdot OD_{647}) + (20.05 \cdot OD_{647} - 4.77 \cdot OD_{664})) \cdot 80$$

2.13 Chlorophyll fluorescence measurements

Chlorophyll fluorescence of PSII was determined by applying the Junior-PAM (Heinz Walz GmbH, Effeltrich, Germany) with the following settings: Dark adapted plants (90 min) were treated with measuring light (450 nm; 0.1 µmol·m^{-2}·s^{-1}, 5 and 100 hz modulation frequencies) for 2 min. Then saturating light pulses (450 nm, <1 s, 10,000 µmol·m^{-2}·s^{-1}) were added every 60 s. Three min thereafter actinic light (450 nm) was switched on and given for a time period of 8 min. Four different light intensities of actinic light (45, 90, 190, 420, or 820 µmol·m^{-2}·s^{-1}) were tested. During the time course of fluorescence measurement leaves were aerated with water saturated air containing 0.07% CO_2. Photochemical (q_P) and non-photochemical quenching (q_N) parameters were calculated according to Schreiber et al., (1986) and van Kooten and Snel (1990).

2.14 Lipid analysis

2.14.1 Lipid extraction

Total lipid extraction of 100 mg plant material was carried out by Chloroform/Methanol according to Bligh and Dyer, 1959. Polar membrane lipids and Arabidopsides were extracted from 150 mg of fresh plant material with 1.5 ml of 2-isopropanol at 80 °C in 15 min. Samples

were centrifuged for 10 min at 14,000 rcf, and each supernatant was collected. The remaining plant material was re-extracted twice with 1.5 ml of chloroform:2-isopropanol (2:1, v/v) and 1.5 ml of chloroform:methanol (1:2, v/v). Samples were centrifuged after each extraction step, and the supernatants were combined. Extracts were dried under a stream of nitrogen at 60 °C.

2.14.2 LC-MS and LC-MS/MS analyses

LC-MS/MS analyses were performed using a Acquity ultra-high-performance liquid chromatograph coupled to a Micromass Quattro Premier triple quadrupole mass spectrometer (Waters, Milford, USA) with an electrospray interface (ESI). All aspects of system operations and data acquisition were controlled by using MassLynx V4.1 software (Waters). LC-MS analyses of fatty acids were performed using an Agilent 1200 liquid chromatography system (Agilent, Waldbronn, Germany) coupled to the mass spectrometer mentioned above.

2.14.2.1 Chromatographic conditions

Chromatographic separations of phospholipids, galactolipids and arabidopsides were carried out using an Acquity BEH column (2.1 x 50 mm, 1.7 µm particle size with a 2.1- x 5 mm guard column; Waters, Milford, USA) with the following solvent systems: solvent A was 1 mM aqueous ammonium acetate and solvent B was 1 mM ammonium acetate in methanol. For phospholipid analysis, a gradient elution was performed on a BEH C18 column at a flow rate of 0.3 ml·min^{-1} at 40 °C as follows: 75% to 100% B in 10 min, followed by 100% B for 2 min, and reconditioning at 75% B for 3 min. For galactolipids and arabidopsides, a linear step gradient (0.3 ml·min^{-1} flow rate, 30 °C) on a BEH C8 column, starting from 75% B for 1 min, followed by 75% to 100% B in 10 min, 100% B for 1 min, and 75% B for 4 min was used.

For the separation of fatty acids a Purospher Star RP-18ec column (2 x 125 mm, 5 µm particle size with a 4 x 4-mm guard column; Merck, Darmstadt, Germany) was used with the following solvent system: solvent A was 1 mM aqueous ammonium acetate and solvent B was acetonitrile. A gradient elution was performed at a flow rate of 0.2 ml·min^{-1} from 70% to 100% B within 10 min, followed by 100% B for 5 min and reconditioning at 75% B for 10 min.

2.14.2.2 Mass spectrometric conditions

For analysis of galactolipids the electrospray source was operated in the negative electrospray mode (ESI-) at 120 °C and a capillary voltage of 2.25 kV. Nitrogen was used as desolvation

and cone gas with flow rates of 850 at 450 °C and 50 $l \cdot h^{-1}$, respectively. The cone voltage (CV) was adjusted to 40 V. Galactolipids were analyzed by multiple reaction monitoring (MRM; 8.2.1, supplemental tables 6 and 7) using argon as collision gas at a pressure of approximately $3 \cdot 10^{-3}$ bar and a collision energy (CE) of 26 eV. The characteristic formation of fatty acid fragments ([M-H]- → [FA]-) for each individual compound during collision-induced dissociation (CID) was monitored for a scan time of 0.025 s per transition. Quantification was carried out using 3 µg of DGDG 18:0-18:0 as internal standards.

Phospholipid analysis was carried out in the negative electrospray mode, except for the detection of phosphatidylethanolamines (ESI+). The capillary voltage was 3.25 kV, the flow rates were adjusted to 800 $l \cdot h^{-1}$ at 400 °C for the desolvation and 50 $l \cdot h^{-1}$ for the cone gas. Cone voltage and collision energy were optimized for each class of phospholipids with the following parameters: CV 40V and CE 26 eV for PC; CV 48 V and CE 40 eV for PG; CV 38 V and CE 42 eV for PI and CV 40V. Quantification of lipids was performed by monitoring specific transitions of lipids (MRM; 8.2.1, supplemental tables 8, 9 and 11) as mentioned above ([M-H]- → [FA]-), using PC 17:0-17:0, PG 17:0-17:0 and PI 16:0-16:0 as internal standards. Quantification of lipids with two different acyl chains in the sn-1 and sn-2 position was performed by integration of the signals of both daughter ions derived from the loss of acyl group from the precursor ion.

Phosphatidylethanolamines were analyzed in the positive ionization mode. The parameters for ionization and CID were optimized as follows: capillary voltage, 3.25 kV; cone voltage, 32 V; collision energy, 22 eV. Determination of PE was carried out by monitoring a specific MRM transition (8.2.1, supplemental table 10) for each individual compound, resulting from a loss of phosphate and ethanolamine ([M+H]+ → [M-P-EA]+), using PC 18:0-18:0 as internal standard.

For fatty acid analyses the electrospray source was operated in the negative ionization mode at a capillary voltage of 3.5 kV and a source temperature of 120 °C. The optimal MS parameters for the detection of fatty acids were the following: desolvation gas, 800 $l \cdot h^{-1}$ at 400 °C; cone gas, 100 $l \cdot h^{-1}$; cone voltage, 30 V. Quantification was performed using selected ion recording (SIR) for fatty acid carboxylate anions with a scan time of 0.1 s for each compound. Heptadecanoid acid was used as internal standard.

2.14.3 Data processing

Signal values of individual lipid species (glycerolipid, fatty acid) were obtained by using the MassLynx V4.1 software (Waters, Milford, USA). The relative amount (mol%) of each lipid

species within the respective lipid pool was quantified. Internal standards were only applied for quantification of the amount of the total lipid pool. The relative amount (mol%) of individual lipid species was calculated as percentage of a respective signal value as part of the total signal values of a respective lipid class as follows:

$$\text{Relative amount of lipid species [mol\%]} = ((s_1 \div mw_{s_1}) \div \sum_{i=s_1}^{n} x_i \div mw_i) \cdot 100$$

mw, molecular weight

S_1, signal value of the respective lipid species

The relative amount of polar lipid species allowed the calculation of the distribution of the fatty acids 16:0, 16:1, 16:2, 16:3, 18:0, 18:1, 18:2 or 18:3 within a respective polar lipid class (MGDG, DGDG, PG, PC, PE and PI). Therefore the relative amounts, divided by two, of each polar lipid species (mol%; see above), containing one of the respective fatty acid, were summarized. For polar lipid species containing two fatty acids of one kind, the relative amount was added one fold. The summarized value is giving the relative amount of the respective fatty acid (%) within the respective polar lipid class.

Based on the relative fatty acid distribution, the desaturation index, which is giving the average number of double bonds of each fatty acid was calculated as follows:

$$\text{Desaturation index} = (p_1 + 2 \cdot p_2 + 3 \cdot p_3) \div 100$$

P_1, relative amount of monounsaturated fatty acid in the respective lipid class (mol%)

P_2, relative amount of diunsaturated fatty acid in the respective lipid class (mol%)

P_3, relative amount dof triunsaturated fatty acid in the respective lipid class (mol%)

For calculation of the total amount of each glycerolipid pool, total amounts of individual glycerolipid species of each glycerolipid class were calculated and summarized as follows:

$$\text{Total amount of glycerolipid pool [µg/ g fresh weight]} = \sum_{i=S_1}^{n} S_1 \div S_{sd} \div m \cdot RF$$

S_1, signal value of the respective lipid species

S_{sd}, signal value of the respective internal standard

m, mass fresh weigh [g]

RF, response factor

3. Results

This study focuses on the role of desaturated lipids in crown gall tumors caused by *Agrobacterium tumefaciens*. A previous genome-wide gene expression study revealed that 27% of genes involved in lipid metabolism are differentially regulated in the crown gall (Deeken et al., 2006). Growth requires the elevated production of macromolecules, such as lipids which serve as essential building blocks of cells and their organelles. Thus, increased lipid biosynthesis is necessary in the emerging crown gall tumor, as it is known from animal tumors (Igal, 2010). The striking change in gene regulation could also reflect alterations in the lipid composition that are related to the physiology of the tumor microenvironment. It has been shown that *Arabidopsis* tumors suffer from hypoxia, oxidative and drought stress. The first part of this study addresses the question whether the lipid pattern differs between stem tissue and the crown gall tumor by applying analytical methods. Tumor development was induced by inoculation of wounded *Arabidopsis* inflorescence stalks (genotype Wassiljewskija) with *Agrobacterium tumefaciens* (strain C58). Mock-inoculated inflorescence stalks of the same age served as reference. Tumor and reference tissue were harvested 21 d after inoculation (2.4.1).

3.1 Unsaturated ER-derived phospholipids dominate the lipid pool of crown gall tumors

In order to obtain an overview over the lipid pattern of *Arabidopsis* crown galls in comparison to the mock inoculated reference stem, the relative distribution of FAs within the total FA pool, including free and bound FAs, was determined (2.14.1, 2.14.2 and 8.3.2, supplemental table 12). The relative amount of the PUFA 18:3 (linolenic acid) was significantly higher in tumors (46±6 mol%) compared to mock-inoculated reference stalks (32±3 mol%;), whereas the relative amounts of the PUFAs 18:2 (linoleic acid) and 16:3 (hexadecatrienoic acid) were significantly reduced in tumors (19±5 mol% and 0.7±0.2 mol%, respectively) compared to the reference (37±3 mol% and 1.5±0.4 mol%, respectively; figure 4; 8.3.2, supplemental table 12). All other FA species were unchanged.

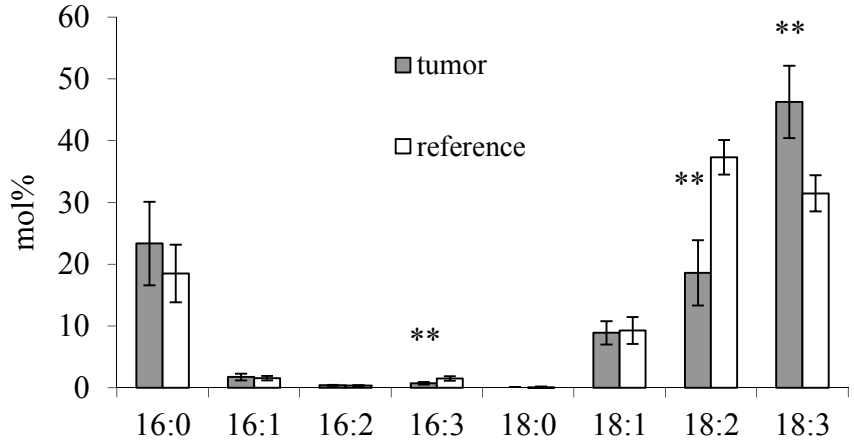

Figure 4. Relative fatty acid distribution within the total fatty acid pool in *Arabidopsis* crown gall tumors.
Mean values (mol%±SD) of each fatty acid species (acyl carbon:double bonds) were calculated from 4-5 independent experiments. Statistical analysis was performed using an unpaired two-tailed Student´s t-test (**, P-value≤0.01).

In order to access the origin of 18:3 PUFA in the tumor, the glycerolipid species of the major plastidic lipid classes (MGDG, DGDG, PG) and of the endoplasmic reticulum (PC, PE, PI) were analyzed (2.14.1 and 2.14.2). Within each of these lipid classes, the relative levels of glycerolipid species, except of the chloroplast-derived PG class, containing 18:3 PUFA, such as MGDG-18:3-18:1, MGDG-18:3-18:3, DGDG-18:3-18:3, PC-18:3-18:3, PC-18:3-18:1, PE-18:3-18:3, PE-18:3-16:0, PE-18:3-16:1, PI-18:3-16:0 were significantly (P-value≤0.05) higher in tumors compared to the reference (figure 5; 8.3.2, supplemental tables 14 to 19).
Calculations of the ratio of relative FA contents within each polar glycerolipid class in crown gall vs. reference (2.14.3) revealed that 18:3 PUFA was again significantly higher in all, except the plastidic PG lipid class of the tumor (table 15). In contrast to 18:3, the precursor was decreased in the tumor lipid classes, but not in the PG class.

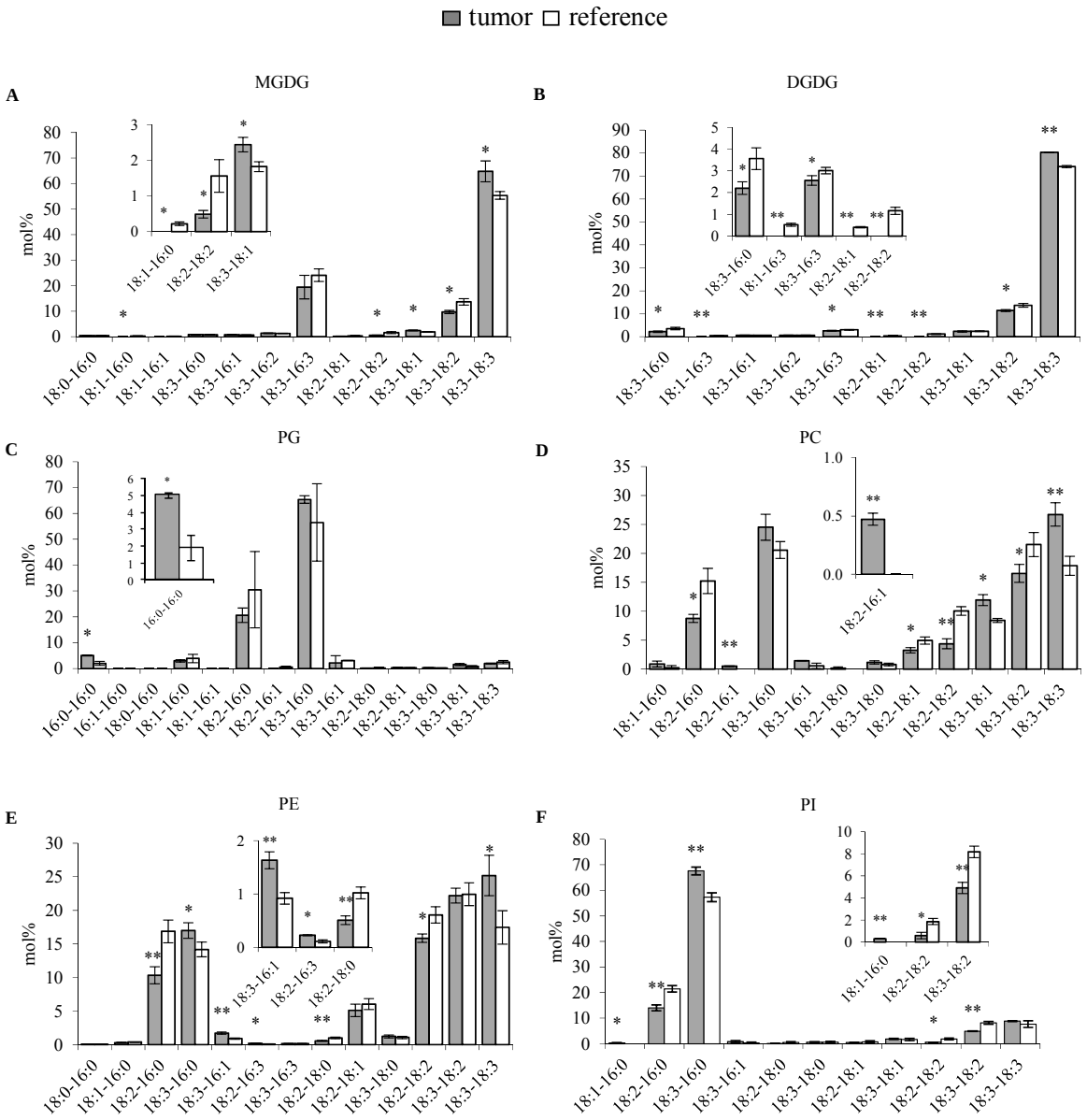

Figure 5. Relative distribution of the lipid species within the major glycerolipid classes in *Arabidopsis* crown galls.

(A) Lipid species of the polar glycerolipid classes monogalactosyldiacylglycerol (MGDG), **(B)** digalactosyldiacylglycerol (DGDG), **(C)** phosphatidylglycerol (PG), **(D)** phosphatidylcholine (PC), **(E)** phosphatidylethanolamine (PE), and **(F)** phosphatidylinositol (PI) were determined by LC-MS/MS. Insets show an enlargement of the lipid species below 10 mol% with significant differences (P-value≤0.05) between tumor and reference tissue. Mean values (mol%±SD) were calculated from 3-4 independent experiments. Statistical analysis was performed by using an unpaired two-tailed Student´s t-test (*, P-value≤0.05; **, P-value≤0.01).

Table 15. Ratios of galactolipid- and phospholipid-derived fatty acids (FA) within major gylcerolipid classes in the *Arabidopsis* crown gall vs. reference.

Ratios were calculated from the relative proportion of FAs (mol%) within each glycerolipid class of galactolipids (MGDG, DGDG) and phospholipids (PG, PC, PE, PI) determined by LC-MS/MS. Not presented are 16:1, 16:2 and 16:3 FA of PC, PE and PI, and 16:2 and 16:3 of PG, which represented only minor fractions of each polar lipid class. Grey boxes with bold italic numbers highlight significantly (P-value≤0.05) lower FA ratios and with bold letters those with higher ratios. Statistical analysis was performed using an unpaired two-tailed Student´s t-test. MGDG, monogalactosyldiacylglycerol; DGDG, digalactosyldiacylglycerol; PC, phosphatidylcholine; PE, phosphatidylethanolamine; PG, phosphatidylglycerol; PI, phosphatidylinositol; nd, not detectable.

	MGDG		**DGDG**		**PG**		**PC**		**PE**		**PI**	
FA	Ratio	P-value	Ratio	P-value	Ratio	P-value	Ratio	P-value	Ratio	P-value	Ratio	P-value
16:0	-1.20	0.070	***-1.62***	***0.023***	1.01	0.795	-1.06	0.381	-1.14	0.116	**1.04**	**0.031**
16:1	1.13	0.533	-1.01	0.960	-1.63	0.493						
16:2	1.04	0.689	1.03	0.881								
16:3	-1.24	0.216	***-1.38***	***0.005***								
18:0	-1.22	0.204	nd		1.16	0.630	1.66	0.192	-1.15	0.282	-1.45	0.603
18:1	1.05	0.532	***-1.42***	***0.021***	-1.00	0.981	1.18	0.145	-1.19	0.245	1.13	0.674
18:2	***-1.58***	***0.031***	***-1.40***	***0.014***	-1.46	0.357	***-1.63***	***0.001***	***-1.21***	***0.005***	***-1.67***	***0.013***
18:3	**1.07**	**0.031**	**1.05**	**0.002**	1.18	0.359	**1.25**	**0.005**	**1.26**	**0.018**	**1.12**	**0.042**

Summarizing the total lipid pool (2.14.3) revealed that the ER-specific phospholipids, PC (1.79-fold, P-value: 0.05), PE (1.31-fold, P-value 0.0294) and PI (2.61-fold, 0.002) were higher, whereas the total amounts of the plastidic lipid pools, MGDG (1.76-fold, P-value: 0.022), DGDG (2.36-fold, P-value: 0.032) and PG (1.25-fold, 0.153) were lower in tumors (figure 6A; 8.3.2, supplemental table 13). Thus, the high levels of the linolenic acid 18:3 in the crown gall mainly derived from the phospolipids PC, PE and PI. This was also supported by the finding that the desaturation index, which represents the average number of double bonds per fatty acid in a lipid pool (2.14.3), was significantly (P-value≤0.05) increased in the tumor within the MGDG, DGDG, PC (P-value 0.055) and PE pools (figure 6B). In summary, the data suggest a role for 18:3 PUFA from ER derived phospolipids in *Arabidopsis* crown galls.

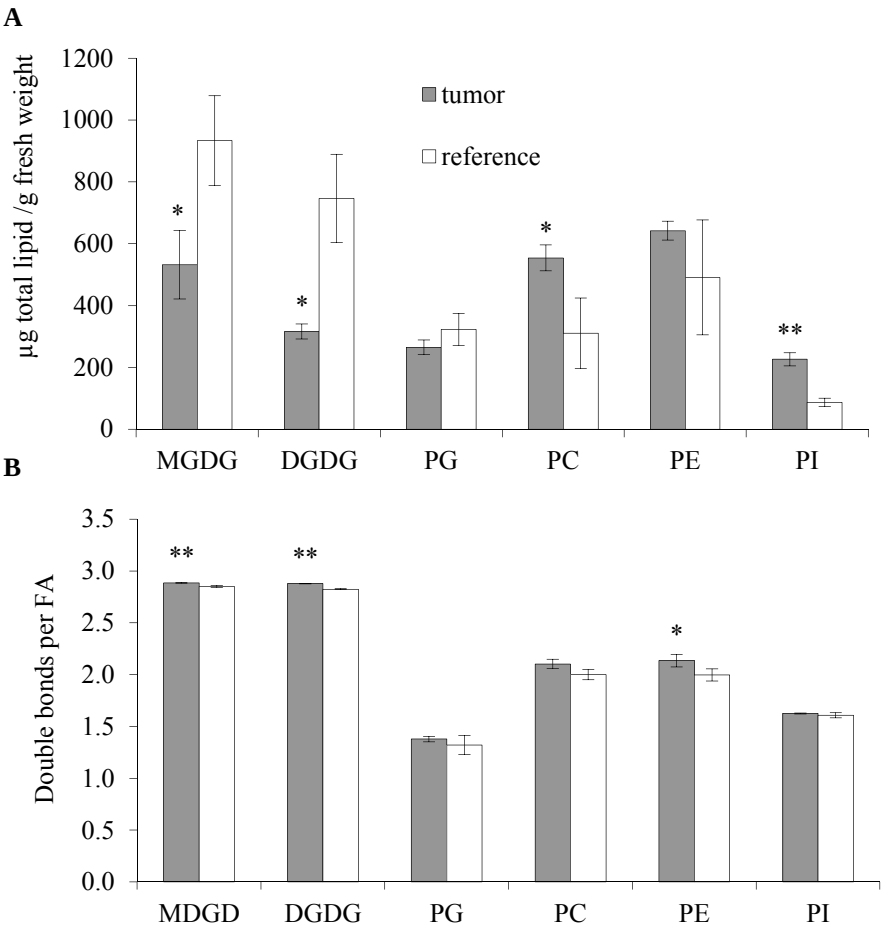

Figure 6. Total amounts and desaturation indices of polar glycerolipid pools in *Arabidopsis* crown galls.
(A) Total amounts of polar glycerolipid pools in *Arabidopsis* crown gall tumors and mock-inoculated inflorescence stalk tissue (reference). Mean values (µg total lipid per g fresh weight±SD) of each lipid pool were calculated from 3-4 independent experiments by summarizing the amounts of individual glycerolipid species determined by LC-MS/MS using internal lipid standards. **(B)** Desaturation index in major glycerolipid pools in *Arabidopsis* crown galls. Mean values (double bonds per FA±SD) of each lipid pool were calculated on the relative lipid profiling by LC-MS/MS from 3-4 independent experiments. Statistical analysis was performed using an unpaired two-tailed Student´s t-test (*, P-value≤0.05; **, P-value≤0.01). MGDG, monogalactosyldiacylglycerol; DGDG, digalactosyldiacylglycerol; PC, phosphatidylcholine; PE, phosphatidylethanolamine; PG, phosphatidylglycerol; PI, phosphatidylinositol.

3.2 Strong expression of two desaturases in *Arabidopsis* crown galls

The lipid profile exhibited a clear alteration in the desaturation pattern in *Arabidopsis* crown galls (figures 4 to 6 and table 15). In order to identify genes that could be responsible for that change, the transcript levels of genes involved in lipid metabolism of crown gall tumors were analyzed from previously published microarray data (Deeken et al., 2006) and compared with the lipid pattern. Two genes, a stearoyl-acyl carrier protein desaturase (*SAD*, 1.3.1), involved in the first desaturation step in plants and a membrane bound fatty acid desaturase, which produces PUFA (FAD, 1.3.2) were strongly activated. The functional unknown *SAD6* gene,

was 25-fold up-regulated in the plant tumor compared to the mock-inoculated reference stalk tissue (figure 7A). The transcriptional activity of two other *SAD* genes of the *SAD* family, *SAD5* and *SSI2* was significantly reduced (figure 7A). Based on the amino acid sequence, SAD6 builds a unique branch in the phylogenetic tree of the SAD family (figure 7B) and is only distantly related to the other six members. The transcription of the ER-membrane bound *FAD3* gene was 8-fold higher in tumors as compared to mock-inoculated stalks (figure 7C). In contrast to *SAD6* is *FAD3* a functional well characterized member of the *FAD* gene family, which encodes an enzyme for the synthesis of the 18:3 PUFA (1.3.2). The endoplasmatic reticulum (ER)-associated FAD3 protein is like SAD6 only distantly related to the other four FADs of the FAD family (figure 7D). The activity of the second ER-localized *FAD* gene, *FAD2*, which converts 18:1 FA to 18:2 PUFA, was unchanged in tumors. The membrane bound fatty acid desaturases of plastids, *FAD6*, *FAD7*, and *FAD8*, which affect the galactolipid pools, were down-regulated (figure 7C). The lower absolute amount of total galactolipids compared to phospholipids in the tumor (figure 6A) correlates with the reduced transcriptional activity of the plastidic *FAD* genes in crown galls. Furthermore, the increased transcriptional activity of the ER-specific *FAD3* parallels the increase in 18:3 unsaturated phospholipids. Quantitative realtime RT-PCR was applied (2.6.9, 2.7, 8.2.1 and 8.2.3, supplemental table 2) to confirm *SAD6* and *FAD3* transcriptional up-regulation in crown gall tumors. *SAD6* transcripts were 152-fold (49,634±32,132 vs. 325±184) and *FAD3* 17-fold (10,101±4,439 vs. 604±18) up-regulated in tumurs vs. mock treated tissue (figure 7E). In contrast, transcription of *SSI2*, the major contributor of 18:1 FA in leaf tissue (Kachroo et al., 2007), was 2.7-fold down-regulated (7,122±63 to 2,608±1,144 figure 7E).

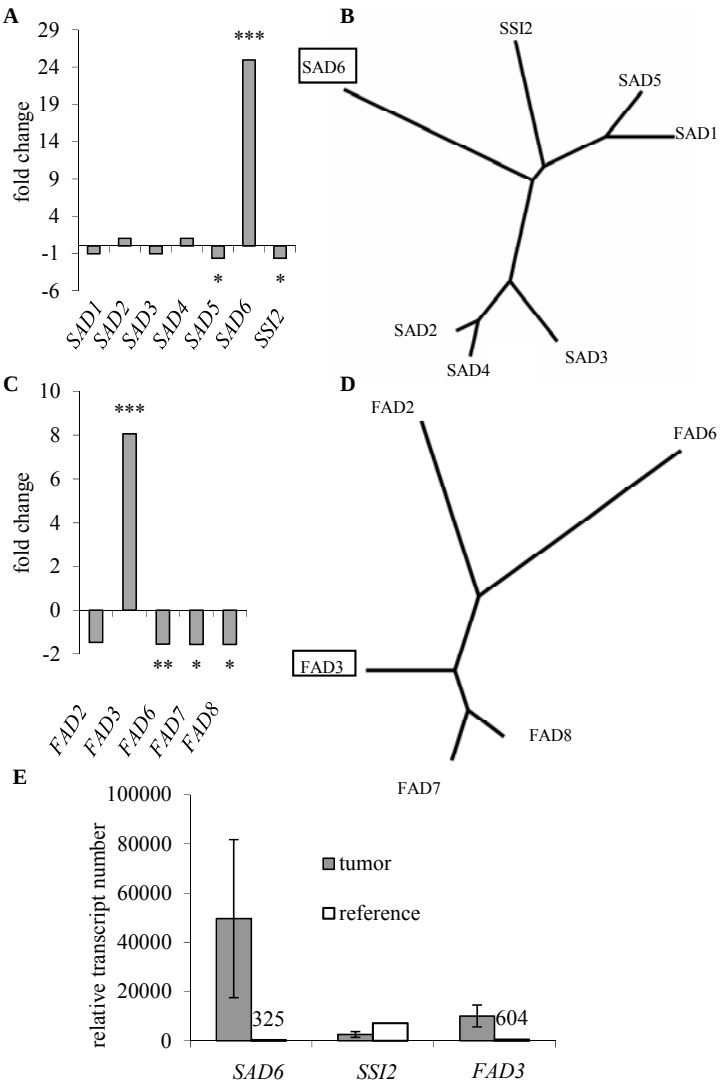

Figure 7. *SAD6* and *FAD3* are the only desaturases strongly up-regulated in *Arabidopsis* (genotype Wassiljewskija) crown gall tumors.

(A) Fold changes of transcriptional activity of stearoyl acyl carrier protein desaturases (*SAD*) in *Arabidopsis* tumors vs. mock-inocculated inflorescence stalk tissues based on microarray data. **(B)** Phylogenetic tree of the seven members comprising the family of *Arabidopsis SAD* proteins (8.2.2). **(C)** Fold changes of gene expression of membrane bound omega-3/6 FA desaturases (*FADs*) based on microarray data. **(D)** Phylogenetic tree of the five members of membrane bound omega-3/6 FA desaturase proteins of *Arabidopsis* (8.2.2). **(E)** Relative transcript number of *SAD6*, *SSI2* and *FAD3* in *Arabidopsis* crown gall tumors and mock inoculated stems (reference). Bars and numbers represent mean values (±SD) of 3-4 independent experiments. Relative transcript numbers were determined and normalized to 10,000 *ACT2/8*-molecules by applying quantitative real time RT-PCR. Statistical analysis was performed using an unpaired two-tailed Student´s t-test (*, P-value≤0.05; **, P-value≤0.01; ***, P-value≤0.001). Phylograms were generated with ClustalX 2.0.12 (Larkin et al., 2007) and drawn by FigTree V.1.3.1 (http://tree.bio.ed.ac.uk/software/figtree/).

3.3 Tumor development on the *fad3* mutants is impaired

In order to test the role of 18:3 and the involvement of FAD3 in desaturation in tumors, *Arabidopsis* mutants (2.3.3) impaired in FA desaturation were analyzed with respect to tumor growth (2.4.1). The tumor weight of *fad3-2* hosted ones was 45% reduced compared to the

WT, Col-0 (figure 8A; 8.34±1.51 vs. 15.15±1.68 mg/cm). The *fad3-2* mutant produces reduced amounts of trienoic FAs, predominantly of phospholipids that represent the major lipid components of extraplastidic membranes (James et al., 1990; Browse et al., 1993). In contrast, the *fad7-1/fad8-1* double mutant (2.3.3) with reduced trienoic fatty acids of the galactolipid class (McConn et al., 1994; Gibson et al., 1994) exhibited no change in tumor growth compared to Col-0 (14.76±1.76 vs. 15.15±1.68 mg/cm). The results of the tumor growth assay indicated that 18:3 PUFAs of extrachloroplastidic phospholipids, but not the plastidic galactolipids impact on tumor growth. This observation is in accordance with the reduced number of chloroplasts as well as the lower absolute amount of galactolipids and PGs in the tumor. Taken together, the ER-derived phospholipids were increased in the tumor and contained high levels of linolenic acid (figure 6A and table 15).

Agrobacterium-induced plant tumor development is associated with increasing water loss (Schurr et al., 1996) and induction of drought stress protection (Efetova et al., 2006). Overexpression of *FAD3* and accumulation of 18:3 PUFAs have been shown to increase tolerance towards drought stress (Zhang et al., 2005). Thus role of *FAD3* in drought stress adaption of the tumor was studied in relation to drop of relative humidity. Tumors on wildtype Col-0 plants exposed to high relative humidity of 75-100% grew 38% larger compared to those facing low humidity of 45-50% (figures 8A and 8B; 20.92±3.24 vs. 15.15±1.68 mg/cm). Furthermore, the significant difference in tumor growth between the *fad3-2* mutant and Col-0 observed at a relative humidity of 45-50% was abolished when plants were grown at 75%-100% humidity (17.15±1.91 vs. 20.92±3.24 mg/cm). According to quantitative real time RT-PCR analysis, however, changes in relative humidity did not affect transcriptional regulation of *FAD3* (Data not shown). The *fad7-1/fad8-1* double mutant exhibited no significant change in tumor size in comparison to Col-0 under high humidity conditions (24.21±14.18 vs. 20.92±3.24 mg/cm). The tumor growth assay suggested that 18:3 PUFAs of the extrachloroplastidic phospholipids, synthesized by FAD3 in the ER, rather than chloroplast-derived 18:3 PUFA, play a role in drought stress protection of tumors.

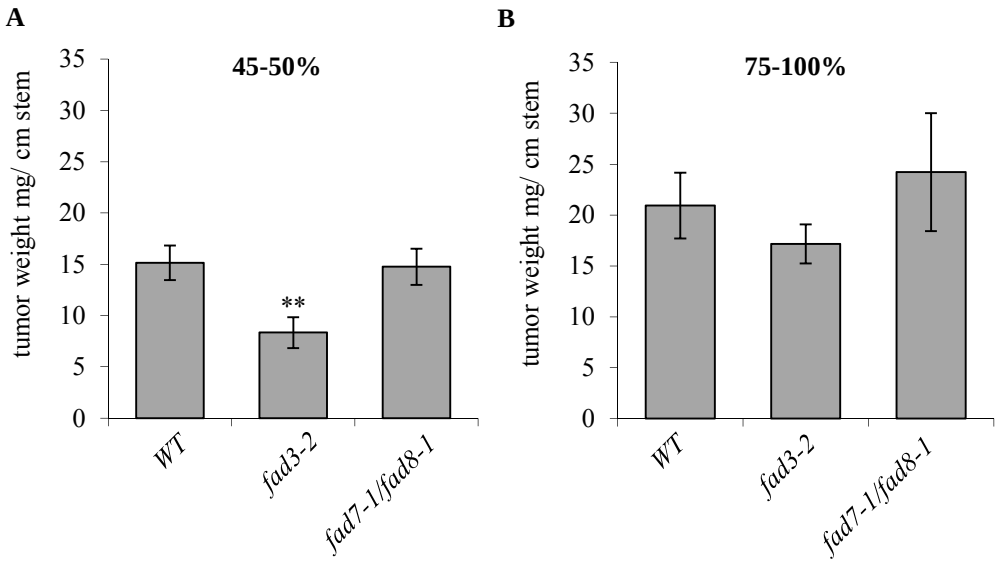

Figure 8. The *Arabidopsis fad3-2* mutant develops smaller tumors under low relative humidity.
(A) Tumor weight from *fad3-2* (Browse et al., 1993) *and fad7-1/8-1* mutants (McConn et al., 1994) and the respective wildtype Col-0 grown at a relative humidity 45-50% and **(B)** at 75-100%. Tumor weights were determined per cm of infected inflorescence stalks 21 d after inoculation with A. tumefaciens strain C58. Mean values (±SE) were calculated in (A) from 22 tumors of *fad3-2*, 18 tumors of *fad7-1/8-1*, 28 tumors of Col-0 and in (B) from 22 tumors of fad3-2, 6 tumors of *fad7-1/8-1*, 24 tumors of Col-0. Statistical analysis was performed using an unpaired two-tailed Student´s t-test (**, P-value ≤ 0.01.

3.4 Transcription of the *SAD6* gene is induced with the onset of tumor development

High activity of *FAD3* (figure 7C) and the overall increased desaturation indices (figure 6B) in tumors depend on the availability of the substrate 18:1, oleic acid. This first step in desaturation is catalysed by *SAD* gene family. *SAD6*, a thus far functionally unknown member of this gene family showed an extraordinary high transcriptional activity in the *Arabidopsis* tumour (figure 7E).

In order to elucidate the role of the *SAD6* gene in tumor lipid metabolism and -development, the spatiotemporal *SAD6* promoter activity was studied. Therefore transgenic *Arabidopsis* plants, expressing the reporter gene glucuronidase (GUS) under control of the *SAD6*-promoter fragment of 1,303 bp 5´-upstream of the *SAD6* coding sequence were generated (2.8.2, 2.8.4, 8.2.1, 8.2.3, supplemental table 3, and 8.2.4, supplemental figure 7). Three independent T3-lines, homozygous for the T-DNA insertion with the $SAD6_{PRO}$:GUS construct, were analyzed (2.10). The GUS reporter lines showed that the *SAD6* promoter was already induced six d after inoculation. This coincides with the onset of tumor development when only a few cells express the T-DNA encoded genes and early signs of tumor growth became visible (figure 9A). This was not observed at earlier time points (data not shown). The *SAD6* gene was active in the whole tumor tissue as visualized by GUS staining of mature tumors of transgenic GUS plants (figure 9B). Applying quantitative real time RT-PCR (2.6.9, 8.2.1 and

8.2.3, supplemental table 2) confirmed a significant increase in *SAD6* transcript numbers (figure 9C). Furthermore increased *SAD6* gene activity was not observed when the disarmed *Agrobacterium* strain GV3101 was inoculated. Thus agrobacterial effector proteins do not have an influence on *SAD6* gene expression, because GV3101 is a derivative of the *Agrobacterium* strain C58. GV3101 only lacks the T-DNA, but not the virulence factors, such as VirD2, VirE2, VirE3, and VirF (Vergunst et al., 2000, 2003).

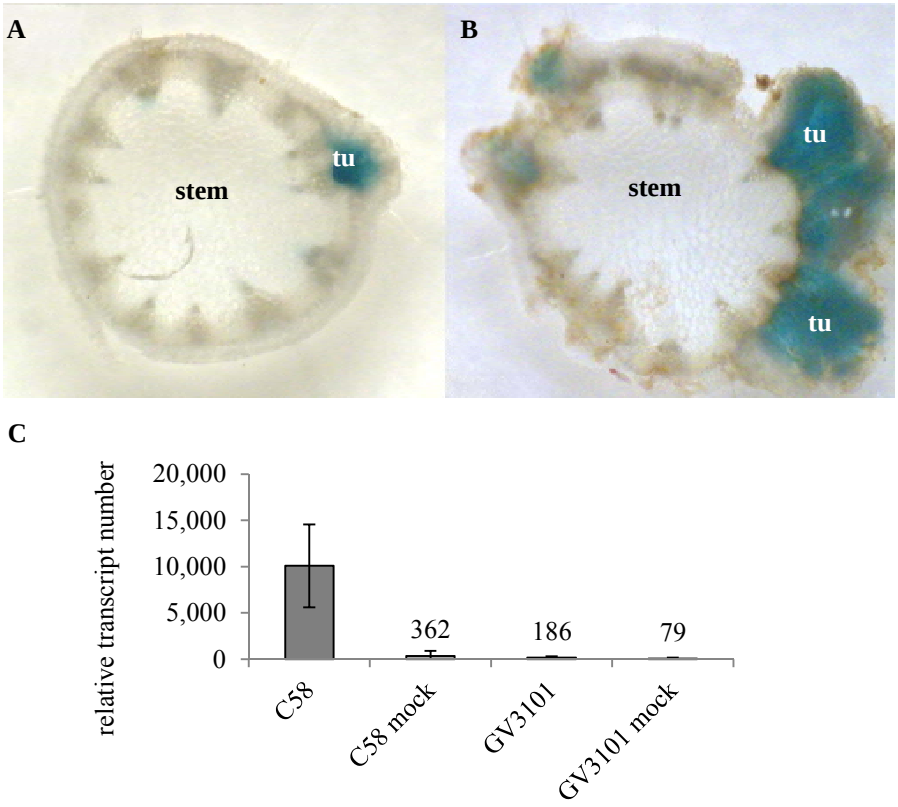

Figure 9 Spatiotemporal expression of the *SAD6* gene in the crown gall and transcriptional regulation of *SAD6* by oncogenic and non-oncogenic *Agrobacterium* strains as well.
Histochemical GUS assay, indicated by the blue color in *Arabidopsis* cross sections of **(A)** a just emerging tumor (tu) six d after inoculation (dai) of *A. tumefaciens* strain C58, and **(B)** a mature tumor (tu) 21 dai. Three independent transgenic GUS-expressing lines of the T3 generation were analyzed and showed the same staining pattern. **(C)** Transcript numbers of *SAD6* in *Arabidopsis* inflorescence stalks six d after inoculation of the oncogenic *Agrobacterium* strain C58 and the non-oncogenic strain GV3101. Inflorescence stalks treated with the respective cultivation medium for agrobacteria served as control. Bars and numbers represent mean values (±SD) of 3-4 independent experiments. Relative *SAD6* transcript numbers were determined by applying quantitative real time RT-PCR and normalized to 10,000 *ACT2/8*-molecules.

Other than the tumor, the *SAD6* gene has a very low activity throughout the plant, in contrast to the ortholog *SSI2* gene. The latter is ubiquitously expressed in *Arabidopsis* and the major contributor of 18:1 FA in *Arabidopsis* leaf tissue (Kachroo et al., 2001, 2007). Histochemical *Arabidopsis* plants expressing GUS under control of *SAD6*-promoter (2.8.2, 2.8.4, 8.2.1, 8.2.3, supplemental table 3, and 8.2.4, supplemental figure 7) demonstrated *SAD6*-promoter

activity in root tips of germinating seeds and seedlings, in stipules, but not in flowers, siliques and leaf tissue (figures 10A to 10G; 2.10), which was confirmed by quantitative realtime RT-PCR. According to quantitative real time RT-PCR (2.6.9, 8.2.1 and 8.2.3, supplemental table 2) the transcript numbers were between 8 and 325 relative to 10,000 actin transcripts in the leaf, root, flower and inflorescence stalk, whereas 49,634±32,132 transcripts were measured in the tumor (figure 10H).

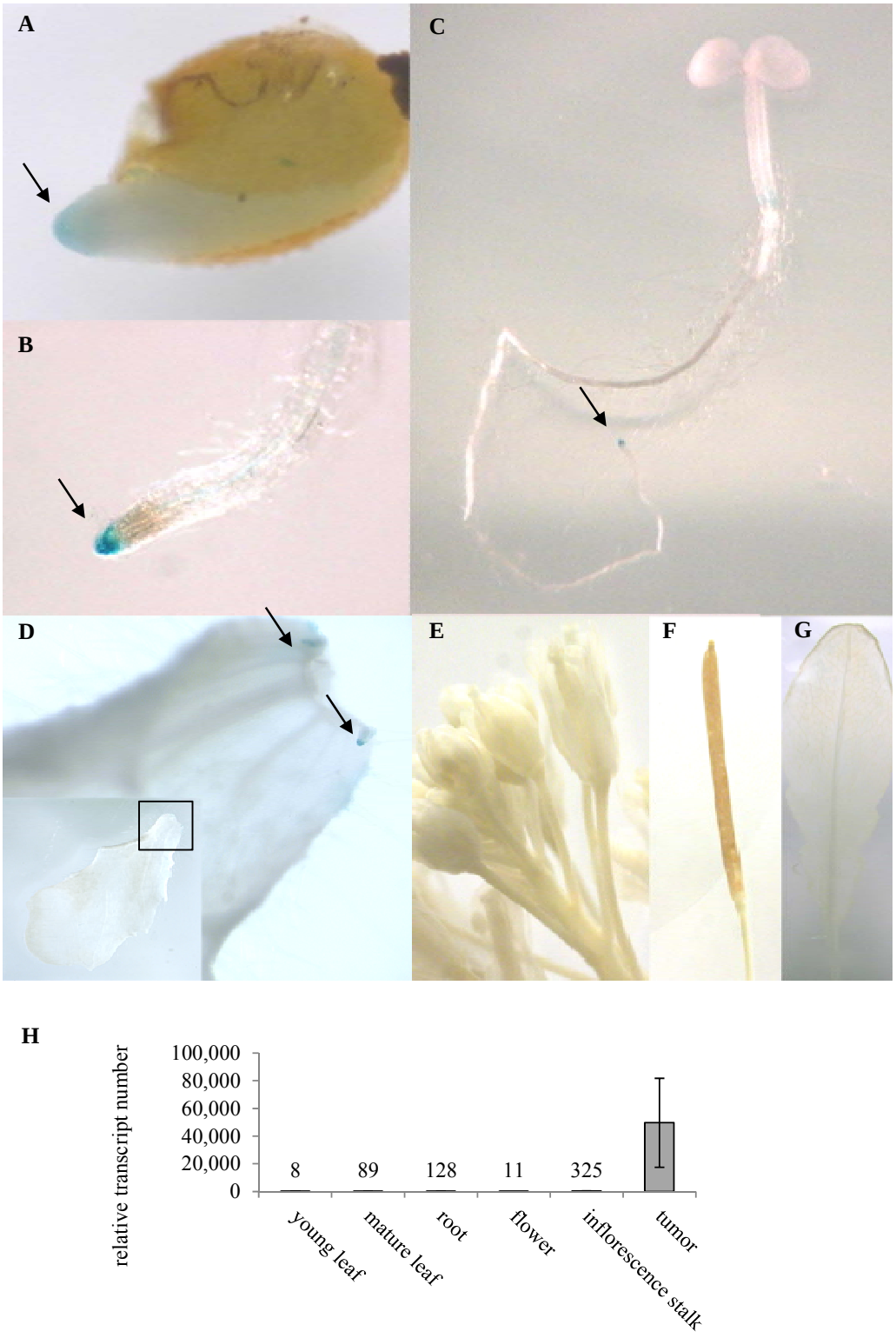

Figure 10. Expression pattern of the *SAD6* gene in *Arabidopsis*

(A-G) Histochemical GUS assay indicated by the blue color: **(A)** root apex of germinating seedling, **(B)** root tip and stele (very weak), **(C)** the developing zone of the hypocotyl of 7 d old seedling **(D)** stipules at the leaf base of 6 week old *Arabidopsis* plant shown in a close up (arrows), no GUS activity was detectable in **(E)** flowers, **(F)** siliques, and **(G)** leaves. Three independent transgenic GUS-expressing lines of the T3 generation were analyzed. **(H)** *SAD6* transcription in different *Arabidopsis* plant organs and in the crown gall. Bars and numbers represent mean values (±SD) of 3-4 independent experiments. Relative *SAD6* transcript numbers were determined by applying quantitative real time RT-PCR and normalized to 10,000 *ACT2/8*-molecules.

3.5 The *SAD6* gene is strongly induced by hypoxia

The tumor-, but not agrobacteria-dependent strong expression of the *SAD6* gene suggested that a plant-specific factor in the tumor, acts as regulator for the *SAD6* gene (3.4). According to the motif database PLACE (http://www.dna.affrc.go.jp/PLACE/index.html) the promoter of the *SAD6* gene contained seven cis-acting regulatory DNA elements which suggests an involvement of hypoxia in gene regulation (figure 11). Earlier studies have shown that *Arabidopsis* crown gall tumors not only suffer from drought stress, but are also deprived of oxygen (Deeken et al., 2006).

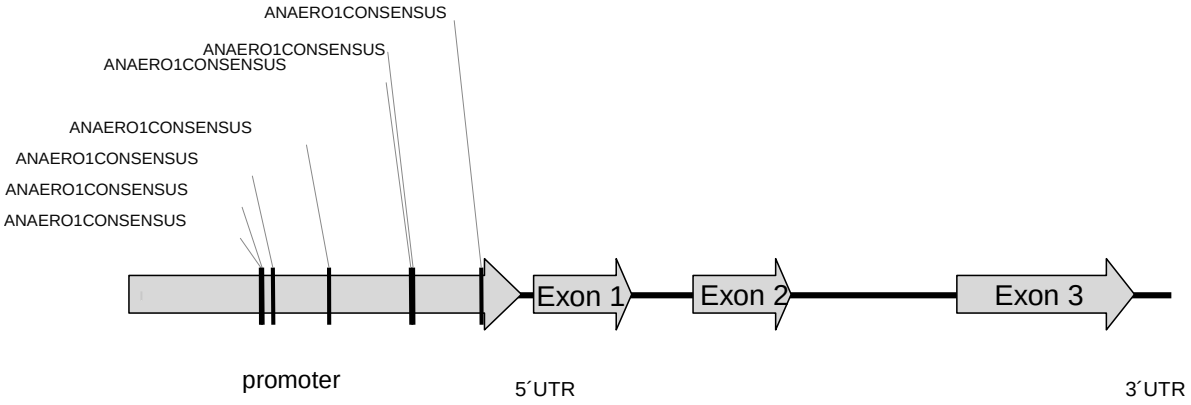

Figure 11. Positions of the hypoxia related ANAERO1CONSENSUS- cis-acting regulatory DNA elements in the promoter region of *SAD6* (At1g43800) locus according to the motif database PLACE (http://www.dna.affrc.go.jp/PLACE/index.html).

When *Arabidopsis* was exposed to hypoxic conditions with air, containing only 0.5% oxygen for 24 h (2.4.2) a more than 500-fold increase in *SAD6* transcription was determined (2.6.9, 8.2.1 and 8.2.3, supplemental table 2) in roots (from 23±15 to 12,977±4,205 relative transcripts) and even 2,500-fold in shoots (from 5±7 to 13,424±2,169 relative transcripts; figure 12A). These results were confirmed by histochemical GUS staining experiments (2.10) with at least three transgenic $SAD6_{PRO}$*:GUS* reporter lines (figures 12C to 12F). Under hypoxic conditions strong GUS-staining was observed in roots and leaves (figures 12C and 12E) which was absent under normoxia (figures 12D and 12F). Furthermore, 24 h of water logging treatment (2.4.2), a natural condition that causes hypoxia, also induced *SAD6* transcription in roots (355±301 to 34,846±5,727 transcripts; figure 12B). In soil with normal water content *SAD6* transcripts were not elevated in roots and shoots (figure 12B). Thus, up-regulation of the *SAD6* gene in the crown gall (3.4) seems to be mediated by hypoxia, which is known to accompany tumor development (Deeken et al., 2006).

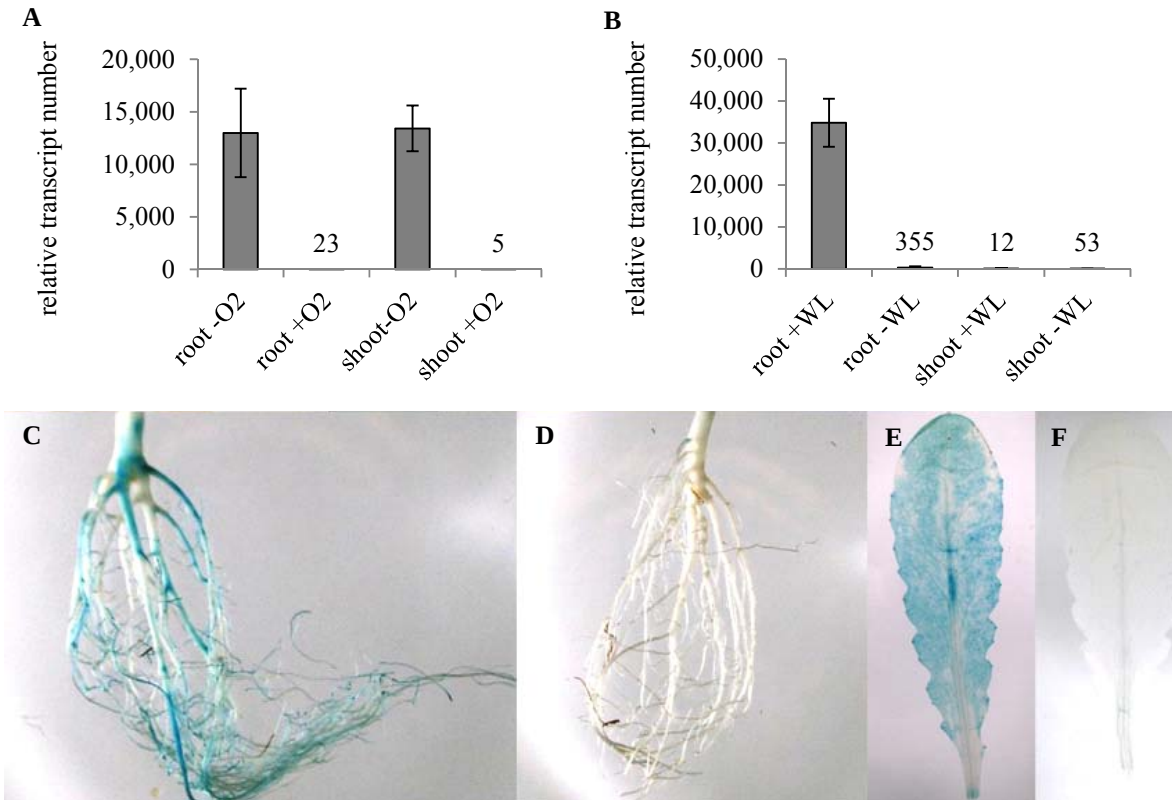

Figure 12. Regulation of the *SAD6* gene expression in *Arabidopsis* by hypoxia
(A) Relative transcript numbers of the *SAD6* gene in root and shoot of *Arabidopsis* plants (genotype: Wassiljewskija) after 24 h of hypoxia (0.5% oxygen, -O2) in comparison to ambient oxygen conditions (+O2) and **(B)** after 24 h of waterlogging treatment of the roots (+WL) in comparison to non-treated plants (-WL). Bars and numbers represent mean values (±SD) of 3-4 independent experiments. Relative *SAD6* transcript numbers were determined by applying quantitative real time RT-PCR and normalized to 10,000 *ACT2/8*-molecules. **(C)** Ubiquitous GUS activity of transgenic $SAD6_{PRO}$*:GUS* plants in the root and **(D)** leaf of plants exposed to hypoxia (0.5% oxygen) for 24 h. No GUS activity was visible in **(D)** roots and **(F)** the leaf under ambient oxygen conditions. Three independent transgenic GUS-expressing lines of the T3 generation were analyzed.

3.6 *SAD6* is able to complement the dwarf-growth phenotype of the *ssi2-2* mutant

SAD6 is according to sequence homology a member of the *S-ACP-Desaturase* (*SAD*) gene family (figure 7B). However, the function of SAD6 catalyzing the first step of FA desaturation and forming mono unsaturated FAs (MUFAs) is thus far unproven. The function as SAD requires the localization of the protein in the chloroplast. Predictions of the subcellular localization by WoLF PSORT (http://wolfpsort.org/) and MultiLoc2 (http://abi.inf.uni-tuebingen.de/Services/MultiLoc2/index.html/) suggested a localization of the SAD6 protein in chloroplasts. In order to verify the subcellular localization of SAD6, a V5/HIS6 epitope-tagged SAD6 protein (49,248 kDa) was transiently overexpressed in tobacco leaves (2.4.4, 2.8.3, 2.8.5, 8.2.1, 8.2.3, supplemental table 3, and 8.2.4, supplemental figures 8 and 9). The chloroplasts from leaves were enriched and the intact chloroplasts were purified with a percoll gradient (2.9.1). The intactness of the chloroplasts was inspected by

phase contrast microscopy. Proteins were extracted from the chloroplast fraction and total leaf tissue (2.9.1). Western blot studies with a V5 specific antibody (2.9.4) revealed an accumulation of the chemiluminescence signal in the chloroplast-specific protein fraction in comparison to the crude extract of total leaf tissue and confirmed the localization of the SAD6 protein in chloroplasts (figures 13A and 13B).

According to the phylogenetic tree the well characterized SSI2 is the nearest neighbor of SAD6 (figure 7B). The function of SSI2 as 18:0 desaturating enzyme has been demonstrated (Kachroo et al., 2001). In order to elucidate the function of the putative desaturase SAD6, complementation studies with a mutant for the *SSI2* gene locus were performed. Therefore a homozygous T-DNA insertion line was selected, harboring an insertion in the intron region of *SSI2* (Salk039862; 2.3.3, 8.1, supplemental figure 3, and 8.2.3, supplemental table 1). Loss of function mutants for the *SSI2* gene locus (*ssi2* and *fab2*) are known to show a dwarf growth phenotype (Kachroo et al., 2001; figure 13C, ssi2-2). The stable transformation of these mutant plants with the *SAD6* coding region under control 35S promoter (2.8.3, 2.8.5, 8.2.1, 8.2.3, supplemental table 3, and 8.2.4, supplemental figure 10) resulted in three independent transformant lines with a WT like phenotype (figure 13C, *ssi2-2-35S$_{PRO}$:SAD6*). These lines expressed *SAD6* transcripts (line #17: 173,765; #21: 52,776; and #22: 53,732 transcripts per 10,000 *ACT2/8*-molecules; 2.6.9, 8.2.1 and 8.2.3, supplemental table 2). Thus, *SAD6* complements the *ssi2-2* dwarf growth phenotype. This result, together with the localization of SAD6 in the chloroplast, strongly suggests that SAD6 is a functional S-ACP-Desaturase like SSI2.

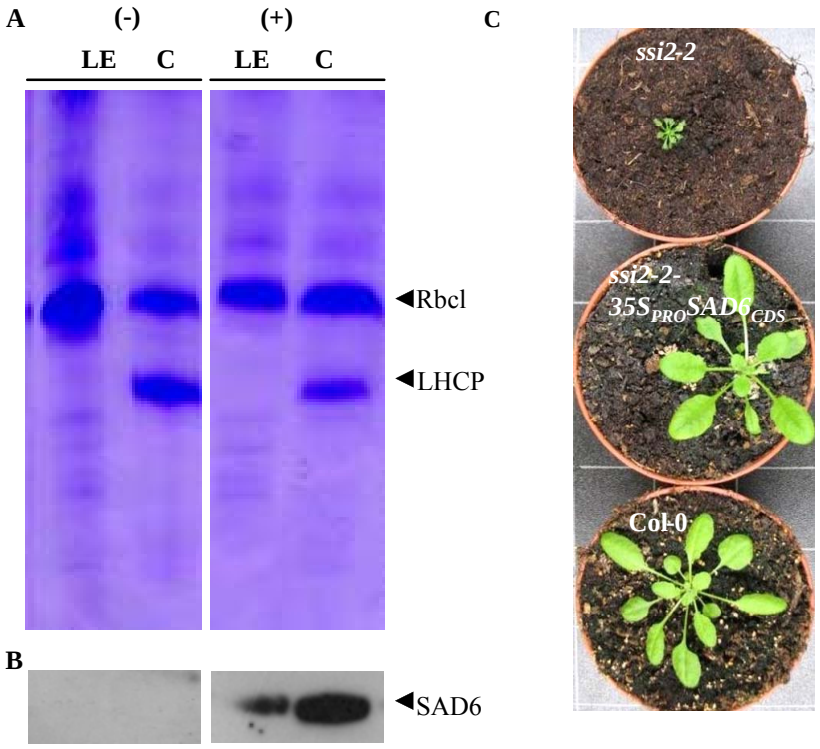

Figure 13. The SAD6 protein is located in chloroplasts and funtionally complements the dwarf growth phenotype of the *ssi2-2* mutant allele.

(A) Coomassie blue stained SDS-PAGE with 10 µg protein of crude leaf extracts (LE) and the chloroplast fraction purified in a percoll gradient of non-transformed (-) and transiently transformed *N. benthamiana* leaves using the $35S_{PRO}$:$SAD6_{CDS}$:*V5:HIS6* construct (+). Arrow heads indicate the position of Ribulose bisphosphate carboxylase large subunit (Rbcl) and light-harvesting chlorophyll a/b-binding protein (LHCP). Note, the latter accumulated only in the purified chloroplast fraction. **(B)** Western blot of non-transformed (-) and transiently transformed (+) N. *benthamiana* leaves using an V5-specific monoclonal antibody for detection of the V5/His6-tagged SAD6 protein. Arrow head indicates the position of the V5/HIS6-tagged SAD6 protein. **(C)** Growth phenotypes of an eight weeks old *A. thaliana* wildtype plant Col-0, of a ssi2-2 plant transformed with $35S_{PRO}$:$SAD6_{CDS}$ construct (*ssi2-2-*$35S_{PRO}$:$SAD6_{CDS}$), and of the salk039682 line with a T-DNA-insertion in the *SSI2* locus. Plants were cultivated under long d conditions (16 h/8 h). One representative independent *ssi2-2-*$35S_{PRO}$:$SAD6_{CDS}$ transformant line out of three is shown. Transgenic plants were characterized by S. Lamberts, University of Würzburg.

3.7 Overexpression of the *SAD6* gene causes a light-dependent chlorosis phenotype

In order to study the impact of SAD6 on the lipid pattern in *Arabidopsis* crown galls *Arabidopsis* lines with a T-DNA insertion in the coding sequence of the *SAD6* gene were not available at any of the stock centers. A homozygous insertion line with a T-DNA insertion located in the *SAD6* promoter region (salk70018; 2.3.3, 8.1, supplemental figure 2, and 8.2.3, supplemental table 1), resulted in a 38-fold reduced *SAD6* transcription under hypoxia in contrast to a strong induction of the gene in the wildtype Col-0 (473±179 to 18,167±12,331 transcripts per 10,000 *ACT2/8*-molecules; 2.6.9, 8.2.1 and 8.2.3, supplemental table 2). However, significant effects on tumor growth and lipid pattern were not observed (data not

shown), most likely due to the remaining *SAD6* gene activity or compensation by close homologs.

The *SAD6* gene is barely transcribed in *Arabidopsis* (figures 10A to 10H) in contrast to its well characterized ortholog *SSI2*. Therefore a homozygous T-DNA activation tagging line (GK30d04; 2.3.3, 8.1, supplemental figure 1, and 8.2.3, supplemental table 1) was selected to study the impact of *SAD6* on the lipid pattern in *Arabidopsis*. The relative transcript number in leaves of *SAD6* overexpressing plants (SAD6-OE) was 49,634±6,781 (figure 14). This very high transcript number was similar to that found in tumors (54,438±32,132).

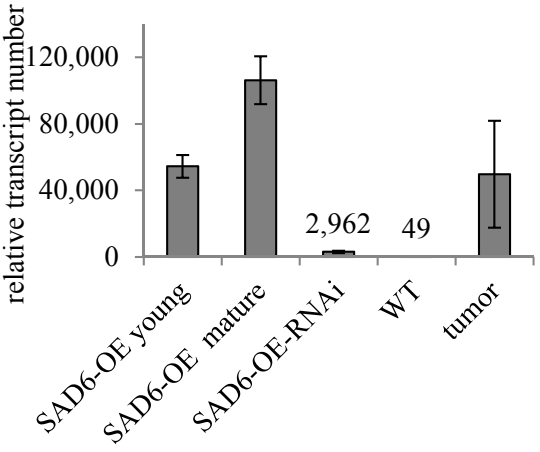

Figure 14. Comparison of *SAD6* gene expression in *Arabidopsis* mutants SAD6-OE and SAD6-OE-RNAi. the crown gall and the wild type.
Relative transcript numbers in young leaves of *SAD6*-overexpressing plants (SAD6-OE), Columbia-0 (WT) and SAD-OE plants, in which *SAD6* transcripts were posttranscriptional silenced by RNAi (SAD6-OE-RNAi), and the tumor. Bars and numbers represent mean values (±SD) of 3-4 independent experiments. Relative *SAD6* transcript numbers were determined by applying quantitative real time RT-PCR and normalized to 10,000 *ACT2/8*-molecules.

When SAD6-OE plants were cultivated under standard conditions with eight h of light (120 µmol·m^{-2}·s^{-2}; 2.3.1), young leaves developed chlorosis symptoms and growth of the plants was slightly retarded in comparison to the WT (figures 15A to 15F). Cotyledons, however, did not develop chlorosis (figure 15B). The reproductive organs of SAD6-OE were also WT-like (figures 15G and 15H). Chlorotic leaves showed a wrinkled appearance along the edges of the leaf blade (figure 15I). Severity of chlorosis gradually decreased with leaf age, letting leaves of the outer whorl appear green, similar to those in WT plants. This observation did not correlate with the relative transcript number of *SAD6* that was two-fold higher in mature leaf tissue (106,291±14,377 relative *SAD6* transcripts) in comparison with young leaf tissue (49,634±6,781).

In order to confirm that the chlorotic phenotype of the T-DNA insertion line SAD6-OE was caused by overexpression of *SAD6* and not by secondary T-DNA insertion, *SAD6* gene expression was reduced by stable RNAi-mediated suppression in the SAD6-OE background (2.8.1, 2.8.5, 8.2.1, 8.2.3, supplemental table 4, and 8.2.4, supplemental figures 4 and 5). The RNAi-mediated 18-fold down-regulation from 49,634±6,781 to 2,962±819 relative *SAD6* transcripts in homozygous SAD-OE lines (figure 14) recovered the wildtype phenotype in

SAD6-OE (figure 15C). This finding showed that the observed chlorotic phenotype of SAD6-OE is due to the overexpression of *SAD6*.

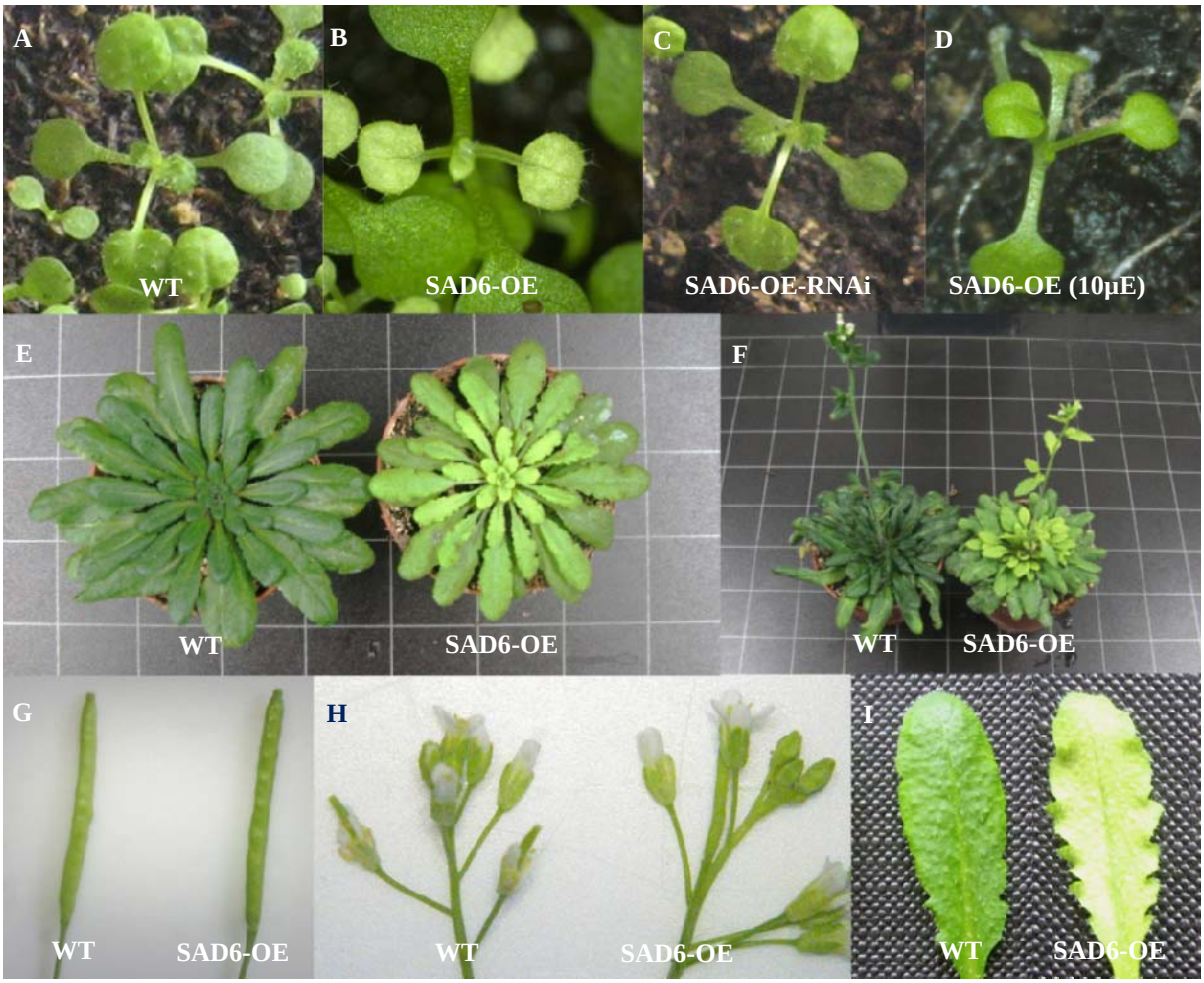

Figure 15. Phenotypes of *Arabidopsis* overexpressing the *SAD6* gene (SAD-OE) and a revertant of *SAD6* overexpressor (SAD6-OE-RNAi).
(A-I) *Arabidopsis* phenotypes of *SAD6* overexpressing (SAD6-OE) plants and plants with RNAi-mediated down-regulation of *SAD6* overexpression (SAD6-OE-RNAi). 14-d-old seedlings: **(A)** Col-0 (WT), **(B)** SAD6-OE with chlorotic first true leaves, **(C)** SAD6-OE-RNAi without chlorotic leaves, and **(D)** rescue of the SAD6-OE chlorotic phenotype under low light conditions of 10 µmol·m^{-2}·s^{-1} (µE). **(E)** Eight-week-old non flowering plants of SAD6-OE and Col-0 (WT) plants and **(F)** twelve-week-old flowering plant of SAD6-OE and Col-0 (WT). Note the chlorotic appearance of young growing leaves of adult SAD6-OE plants. **(G)** Siliques and **(H)** flowers of twelve-week-old SAD6-OE and Col-0 (WT) plants. **(I)** Inner leaves of eight-week-old Col-0 (WT) and SAD6-OE plants. If not otherwise indicated, all plants were cultivated with 120 µmol·m^{-2} ·s^{-1} of light.

The occurrence of chlorosis in young leaves was due to 4.5-fold reduced chlorophyll content in SAD6-OE plants (from 1,018±100 to 226±51 µg chlorophyll/g fresh weight; 2.12), whereas in mature leaves (from 53±102 to 662±102 µg chlorophyll/g fresh weight; figure 16A). The number of chloroplasts calculated counted in mesophyll protoplasts of five weeks old plants was, however, not significantly altered between both plant types (figure 16B; 2.11). Photosynthesis of chlorotic SAD6-OE leaves was compared with that of green Col-0 leaves

by measuring chlorophyll fluorescence of photosystem II (PSII) with a pulse amplitude modulated fluorimeter (PAM; 2.13). The fluorescence parameters of photochemical quenching (q_P) and non-photochemical quenching (q_N) of photosystem II (PSII) were calculated for five different actinic light intensities. At all light intensities q_P was lower in chlorotic leaves of SAD6-OE compared to green leaves of Col-0 plants and non-photochemical (q_N) quenching was increased (figure 16C). In chlorotic leaves a lower proportion of PSII reaction centers were open and a larger proportion of photochemical energy dissipated as heat. Thus, the photochemistry but not biogenesis of chloroplasts was affected by overexpression of *SAD6*.

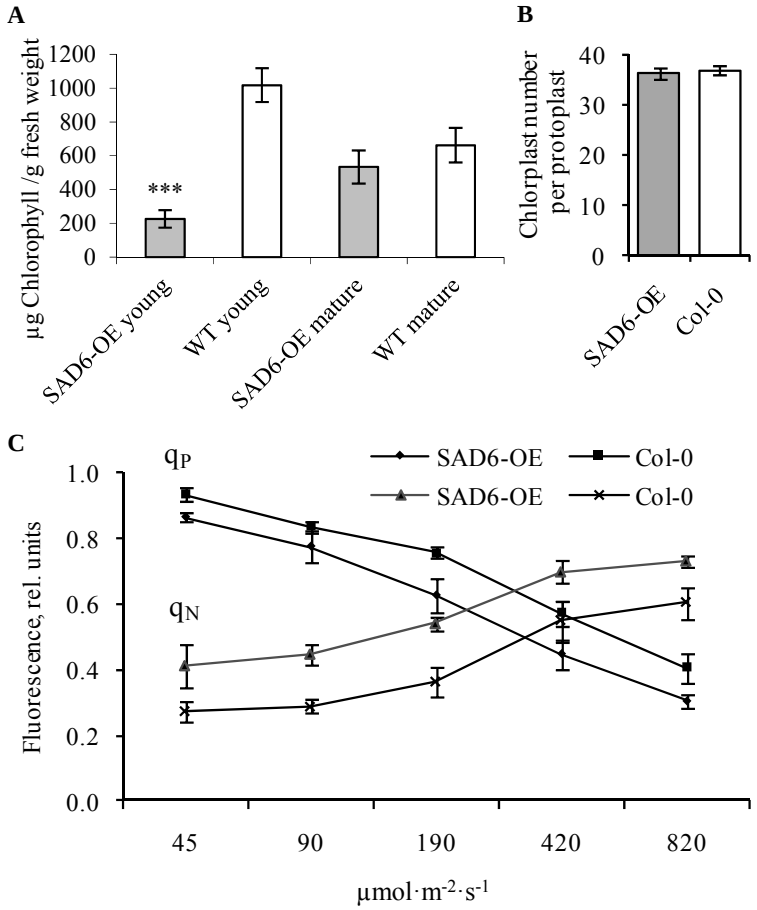

Figure 16. Characteristics of the chlorotic phenotype of *Arabidopsis*, overexpressing the *SAD6* gene (SAD6-OE).

(A) Total chlorophyll content of young chlorotic and mature leaves of SAD6-OE plants as well as young green and mature leaves of Col-0 plants (WT). Mean values (µg/g fresh weight±SD) of chlorophyll a and chlorophyll b of 3-4 independent experiments are shown. **(B)** Number of chloroplasts in mesophyll protoplasts from SAD6-OE leaves. Mean values +/-SE were calculated from three independent experiments with 20 protoplasts each. **(C)** Pulse amplitude modulated fluorimeter (PAM) measurements were conducted to compare the photochemical (qP) and non-photochemical quenching (qN) at different actinic light intensities in SAD6-OE and Col-0 plants. Statistical analysis was performed by using an unpaired two-tailed Student´s t-test (***, P-value≤0.001). Determination of chloroplast number and PAM measurements were carried out by S. Lamberts, University of Würzburg.

The development of chlorosis by SAD6-OE plants was light-dependent and did not occur under low light intensity of 10 $\mu mol \cdot m^{-2} \cdot s^{-1}$ (figure 15D). This pointed to a possibly enhanced photo-oxidative stress, which is a result of increased illumination of the photosystems in plants.

3.8 The lipid profile of SAD6-OE is similar to that of crown galls

Having learned that SAD6 protein is associated with S-ACP-Desaturase function (3.6), the influence of *SAD6* dose on the lipid profile was analyzed. Therefore, glycerolipid species of the polar glycerolipid classes MGDG, DGDG, PG, PC, PE and PI in chlorotic leaves of *SAD6*-overexpressing plants (SAD6-OE) and in wildtype leaves were determined (2.14.1, 2.14.2 and 8.3.2, supplemental tables 21 to 26).

The data revealed significant differences in the relative distribution of several lipid species except PG (figure 17). The relative levels of glycerolipid species, containing unsaturated FAs, such as DGDG-18:3-18:2, DGDG-18:3-18:3, PC-18:2-16:1 PC-18:1-18:1, PC-18:2-18:1, PC-18:3-18:2, PC-18:3-18:3, PE-16:2-16:0, PE-18:3-16:1, PE-18:2-16:3, PE-18:3-16:3, PE-18:3-18:2, PE-18:3-18:3, PI-18:3-18:1 were significantly (P-value≤0.05) higher in SAD6-OE compared to the reference. Exceptions to this are significantly (P-value≤0.05) lower relative levels of the glycerolipids MGDG-18:3-16:1, MGDG-18:3-16:2, DGDG-18:3-16:1 and PC-18:3-16:3 in SAD6-OE. The relative levels of glycerolipid species containing saturated FAs, such as DGDG-18:3-16:0, PC-18:2-16:0, PC-18:0-16:3, PC-18:1-18:0, PC-18:2-18:0, PC-18:3-18:0, PE-18:2-16:0, PE-18:3-16:0, PI-18:2-16:0, were significantly (P-value≤0.05) lower in SAD6-OE compared to the reference.

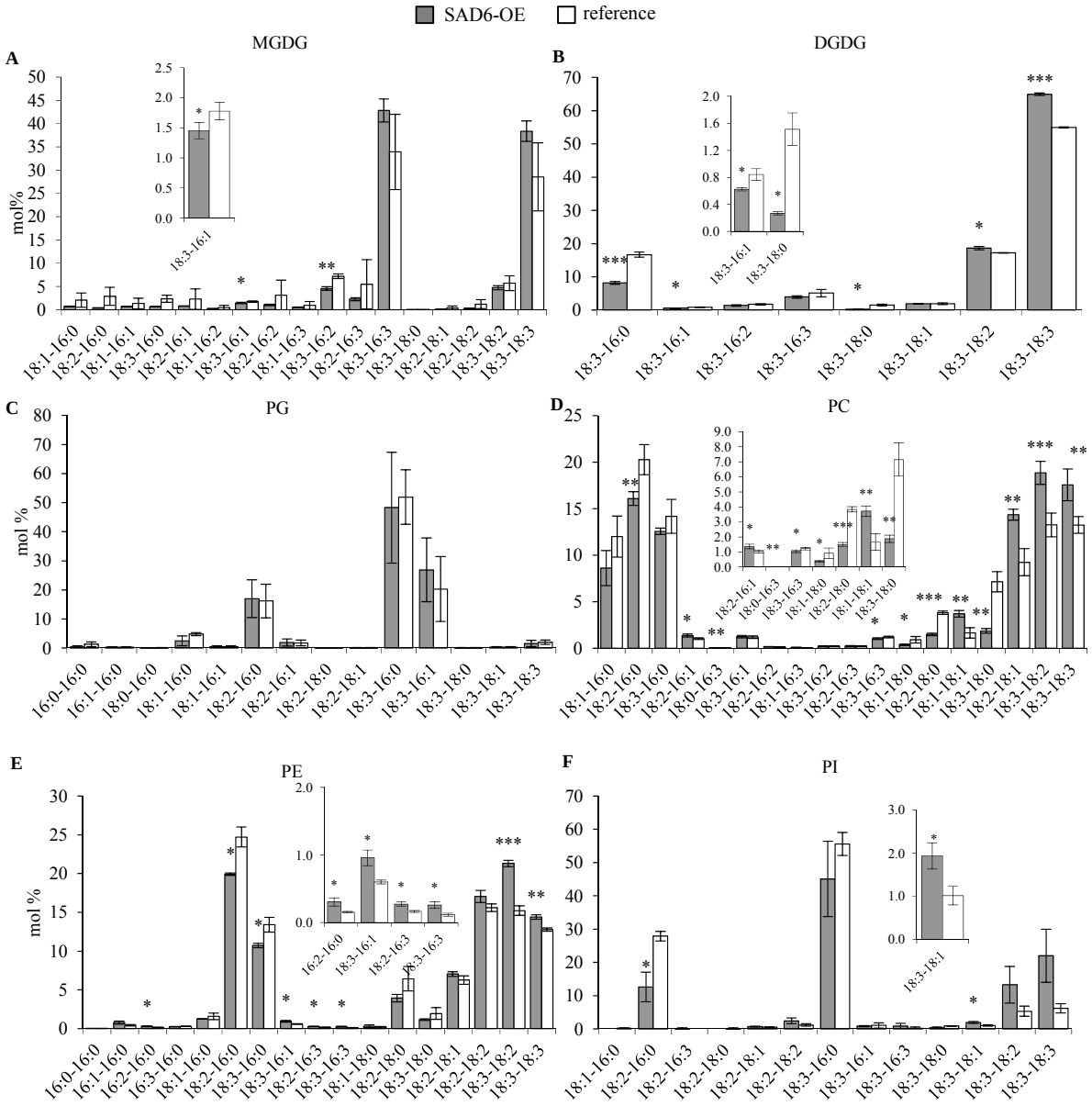

Figure 17. Relative distribution of the lipid species within the major glycerolipid classes in SAD6-OE.

(A) Lipid species of the polar lipid classes monogalactosyldiacylglycerol (MGDG), **(B)** digalactosyldiacylglycerol (DGDG), **(C)** phosphatidylglycerol (PG), **(D)** phosphatidylcholine (PC), **(E)** phosphatidylethanolamine (PE), and **(F)** phosphatidylinositol (PI) were determined by LC-MS/MS. Insets show an enlargement of the lipid species below 10 mol% with significant differences (P-value≤0.05) between SAD6-OE and reference tissue. Wildtype *Arabidopsis* (ecotype: Col-0) served as reference. Mean values (mol%±SD) were calculated from 3-4 independent experiments. Statistical analysis was performed by using an unpaired two-tailed Student´s t-test (*, P-value≤0.05; **, P-value ≤0.01; ***, P-value ≤0.001.

Leaves of SAD6-OE plants, in which *SAD6* overexpression was reverted by RNAi (SAD6-OE-RNAi) exhibited no significant difference in the lipid pattern in comparison to the reference (figure 18; 2.14.1, 2.14.2 and 8.3.3, supplemental tables 27 to 32), thus indicating that *SAD6* overexpression was responsible for the altered lipid species pattern in SAD6-OE.

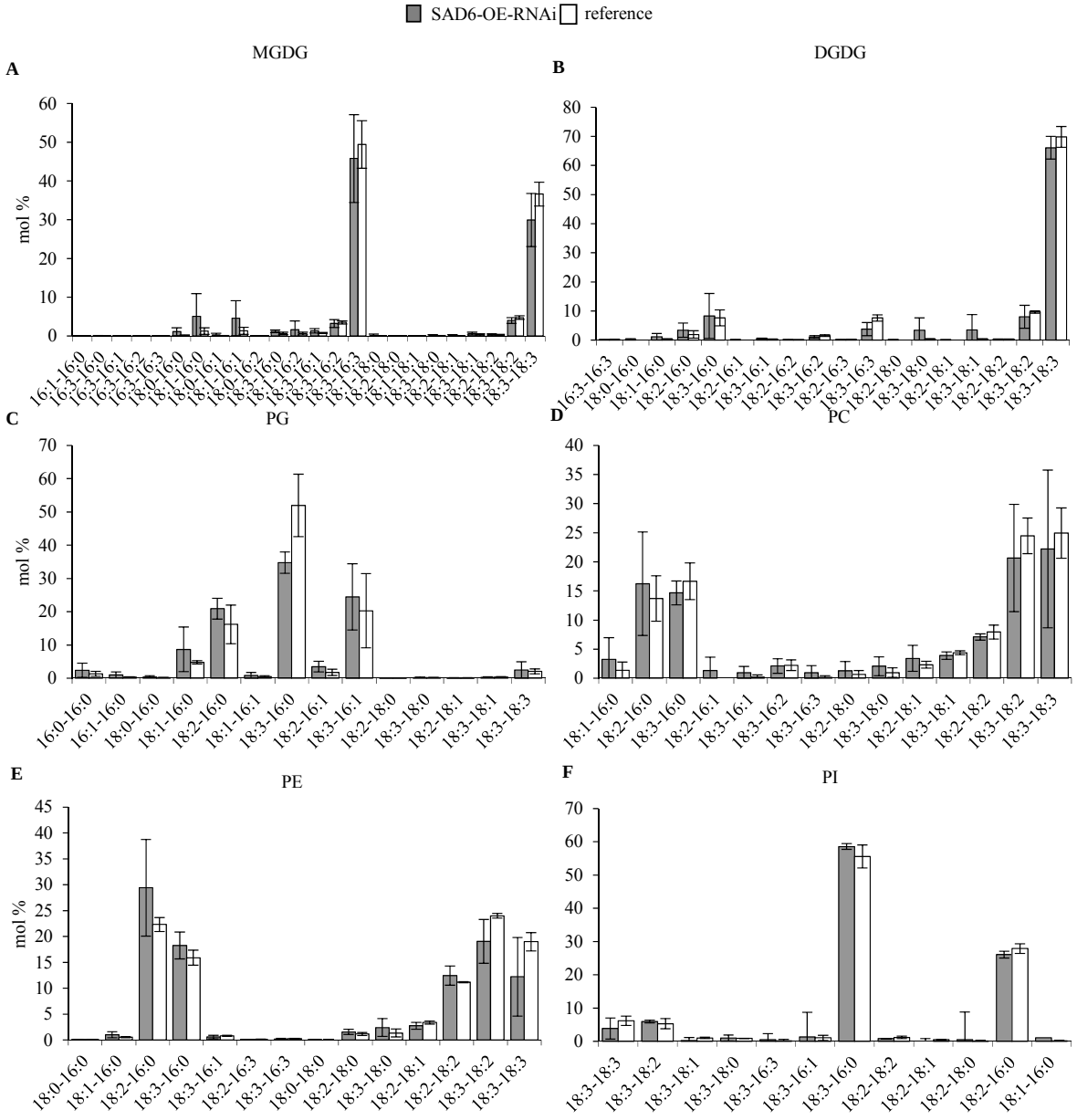

Figure 18. Relative distribution of the lipid species within the major glycerolipid classes in SAD6-OE-RNAi. **(A)** Lipid species of the polar lipid classes monogalactosyldiacylglycerol (MGDG), **(B)** digalactosyldiacylglycerol (DGDG), **(C)** phosphatidylglycerol (PG), **(D)** phosphatidylcholine (PC), **(E)** phosphatidylethanolamine (PE), and **(F)** phosphatidylinositol (PI) were determined by LC-MS/MS. Wildtype *Arabidopsis* (ecotype: Col-0) served as reference. Mean values (mol%±SD) were calculated from 3 independent experiments. Statistical analysis was performed by using an unpaired two-tailed Student´s t-test. MGDG, monogalactosyl diacylglycerol; DGDG, digalactosyl diacylglycerol; PC, phosphatidyl choline; PE, phosphatidyl ethanolamine; PG, phosphatidyl glycerol; PI, phosphatidyl inositol.

In order to access the nature of the differences in the lipid pattern of SAD6-OE and for comparison of the SAD6-OE lipid pattern with that of the tumor, the ratios of the relative FA contents within each glycerolipid class in SAD6-OE, SAD6-OE-RNAi and in the crown gall vs. the respective reference were calculated (2.14.3; tables 15 and 16A). Strikingly, in SAD6-OE the 18:0 FA which is part of the SAD substrate, was in all lipid classes, except MGDG, significantly reduced, thus indicating most likely elevated SAD activity in SAD6-OE. Furthermore, in SAD6-OE relative contents of unsaturated FAs, such as 18:1 FA, 18:2 FA and 18:3 FA, were significantly increased in DGDG, PC, PE and PI. An increase of 18:3 PUFA was also observed in all lipid classes of the crown gall except PG (table 15). In the revertant of the *SAD6* overexpressor, SAD6-OE-RNAi, the relative FA contents were not significantly altered (table 16B).

Table 16. Ratios of galactolipid and phospholipid fatty acids (FA).
(A) Young leaves of SAD6-OE vs. wildtype plants (ecotype Col-0), and **(B)** young leaves of SAD6-OE-RNAi vs. wildtype plants (ecotype Col-0). Ratios were calculated from the relative proportion of FAs (mol%) within each polar lipid class of galactolipids (MGDG, DGDG) and phospholipids (PG, PC, PE, PI) determined by LC-MS/MS. Not presented are 16:1, 16:2 and 16:3 FA of PC, PE and PI, and 16:2 and 16:3 of PG, which represented only minor fractions of each polar lipid class. Grey boxes with bold italic numbers highlight significantly (P-value≤0.05) lower FA ratios and with bold letters those with higher ratios. Statistical analysis was performed using an unpaired two-tailed Student´s t-test. MGDG, monogalactosyl diacylglycerol; DGDG, digalactosyldiacylglycerol; PC, phosphatidylcholine; PE, phosphatidylethanolamine; PG, phosphatidylglycerol; PI, phosphatidylinositol.

FA	**MGDG**		**DGDG**		**PG**		**PC**		**PE**		**PI**	
	Ratio	P-value	Ratio	P-value	Ratio	P-value	Ratio	P-value	Ratio	P-value	Ratio	P-value
(A) SAD6-OE vs. wildtype												
16:0	-3.93	0.07	***-2.03***	***0.001***	-1.10	0.544	***-1.25***	***0.000***	***-1.22***	***0.020***	-1.45	0.097
16:1	-1.85	0.34	***-1.35***	***0.039***	1.29	0.548						
16:2	-1.85	0.11	-1.24	0.092								
16:3	1.13	0.05	-1.28	0.217								
18:0	2.09	0.32	***-5.65***	***0.012***	-2.74	0.334	***-3.17***	***0.001***	-1.59	0.068	***-3.32***	***0.027***
18:1	-2.24	0.37	-1.00	1.000	-1.65	0.217	1.21	0.133	1.07	0.455	**1.60**	**0.041**
18:2	-2.22	0.25	**1.08**	**0.034**	1.05	0.867	**1.09**	**0.001**	1.03	0.054	-1.15	0.109
18:3	1.21	0.26	**1.06**	**0.000**	1.03	0.787	1.11	0.054	**1.11**	**0.002**	**1.39**	**0.043**
(B) SAD6-OE-RNAi vs. wildtype												
16:0	4.03	0.24	1.32	0.67	-1.08	0.63	1.08	0.81	1.26	0.28	1.03	0.41
16:1	2.97	0.28	1.82	0.12	1.30	0.50						
16:2	1.25	0.40	-1.41	0.24								
16:3	-1.08	0.65	-2.00	0.09								
18:0	5.39	0.23	9.80	0.31	2.51	0.44	2.04	0.47	1.59	0.30	1.48	0.67
18:1	3.28	0.36	7.93	0.30	1.69	0.44	1.31	0.52	-1.04	0.72	-1.24	0.73
18:2	1.42	0.46	1.01	0.96	1.36	0.15	1.00	1.00	1.06	0.16	-1.06	0.66
18:3	-1.18	0.18	-1.04	0.31	-1.19	0.25	-1.10	0.67	-1.24	0.25	-1.01	0.88

In SAD6-OE, the desaturation index which gives the average number of double bonds per FA was increased in all lipid classes (MGDG, 8.53%, P-value: 0.2; DGDG, 5.47%, P-value: 0.001; PG, 4.13%, P-value: 0.42; PC, 11.25%; P-value: 0.003; PE, 7.53%, P-value: 0.001; PI, 6.9%, P-value: 0.074; 2.14.3). This was similar to the desaturation index in the tumor, but was not observed in SAD6-OE-RNAi plants (figure 19A).

Quantification of the size of the different lipid pools using internal lipid standards (2.14.3) revealed that the amount of the ER-specific phospholipid pool was increased in SAD6-OE leaves (PC, 1.32-fold, P-value: 0.072; PE, 1.25-fold, P-value: 0.18, PI, 1.3-fold, P-value: 0.42;

figure 19B) whereas the plastid-derived galactolipid pools were significantly reduced (MGDG, -1.82 fold, P-value: 0.013; DGDG, -2.46 fold, P-value: 0.016; figure 19B). This lipid pattern was similar to that found in the *SAD6* overexpressing tumor, but was not observed in leaves of SAD6-OE-RNAi plants.

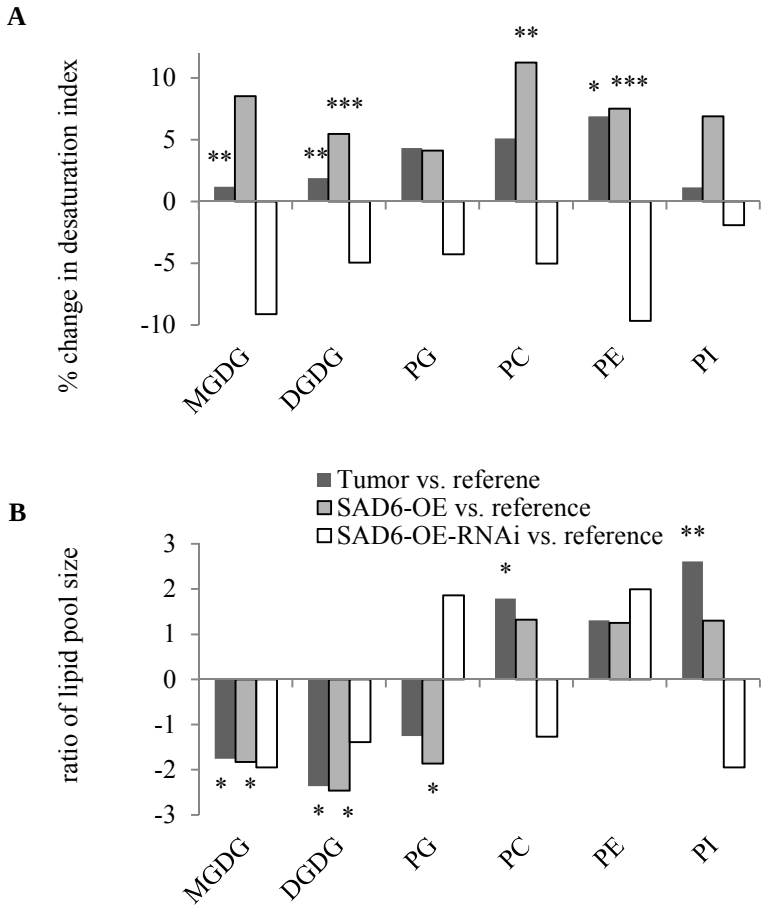

Figure 19. Ratios of the total amounts of galacto- and phospholipids and the change in desaturation indexes of fatty acids (FA) as well.

(A) The relative (%) change in desaturation indexes of C16 and C18 fatty acids of the polar glycerolipid classes MDGD, DGDG, PG, PC, PE, and PI in crown gall tumors vs. mock inoculated reference, SAD6-OE and SAD6-OE-RNAi vs. the wildtype Col-0 of *Arabidopsis*. The desaturation index gives the average number of double bonds per fatty acid in a lipid pool and was calculated according the relative lipid profiling by LC-MS/MS of the respective galacto- and phospholipid class of three to four independent experiments. **(B)** Ratios of the total amount of each of the polar lipid classes monogalactosyldiacylglycerol (MDGD), digalactosyldiacylglycerol (DGDG), phosphatidylglycerol (PG), phosphatidylholine (PC), phosphatidylethanolamine (PE), and phosphatidylinositol (PI) in crown gall tumors vs. mock inoculated reference, SAD6-OE and SAD6-OE-RNAi vs. the wildtype Col-0 of *Arabidopsis*. The ratios were calculated from the absolute amounts of each lipid species according LC-MS/MS lipid profiling of the respective galacto- and phospholipid class of 3-4 independent experiments. Statistical analysis was performed using an unpaired two-tailed Student´s t-test (*, P-value≤0.05; **, P-value≤0.01; ***, P-value≤0.001.

Since substantially amounts of unsaturated MGDGs can be converted into oxylipins the content of arabidopsides, a class of *Arabidopsis* oxylipins (Mosblech et al., 2009), was determined (figure 20; 2.14 and 8.3.2, supplemental table 20). In SAD6-OE leaves, exposed to 120 µmol·m^{-2}·s^{-2} of light for 8h (standard condition), the arabidopsides A to G, but not E appeared 3 to 6-fold increased. Thus, the elevated Arabidopside levels indicated that conversion of MGDGs into oxylipins could result in the observed lowered amounts of MGDG in SAD6-OE. However in the crown gall tumor levels of Arabidopsides were not altered (data not shown).

In summary, the elevation of unsaturated lipids and a rise in ER-derived phospholipids in SAD6-OE plants reflected the situation in the tumor that produces a high *SAD6* dose, whereas the lipid pattern in SAD6-OE-RNAi transgenics was wildtype-like.

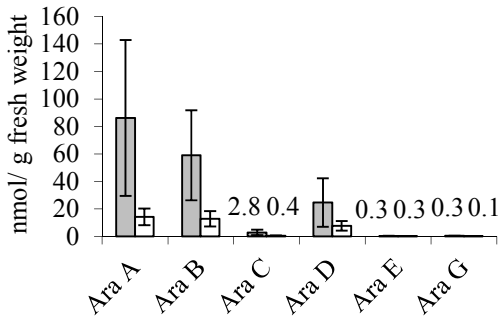

Figure 20. Oxylipin class of Arabidopsides in SAD6-OE.
Amount of the oxidized membrane lipid species arabidopsides in young chlorotic leaves of SAD6-OE plants and young leaves of wildtype Col-0. Mean values (nmol/g fresh weight±SD) were calculated from 3-4 independent experiments of each arabididopside type: Ara A, Ara B, Ara C, Ara D, Ara E, and Ara G. For statistical analysis an unpaired two-tailed Student´s t-test was performed (***, P-value≤0.001).

4. Discussion

Molecular processes underlying host cell transformation and cellular reprogramming mediated by *Agrobacterium tumefaciens* was studied extensively (Tzfira and Citovsky, 2006). In contrast to that the knowledge about metabolical changes during crown gall development is limited and most studies were focused on phytohormone-related processes (Aloni and Ulrich, 2008). In a comprehensive study, Deeken and coworkers (2006) elucidated that *Arabidopsis* crown gall development is accompanied by a transition of the metabolism from autotrophy to heterotrophy. Furthermore, it was demonstrated that tumor development requires adaptions in order to cope with abiotic stress factors, such as hypoxia (Deeken et al., 2006), oxidative (Lee et al., 2009) and drought stress (Efetova et al., 2007). Lipids, predominantly unsaturated fatty acids are extraordinarily sensitive to these stress factors (Upchurch, 2008). Therefore, adaption of the lipid metabolism seems to be required in crown gall development. From animal and human tumors major alterations in lipid biosynthesis and desaturation are well known and confer proliferative advantages and thus survival of the cancer cell in its microenvironment formed by oxidative stress and hypoxia (Hsu and Sabatini, 2008; Fritz and Fajas, 2010).

4.1 The novel S-ACP-desaturase SAD6 and FAD3 shape the lipid profile of *Arabidopsis* tumors

The lipid profiling of *Arabidopsis* crown galls revealed a significant change in the composition of FA and glycerolipid species in comparison with the reference (3.1). The ER-derived phospholipid pools, PC, PE, and PI were elevated, whereas those of the plastidic lipids, MGDG, DGDG, and PG were decreased (figure 6A). The shift from plastidic to ER-derived phospholipids was accompanied with an increase in 18:3 PUFAs (figures 4, 5A to 5F and table 15). The tumor lipid pattern exhibits a strong similarity to that of other heterotrophic tissues with no or reduced photosynthesis, such as roots, callus, and young growing tissues. In chlorotic tissues the eukaryotic phospholipid biosynthesis pathway of the ER is known to be the major pathway resulting in an increase in unsaturated phospholipids. Young developing pale green leaves of *Zea mays* or *Citrus sinensis* or non-green callus tissues *of Datura innoxia* exhibit elevated levels of ER-derived phospholipids (Freeman et al., 1978; Leech et al., 1973; Manoharan et al., 1987). Furthermore callus of *Brassica napus* and galls on *Quercus palustris* or *Solidago altissima* show an overall increased degree of phospholipid desaturation (Bayer, 1991; Zur et al., 2002; Tooker et al., 2009). In plant tumors the number of chloroplasts is considerably decreased during development and the remaining ones exhibit modified and

reduced thylacoid ultrastructures (Gee et al., 1967). For *Arabidopsis* tumors it was shown that photosynthesis is reduced which contributes to the development of hypoxic conditions and results in the heterotrophic and anaerobic metabolism (Deeken et al., 2006). The alteration in chloroplasts is reflected by the lower plastidic lipid pools (figure 6A). Thus, the observation that unsaturated FAs from phospholipids dominate the lipid pool of growing and heterotrophic tissues is consistent with our findings in *Arabidopsis* tumors.

The elevated degree of unsaturated FAs observed in crown gall tumors (figure 6B) requires an increased activity of desaturase enzyme function. The high levels of the 18:3 PUFAs, predominantly of the ER derived phospholipids PC, PE and PI correlated with the strong induction of the *FAD3* gene in tumors (3.2, figure 7C). *FAD3* encodes a membrane bound fatty acid desaturase enzyme which is the only desaturase in *Arabidopsis* synthesizing 18:3 PUFAs in the ER (Browse et al., 1993; Li-Beisson et al., 2010). It is known that *FAD3* transcript numbers and the levels of ER-derived 18:3 PUFAs are positively correlated, like it was observed in the crown gall (Kang et al., 1996; Collados et al., 2006). Above all, the *fad3-2* mutant, which has reduced levels of ER-derived 18:3 PUFAs, developed significantly smaller tumors compared to the respective wildtype (3.3, figure 8A). This observation strongly suggested that FAD3 is responsible for the production of ER-derived phospholipid 18:3 PUFAs in *Arabidopsis* tumors. In contrast, *FAD7* and *FAD8*, involved in biosynthesis of plastidic 18:3 PUFAs were down-regulated in *Arabidopsis* tumors and did not alter their development did not play a role in tumor development (3.3, figure 8A). Thus, *FAD3*, rather than the plastic-localized desaturases, *FAD7* and *FAD8*, is contributing to the 18:3 PUFA pools in crown galls.

In addition to *FAD3*, *SAD6*, with homology to S-ACP-desaturases (SADs), was strongly expressed in *Arabidopsis* tumors (3.2, figure 7A). Among the seven members of the *SAD* gene family the function of the *SAD6* gene is not known. Expression of the *SAD6* gene is almost undetectable in *Arabidopsis* under normal growth conditions, but strongly activated upon hypoxia (3.5, figure 12A; Loreti et al., 2005; Kachroo et al., 2007; Mustroph et al., 2009). Since the tumor is hypoxic this stress condition most likely induces SAD6 transcription there.

Constitutive expression of *35S:SAD6$_{PRO}$* reverted the extreme dwarf phenotype of the loss of *SSI2/FAB2* function in the T-DNA insertion line, *ssi2-2* (3.6, figure 13C). In addition, SAD6 was localized in chloroplasts like it is known for SSI2/FAB2 (Peltier et al., 2006; Olinares et al., 2010). A further indication that SAD6 functions as SAD came from *SAD6* overexpressing plants (SAD6-OE). In these plants the content of the saturated FAs 16:0 and 18:0, substrates for SAD enzymes, was considerably reduced (3.8, table 16A). A strong decrease of the levels

of the SAD substrate 18:0 was also reported for *Oryza sativa* overexpressing the *Arabidopsis SSI2* ortholog, *OsSSI2* (Jiang et al., 2009), but not for *SSI2* when overexpressed in *Arabidopsis* (Kachroo et al., 2007). SADs can desaturate both 16:0 and 18:0 FAs (Kachroo et al., 2007), however, SSI2, SAD1 and SAD5 prefer C18:0-ACP as substrate, whereas SAD3 preferentially utilizes C16:0-ACP (Kachroo et al., 2007). Therefore the reduced 16:0 and 18:0 FA contents in SAD6-OE plants suggest that SAD6 utilizes both substrates. Furthermore, the higher desaturation index of SAD6-OE plants and the tumor as well as the lower desaturation index of SAD6-OE-RNAi plants, also supported the desaturating function of SAD6 (figure 19A). These observations strongly suggested that SAD6 functions as S-ACP-desaturase enzyme.

In apparent contradiction to the proposed function of SAD6 in SAD6-OE plants, 18:1 FA levels were not increased with the exception of the ER-derived polar glycerolipid class PI. In plant tumors with strong *SAD6* overexpression the relative levels of 18:1 FAs were also not significantly altered. The increased levels of 18:2 and 18:3 PUFAs, observed in SAD6-OE, suggest a feed-forward mechanism in which the strong *SAD6* expression stimulates desaturation of 18:1 FA. An increase of PUFAs was also reported for *Arabidopsis* overexpressing an acyl carrier protein, promoting 18:1 FA biosynthesis (Branen et al., 2001).

In the plant tumor, transcription of *SSI2,* the major contributor to the 18:1 MUFA pool in *Arabidopsis* leaves (Kachroo et al., 2007) was significantly reduced (3.2, figure 7A). Thus, SAD6 seems to be the only candidate that provides 18:1 for further desaturation in *Arabidopsis* crown galls and together with *FAD3* is shaping the lipid profile of crown galls.

4.2 Unsaturated fatty acids confer resistance of the plant tumor to oxidative and drought stress

Agrobacterium mediated crown gall development is accompanied by hypoxia, oxidative and drought stress (Jia et al., 1996; Deeken et al., 2006; Efetova et al., 2007; Lee et al., 2009). These factors are known to impair lipid biosynthesis and initiate degradation processes, such as the massive release of FAs from polar lipids during oxygen deprivation (Rawyler et al., 1999; Pavelic et al., 2000; Upchurch, 2008). A measure for oxygen deprivation as e. g. experienced by flooded roots is the change in the lipid content and composition (Hetherington et al., 1982; Chirkova et al., 1989). The detrimental effect of oxygen deprivation on lipids is due to the increased production of reactive oxygen species (ROS; Blokhina et al., 2003; 2010). Unsaturated FAs are prone to damage by reactive oxygen species (ROS) and are converted to lipid peroxides which affect membrane integrity (Blokhina et al., 1999). A decrease in unsaturated to saturated FA ratios can occur by lipid peroxidation (Blokhina et al.,

2003; Blokhina and Fagerstedt, 2010). In crown galls, however, the levels of unsaturated FAs were increased despite hypoxic conditions and ROS production, (3.1). Under these stress conditions the strong expression of the *SAD6* and *FAD3* genes in the tumor (3.2, figure 7A) may be a means to compensate for the loss of unsaturated FAs in order to maintain membrane integrity and fluidity. From animals it is known that cells maintain their membrane lipid homeostasis by replacing peroxidized lipids with newly synthesized unsaturated FAs (Bordoni et al., 2005).

Microarray data from different hypoxia experiments have shown that in particular fatty acid desaturase genes which include *SAD6* and *FAD3* are up-regulated (Liu et al., 2005; Loreti et al., 2005). Hypoxia, as observed in the tumor and in other metabolically active tissues with higher rates of oxygen consumption, such as growing root tips, strongly activated *SAD6* gene activity (3.5, figure 12A to 12F). It has been shown that root apical zones are prone to hypoxia even in air (Armstrong and Becket, 1985). Sensitivity to hypoxia is unique for the *SAD6* gene and was not observed on any other member of the *SAD* gene family (Loreti et al., 2005; Mustroph et al., 2009). Under low oxygen concentrations the *SAD6* gene may be activated in order to compensate for the inhibition of desaturation activity for which oxygen is required (Shanklin and Sommerville, 1991). In this respect SAD6 is similar to the ER-localized delta-9-FA-Desaturase, OLE1, in yeast. As a response to the depletion of unsaturated FAs under hypoxic conditions transcription of the *OLE1* gene is induced (Kwast et al., 1998; Nakagawa et al., 2001; Vasconcelles et al., 2001). Gene expression of *SAD6* also resembles that of the ER-localized stearoyl-coenzyme A desaturase SCD1 from animals. *SCD1* is strongly up-regulated in animal tumors (Igal et al., 2010) and induced under hypoxic conditions (Li et al., 2005; Igwe et al., 2008). It was proposed that SCD1 modulates metabolic and signaling processes related to cell proliferation, survival and malignant transformation to cancer cell (Igal et al., 2010).

Furthermore, the hypoxia dependent *SAD6* may prime the lipid profile for the post-anoxic period by increasing the degree of unsaturation. It is well known that ROS production peaks after hypoxia when the oxygen concentration increases to normoxia and has detrimental effects on lipids, predominantly unsaturated FAs (Hunter et al., 1983 Albrecht et al., 1994; Blokhina and Fagerstedt, 2010). It is well known that several genes encoding enzymes to protect against oxidative stress are up-regulated during hypoxia (Blokhina and Fagerstedt, 2010), like it was observed in the crown gall (Deeken et al., 2006; Lee et al., 2009). Survivability of the cell depends on the ability to preserve its lipid composition and FA

unsaturation after oxygen deprivation (Blokhina et al., 2003). Thus, high activity of *SAD6,* together with *FAD3,* may prime the tumor for survival in the postanoxic period.

For SSI2, the ortholog of SAD6, and free 18:1 FA of *Arabidopsis* it was shown that they are involved in regulation of NPR1-dependent and -independent pathogen defense responses (Kachroo et al., 2001; Kachroo et al., 2003). *SAD6*, however, seems not to be involved in signaling, since no alteration in pathogenesis related (PR) gene regulation in SAD6-OE plants was observed (data not shown). In contrast to *SAD6*, *SSI2* is expressed throughout *Arabidopsis* (Kachroo et al., 2001; Kachroo et al., 2007) and is according to genevestigator (https://www.gene-vestigator.com/gv/index.jsp) not specifically regulated at the transcriptional level. Overexpression of the *SSI2* gene in *Arabidopsis* or rice does not cause chlorosis (Jiang et al., 2009; Kachroo et al., 2007) which was characteristic for *SAD6* overexpressing tissues (tumors and SAD6-OE; 3.7, figure 15A, 15B, 15E and 15F).

The chlorotic phenotype of SAD6-OE was light dependent (3.7, figure 15D). The altered lipid homoeostasis as result of *SAD6* activity impairs the function of membranes involved in photosynthesis. This idea was supported by the observation that overexpression of *SAD6* is accompanied by a reduction in chlorophyll content and number in open PSII centers (q_P). Light-exposed chloroplasts are the main source of ROS (in particular singlet oxygen) generation (Foyer and Noctor, 2003). *SAD6* overexpressing leaves appear to suffer photooxidative stress that is accompanied by excessive formation of singlet oxygen, ultimately leading to the development of chlorosis in the light (Triantaphylides et al., 2008). Photooxidative stress also activates the jasmonate pathway, lipoxygenase-dependent plastid membrane oxidation, and arabidopside accumulation (op den Camp et al., 2003). Arabidopside accumulation was also observed in SAD6-OE leaves (3.8, figure 20). Thus, the altered lipid homeostasis leads most likely to an enhanced susceptibility against photooxiative stress resulting in the degradation of plastidic lipid pools. Finally chlorosis in SAD6-OE leaves may activate the eukaryotic phospholipid-biosynthesis pathway as indicated by an increase in the levels of unsaturated FAs, like 18:1, 18:2 and 18:3 of the eukaryotic pathway. The observation that *ssi2-2* mutants, overexpressing the *SAD6* gene (3.6, figure 13C), and mature leaves of SAD6-OE plants as well as heterozygous SAD6-OE lines (data not shown) did not develop chlorosis under illumination, suggests a threshold dependent chlorotic phenotype. In these plants the impact on fatty acids that leads to an altered lipid homeostasis seems to stay below the threshold that confers an increased susceptibility against photooxidative stress that causes chlorosis. The molecular mechanism behind the threshold-dependent phenotype remains to be uncovered.

Crown galls have not only to cope with hypoxia and oxidative stress, but also with drought stress. The loss of water is increased (Schurr et al., 1996) and ABA-mediated drought stress adaptions were shown to be crucial for tumor development (Efetova et al., 2007). The rate of water evaporation by the tumor is dependent on the degree of humidity (Grantz, 1990). A relative humidity of 85%-100% diminished the observed difference in tumor size of the *Arabidopsis fad3-2* mutant and WT plants at 45-50% humidity (3.3, figure 8B). Thus, the impaired tumor growth on *fad3-2* mutants in dry air suggests a role of ER-derived 18:3 PUFAs in protection against drought stress. Drought stress decreases the membrane lipid content by inhibition of lipid biosynthesis (Monteiro de Paula et al., 1993) and stimulation of peroxidative and lypolytic activities (Ferrari-Iliou et al., 1993; Matos et al., 2001). For drought stress-sensitive plants a reduction of PUFAs was reported (Pham-Thi et al., 1983; Monteiro de Paula et al., 1993; Dakhma et al., 1995). In drought tolerant cowpea cultivars omega-3 fatty acid desaturase (*FAD*) genes, homologous to *Arabidopsis FAD3*, are transcriptionally up-regulated and biosynthesis of 18:3 PUFAs is induced. *FAD* transcription is not regulated in drought stress sensitive cowpea cultivars (Gigon et al., 2004; Torres-Franklin et al., 2009). Moreover, FADs and their product 18:3 PUFA are involved in enhancing drought stress tolerance (Zhang et al., 2005). Therefore, it seems reasonable that *FAD3* is responsible for the increase of 18:3 PUFAs in tumors, preventing the negative effect of drought stress on membrane structures.

The scheme in figure 21 summarizes the role of lipids in crown gall tumors. The lipid profile reflects that of a heterotrophic lipid metabolism of growing and chlorotic tissues. Two desaturases, the ER-bound *FAD3* and the chloroplast-specific *SAD6* gene encoding a novel S-ACP-desaturase increase the levels of unsaturated FAs thereby conferring resistance to drought and hypoxic stress both resulting in oxidative stress in the crown gall tumor.

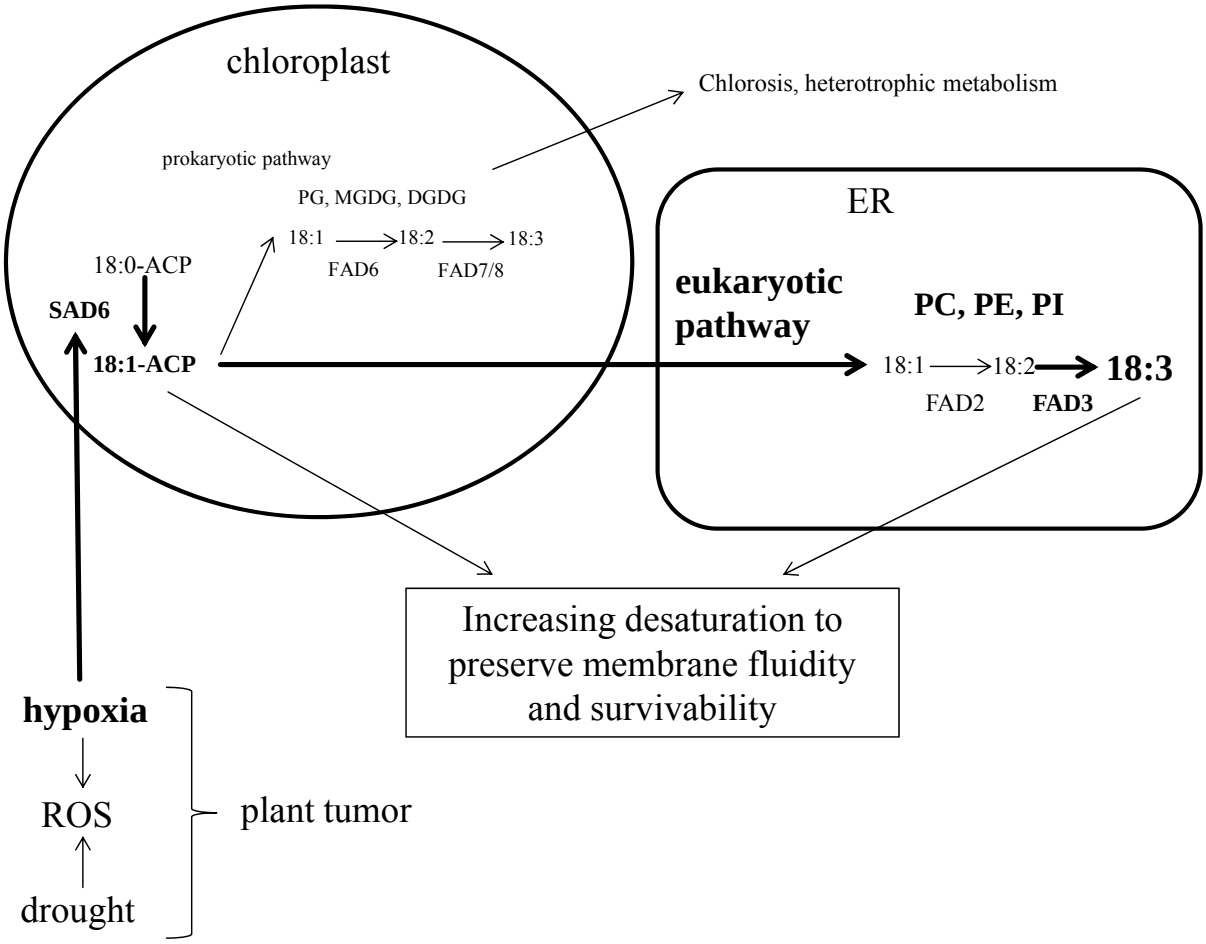

Figure 21. Model of the acyl lipid metabolism in *Agrobacterium* induced crown galls of *Arabidopsis thaliana.* The eukaryotic lipid biosynthesis pathway is favoured over the prokaryotic pathway to produce glycerolipids. The chlorotic tumor, characterized by a heterotrophic metabolism and hypoxia specifically up-regulates the S-ACP-desaturase *SAD6. SAD6* replaces *SSI2* function under hypoxia to cope with limitation of desaturation. The activity of the ER bound desaturase, FAD3, elevates the 18:3 PUFA content in the crown gall, a process known to preserve the lipid profile under drought stress. Both, *SAD6* and *FAD3*, mediate FA desaturation in the crown gall in order to preserve fluidity of membranes that is challenged by hypoxia and drought stress in the tumor, both of which cause oxidative stress. PG, phosphatidylglycerol; MGDG, monogalactosyldiacylglycerol; DGDG, digalactosyldiacylglycerol, PC, phosphatidylcholine; PI, phosphatidylinositol; PE, phosphatidyl-ethanolamine.

5. Summary

Crown gall development is accompanied by hypoxia, drought and oxidative stress. These abiotic stress factors are known to have an impact on fatty acid (FA) desaturation. Thus, an alteration in the lipid profile of plant tumors was expected. A comprehensive lipid analysis of *Arabidopsis thaliana* crown galls induced by *Agrobacterium tumefaciens* showed an increase in the degree of FA desaturation. The poly unsaturated fatty acid (PUFA) linolenic acid (18:3) of endoplasmic reticulum (ER) derived phospholipids was especially affected. The increased levels of desaturated FAs were reflected by a strong induction of two genes encoding desaturases, *FAD3* and *SAD6*. In contrast to *FAD3*, which encodes the ER membrane bound fatty acid desaturase enzyme that synthesizes 18:3 PUFAs in the ER, the function of *SAD6* is unknown. The ability of *SAD6* to complement the extreme dwarf growth phenotype of the *ssi2-2* mutant allele suggests that *SAD6* is a functional stearoyl-acyl-carrier-protein delta-9 desaturase (SAD) which catalyzes the first step in FA desaturation and forms stearic acid (18:1). Overexpression of the *SAD6* gene in *Arabidopsis* (SAD6-OE) to a similar degree as in tumors resulted in a light-dependent chlorosis phenotype and caused a similar shift in the lipid profile towards unsaturated phospholipids. Posttranscriptional down-regulation of *SAD6* overexpression by RNA reverted the chlorosis phenotype and the changes in the lipid profile, showing that SAD6 overexpression forms the unsaturated FA profile and the phenotype in SAD6-OE. The subcellular localization of the SAD6 protein in chloroplasts, which is obligatory for SAD function was demonstrated. *SSI2*, which encodes the major contributor to the 18:1 FA levels in *Arabidopsis* is down-regulated in crown galls pointing to a replacement of *SSI2* function by *SAD6* in the tumor. *SAD6* transcripts were almost undetectable in *Arabidopsis* under normal growth condition, whereas under hypoxia the gene was strongly activated. In the tumor hypoxia most likely caused the very high transcription of *SAD6*. Hypoxia is known to limit FA desaturation and it is associated with an elevated reactive oxygen species (ROS) production which is detrimental for unsaturated FAs. Thus, up-regulation of *SAD6* in the crown gall, most likely serves as an adaptive mechanism to activate desaturation under low oxygen concentrations and to maintain the levels of unsaturated FA under oxidative stress. The ER localized FAD3 most likely is responsible for the rise in 18:3 of the phospholipid class to cope with drought stress in crown galls. This hypothesis was supported by the loss of function mutant, *fad3-2,* which developed significantly smaller tumors as the wild type under low relative humidity.Taken together, this study suggests that the induction of *SAD6* and *FAD3* shapes the tumor lipid profile by increasing the levels of

unsaturated FAs. Unsaturated fatty acids prepare the crown gall to cope with ongoing hypoxia, drought and oxidative stress during growth and development.

6. Zusammenfassung

Die Physiologie der durch *Agrobacterium tumefaciens* hervorgerufenen Wurzelhalsgallen ist geprägt von Sauerstoffmangel, Trocken- und oxidativen Stress. Diese Stressfaktoren beeinflussen die Umwandlung gesättigter zu ungesättigten Fettsäuren (Desaturierung). Somit sind Änderungen im Lipidmuster des durch *Agrobacterium tumefaciens* ausgelösten Pflanzentumors wahrscheinlich. Eine umfassende Analyse des Wurzelhalsgallenlipidmusters ergab, dass der Anteil an ungesättigten Fettsäuren erhöht war. Am auffälligsten war vor allem die Erhöhung der mehrfach ungesättigten Fettsäure Linolensäure (18:3) in den mit dem endoplasmatischen Retikulum (ER) assoziierten Phospholipiden. Dieser Anstieg ging einher mit der stark erhöhten transkriptionellen Aktivität des *FAD3*-Gens, das eine membrangebundene Fettsäure-Desaturase kodiert, die Linolensäure (18:3) im ER synthetisiert. Darüber hinaus war ein weiteres funktionell unbekanntes Desaturase-Gen, *SAD6*, stark aktiviert. Das SAD6 Protein war in Chloroplasten lokalisiert und in der Lage den extremen Zwergwuchs-Phänotyp der *ssi2-2* Mutante zum Wildtyp zu komplementieren. Damit wurde nahegelegt, dass SAD6, wie SSI2, eine funktionelle „delta-9 Stearoyl-Acyl-Carrier-Protein-Desaturase“ (SAD) ist. Die Überexpression des *SAD6*-Gens in *Arabidopsis* (SAD6-OE), vergleichbar der in Wurzelhalsgallen, führte zu einem Anstieg ungesättigter Phospholipide und einem lichtabhängigen chlorotischen Phänotyp. Eine posttranskriptionelle Reduzierung der *SAD6* Überexpression durch RNAi revertierte den Chlorosephänotyp und die Veränderungen im Lipidprofil zum Phänotyp des Wildtyps. Da *SSI2*, welches das SAD-Enzym für die Ölsäure (18:1)-Produktion in *Arabidopsis* kodiert, in Wurzelhalsgallen stark herunterreguliert ist, übernimmt hier sehr wahrscheinlich *SAD6* die Funktion von *SSI2*. Insbesondere deshalb, weil der im Tumor vorherrschende Sauerstoffmangel zu einer starken Aktivierung des *SAD6*-Gens führt. Die Produktion ungesättigter Fettsäuren wird unter hypoxischen Bedingungen limitiert, weshalb eine erhöhte Expression von *SAD6* die reduzierte Synthese ungesättigter Fettsäuren kompensieren könnte. Hypoxie und vor allem die posthypoxische Phase führen zur Produktion reaktiver Sauerstoffspezies (ROS), die ungesättigte Fettsäuren peroxidieren, so dass das Hypoxie-sensitive *SAD6*-Gen darüber hinaus das Niveau ungesättigter Fettsäuren unter oxidativem Stress zu erhalten scheint.

Die ER lokalisierte Desaturase FAD3 ist ursächlich für die spezifische Erhöhung von Linolensäure (18:3) in den ER assoziierten Phospholipiden und führt somit zu einer

Anpassung an den Trockenstress im Tumor. Dies wird dadurch unterstützt, dass an *fad3-2* Mutanten unter erhöhtem Trockenstress deutlich kleinere Tumore wachsen.

Diese Studie hat gezeigt, dass die Induktion von *SAD6* und *FAD3* in der Wurzelhalsgalle mit einer erhöhten Produktion ungesättigter Fettsäuren einhergeht und somit die Entwicklung und das Wachstum von Wurzelhalsgallen unter Sauerstoffmangel, oxidativem Stress und Wasserverlust ermöglicht wird.

7. References

Aisenberg, A.C., and Morris, H.P. (1961). Energy pathways of hepatoma No. 5123. Nature **191,** 1314-1315.

Albrecht, G., and Wiedenroth, E.M. (1994). Protection against activated oxygen following re-aeration of hypoxically pretreated wheat roots. The response of the glutathione system J. Exp. Bot. **45,** 449-455.

Aloni, R., Pradel, K., and Ullrich, C. (1995). The 3-dimensional structure of vascular tissues in *Agrobacterium tumefaciens*-induced crown galls and in the host stems of *Ricinus-communis* L. Planta **196,** 597-605.

Aloni, R., and Ullrich, C.I. (2008). Biology of Crown Gall Tumors. In *Agrobacterium*: From Biology to Biotechnology, T. Tzfira and V. Citovsky, eds. (New York, USA: Springer) pp. 565-591.

Andersson, M.X., Hamberg, M., Kourtchenko, O., Brunnstrom, A., McPhail, K.L., Gerwick, W.H., Gobel, C., Feussner, I., and Ellerstrom, M. (2006). Oxylipin Profiling of the Hypersensitive Response in *Arabidopsis thaliana*. Formation of a novel oxo-phytodienoic acid-containing galactolipid, arabidopside *E*. J Biol. Chem. **281,** 31528-31537.

Armstrong, W., and Beckett, P.M. (1985). Root Aeration in Unsaturated Soil: A Multi-Shelled Mathematical Model of Oxygen Diffusion and Distribution with and without Sectoral Wet-Soil Blocking of the Diffusion Path. New Phytol. **100,** 293-311.

Baier, M., and Dietz, K.J. (2005). Chloroplasts as source and target of cellular redox regulation: a discussion on chloroplast redox signals in the context of plant physiology. J. Exp. Bot. **56,** 1449-1462.

Bayer, M.H. (1991). Fatty acid composition of galactolipids and phospholipids in neoplasmatic plant tissues (cecidia) and normal leaf tissue. Physiol. Plant. **81,** 313-318.

Berberich, T., Harada, M., Sugawara, K., Kodama, H., Iba, K., and Kusano, T. (1998). Two maize genes encoding omega-3 fatty acid desaturase and their differential expression to temperature. Plant Mol Biol **36,** 297-306.

Birnboim, H.C., and Doly, J.A. (1979). A rapid alkaline extraction procedure for screening recombinant plasmid DNA. Nucleic Acid.Res. **7,** 1513-1523.

Bligh, E.G., and Dyer, W.J. (1959). A rapid method of total lipid extraction and purification. Can. J. Biochem. Physiol. **37,** 911-917.

Blokhina, O.B., Fagerstedt, K.V., and Chirkova, T.V. (1999). Relationships between lipid peroxidation and anoxia tolerance in a range of species during post-anoxic reaeration. Physiol. Plant. **105,** 625-632.

Blokhina, O., Virolainen, E., and Fagerstedt, K.V. (2003). Antioxidants, oxidative damage and oxygen deprivation stress: a review. Ann. Bot. **91,** 179-194.

Blokhina, O., and Fagerstedt, K.V. (2010). Oxidative metabolism, ROS and NO under oxygen deprivation. Plant Physiol. Biochem. **48,** 359-373.

Bordoni, A., Angeloni, C., Leoncini, E., Danesi, F., Maranesi, M., Biagi, P.L., and Hrelia, S. (2005). Hypoxia/reoxygenation alters essential fatty acids metabolism in cultured rat cardiomyocytes: protection by antioxidants. Nutr. Metab. Cardiovasc. Dis. **15,** 166-173.

Bradford, M.M. (1976). A rapid and sensitive method for the quantitation of microgram quantities of protein utilizing the principle of protein-dye binding. Anal. Biochem. **72,** 248-254.

Branen, J.K., Chiou, T.J., and Engeseth, N.J. (2001). Overexpression of acyl carrier protein-1 alters fatty acid composition of leaf tissue in *Arabidopsis*. Plant Physiol. **127,** 222-229.

Braun, A. (1952). Conditioning of the host cell as a factor in the transformation process in crown gall. Growth **16,** 65-74.

Brown, D.J., and Beevers, H. (1987). Fatty Acids of Rice Coleoptiles in Air and Anoxia. Plant Physiol. **84,** 555-559.

Browse, J., McConn, M., James, D., Jr., and Miquel, M. (1993). Mutants of *Arabidopsis* deficient in the synthesis of alpha-linolenate. Biochemical and genetic characterization of the endoplasmic reticulum linoleoyl desaturase. J. Biol. Chem. **268,** 16345-16351.

Bullock, W., Fernandez, J., and Short, H. (1987). Xl1-Blue - a high-efficiency plasmid transforming recA *escherichia-coli* strain with beta-galactosidase selection. Biotechniques **5,** 376.

Cahoon, E.B., Mills, L.A., and Shanklin, J. (1996). Modification of the fatty acid composition of *Escherichia coli* by coexpression of a plant acyl-acyl carrier protein desaturase and ferredoxin. J. Bacteriol. **178,** 936-939.

Cahoon, E.B., Shah, S., Shanklin, J., and Browse, J. (1998). A determinant of substrate specificity predicted from the acyl-acyl carrier protein desaturase of developing cat´s claw seed. Plant Physiol. **117,** 593-598.

Chirkova, T.V., Thukova, T.M., and Tretiakov, A.L. (1984). Adeine nucleotides in wheat and rice seedlings under aeration and anoxia. Vestnik LGU **15,** 74-81.

Clough, S.J., and Bent, A.F. (1998). Floral dip: a simplified method for *Agrobacterium*-mediated transformation of *Arabidopsis thaliana*. Plant J. **16,** 735-743.

Collados, R., Andreu, V., Picorel, R., and Alfonso, M. (2006). A light-sensitive mechanism differently regulates transcription and transcript stability of omega 3 fatty-acid desaturases (FAD3, FAD7 and FAD8) in soybean photosynthetic cell suspensions. FEBS Lett. **580,** 4934-4940.

Dakhma, W.S., Zarrouk, M., and Cherif, A. (1995). Effects of drought-stress on lipids in rape leaves. Phytochemistry. **40,** 1383-1386.

Deeken, R., Engelmann, J.C., Efetova, M., Czirjak, T., Muller, T., Kaiser, W.M., Tietz, O., Krischke, M., Mueller, M.J., Palme, K., Dandekar, T., and Hedrich, R. (2006). An integrated view of gene expression and solute profiles of *Arabidopsis* tumors: a genome-wide approach. Plant Cell **18,** 3617-3634.

Dessaux, Y., Petit, A., and Tempe, J. (1993). Chemistry and biochemistry of opines, chemical mediators of parasitism. Phytochemistry **34,** 31-38.

Efetova, M., Zeier, J., Riederer, M., Lee, C.W., Stingl, N., Mueller, M., Hartung, W., Hedrich, R., and Deeken, R. (2007). A central role of abscisic acid in drought stress protection of *Agrobacterium*-induced tumors on *Arabidopsis*. Plant Physiol. **145,** 853-862.

Fabre, E., and Dunal, F. (1853). Observations sur les maladies regantes de la vigne. Bull. Soc. Cent. Agric. Dep. Herault. **40,** 46.

Falcone, D.L., Gibson, S., Lemieux, B., and Somerville, C. (1994). Identification of a gene that complements an *Arabidopsis* mutant deficient in chloroplast omega 6 desaturase activity. Plant Physiol **106,** 1453-1459.

Ferrari-Iliou, R., D´Arcy-Lameta, A., Iliou, J.P., Thi, A.T., Monteiro de Paula, F., Da Silva, J.V., and Mazliak, P. (1993). In vitro photodynamic lipid peroxidation of total lipophilic extracts from leaves of bean plants. Biochim. Biophys. Acta **1166,** 48-54.

Foyer, C.H., and Allen, J.F. (2003). Lessons from redox signaling in plants. Antioxid. Redox Signal. **5,** 3-5.

Freeman, B.A., Platt-Aloia, K., Mudd, J.B., and Thomson, W.W. (1978). Ultrastructural and lipid changes associated with the aging of citrus leaves. Protoplasma **94,** 221-233.

Fritz, V., and Fajas, L. (2010). Metabolism and proliferation share common regulatory pathways in cancer cells. Oncogene **29,** 4369-4377.

Gee, M.M., Sun, C.N., and Dwyer, J.D. (1967). An electron microscope study of sunflower crown gall tumor. Protoplasma **64,** 195-200.

Gibson, S., Arondel, V., Iba, K., and Somerville, C. (1994). Cloning of a temperature-regulated gene encoding a chloroplast omega-3 desaturase from *Arabidopsis thaliana*. Plant Physiol. **106,** 1615-1621.

Gigon, A., Matos, A.R., Laffray, D., Zuily-Fodil, Y., and Pham-Thi, A.T. (2004). Effect of drought stress on lipid metabolism in the leaves of *Arabidopsis* thaliana (ecotype Columbia). Ann. Bot. **94,** 345-351.

Grantz, D.A. (1990). Plant response to atmospheric humidity. Plant, Cell and Environ. **13,** 667-679.

Hamilton, R.H., and Fall, M.Z. (1971). The loss of tumor-initiating ability in *Agrobacterium tumefaciens* by incubation at high temperature. Experientia. **27,** 229-230.

Hanahan, D. (1985). In DNA cloning: A Practival Approach Vol. 1,. D.M. Glover, eds (McLean, Virginia, USA: IRL Press) pp. 109.

Hendry, G.A.F., and Crawford, R.M.M. (1994). Oxygen and enviromental stress in plants - an overview. Proceedings of the Royal Society of Edinburgh **102B**, 1-10.

Henzi, T., and Braendle, R. (1993). Long term survival of rhizimatous species under oxygen deprivation. In Interacting stresses on plants in a changing climate, NATO ASI series 116, MB. Jackson and CR Black, eds (Berlin, Germany: Springer Verlag) pp. 305-314.

Hetherington, A.M., S. Hunter, M.I., and Crawford, R.M.M. (1982). Contrasting effects of anoxia on rhizome lipids in *Iris* species. Phytochemistry **21,** 1275-1278.

Hisamatsu, Y., Goto, N., Hasegawa, K., and Shigemori, H. (2003). Arabidopsides A and B, two new oxylipins from *Arabidopsis* thaliana. Tet. Lett. **44,** 5553-5556.

Hisamatsu, Y., Goto, N., Sekiguchi, M., Hasegawa, K., and Shigemori, H. (2005). Oxylipins arabidopsides C and D from *Arabidopsis* thaliana. J. Nat. Prod. **68,** 600-603.

Hsu, P.P., and Sabatini, D.M. (2008). Cancer cell metabolism: Warburg and beyond. Cell **134,** 703-707.

Hunter, M.I.S., Hetherington, A.M., and Robert, M.M. (1983). Lipid peroxidation-a factor in anoxia intolerance in *iris* species? Phytochemistry **22,** 1145-1147.

Iba, K., Gibson, S., Nishiuchi, T., Fuse, T., Nishimura, M., Arondel, V., Hugly, S., and Somerville, C. (1993). A gene encoding a chloroplast omega-3 fatty acid desaturase complements alterations in fatty acid desaturation and chloroplast copy number of the fad7 mutant of *Arabidopsis thaliana*. J. Biol. Chem. **268,** 24099-24105.

Igal, A.R. (2010). Stearoyl-CoA desaturase-1: a novel key player in the mechanisms of cell proliferation, programmed cell death and transformation to cancer. Carcinogenesis **31,** 1509-1515.

Igwe, E.I., Essler, S., Al-Furoukh, N., Dehne, N., and Brune, B. (2009). Hypoxic transcription gene profiles under the modulation of nitric oxide in nuclear run on-microarray and proteomics. BMC Genomics **10,** 408.

James, D.W., and Dooner, H.K. (1990). Isolation of EMS-induced mutants in *Arabidopsis* altered in seed fatty acid composition. Theor. Appl. Genet. 80**,** 241-245.

Jia, S.R., Kumar, P.P., and Kush, A. (1996). Oxidative stress in *Agrobacterium*-induced tumors on *Kalanchoe* plants. Plant J. **10,** 545-551.

Jiang, C.J., Shimono, M., Maeda, S., Inoue, H., Mori, M., Hasegawa, M., Sugano, S., and Takatsuji, H. (2009). Suppression of the rice fatty-acid desaturase gene OsSSI2 enhances resistance to blast and leaf blight diseases in rice. Mol. Plant Microbe Interact. **22,** 820-829.

Kachroo, P., Shanklin, J., Shah, J., Whittle, E.J., and Klessig, D.F. (2001). A fatty acid desaturase modulates the activation of defense signaling pathways in plants. Proc. Natl. Acad. Sci. USA **98,** 9448-9453.

Kachroo, P., Kachroo, A., Lapchyk, L., Hildebrand, D., and Klessig, D.F. (2003). Restoration of defective cross talk in *ssi2* mutants: role of salicylic acid, jasmonic acid, and fatty acids in SSI2-mediated signaling. Mol. Plant Microbe Interact **16,** 1022-1029.

Kachroo, A., Shanklin, J., Whittle, E., Lapchyk, L., Hildebrand, D., and Kachroo, P. (2007). The *Arabidopsis* stearoyl-acyl carrier protein-desaturase family and the contribution of leaf isoforms to oleic acid synthesis. Plant Mol Biol **63,** 257-271.

Kang, H.K., Min, B., Park, H., Lim, K.J., Huh, T.-L., and Lee, S.Y. (1996). Increase in Linolenate Contents by Expression of the *fad3* gene In Transgenic Tobacco Plants. J. Biochem. Mol. Biol. **29,** 308-313.

Kasajima, I., Ide, Y., Ohkama-Ohtsu, N., and Hayashi, H. (2004). A protocol for rapid DNA extraction from *Arabidopsis* thaliana for PCR analysis. Plant Mol. Biol. Rep. **22,** 49-52.

Kennedy, B.W. (1980). Estimates of U.S. crop losses to prokaryote plant pathogens. Plant Dis **647,** 674-676.

Klaunig, J.E., and Kamendulis, L.M. (2004). The role of oxidative stress in carcinogenesis. Annu. Rev. Pharmacol. Toxicol. **44,** 239-267.

Klee, H., Montoya, A., Horodyski, F., Lichtenstein, C., Garfinkel, D., Fuller, S., Flores, C., Peschon, J., Nester, E., and Gordon, M. (1984). Nucleotide sequence of the *tms* genes of the pTiA6NC octopine Ti plasmid: two gene products involved in plant tumorigenesis. Proc Natl Acad Sci USA **81,** 1728-1732.

Koncz, C., and Schell, J. (1986). The promoter of TL-DNA gene *5* controls the tissue-specific expression of chimaeric genes carried by a novel type of *Agrobacterium* binary vector. Mol. Gen. Genet. **204,** 383-396.

Krysan, P.J., Young, J.C., and Sussman, M.R. (1999). T-DNA as an insertional mutagen in *Arabidopsis*. Plant Cell **11,** 2283-2290.

Kwast, K.E., Burke, P.V., and Poyton, R.O. (1998). Oxygen sensing and the transcriptional regulation of oxygen-responsive genes in yeast. J. Exp. Biol. **201,** 1177-1195.

Laemmli, U.K. (1970). Cleavage of structural proteins during the assembly of the head of bacteriophage T4. Nature **227,** 680-685.

Larkin, M.A., Blackshields, G., Brown, N.P., Chenna, R., McGettigan, P.A., McWilliam, H., Valentin, F., Wallace, I.M., Wilm, A., Lopez, R., Thompson, J.D., Gibson, T.J., and Higgins, D.G. (2007). Clustal W and Clustal X version 2.0. Bioinformatics **23,** 2947-2948.

Lee, C.W., Efetova, M., Engelmann, J.C., Kramell, R., Wasternack, C., Ludwig-Muller, J., Hedrich, R., and Deeken, R. (2009*). Agrobacterium tumefaciens* promotes tumor induction by modulating pathogen defense in *Arabidopsis thaliana*. Plant Cell **21,** 2948-2962.

Leech, R.M., Rumsby, M.G., and Thomson, W.W. (1973). Plastid differentiation, acyl lipid, and Fatty Acid changes in developing green maize leaves. Plant Physiol. **52,** 240-245.

Li, J., Grigoryev, D.N., Ye, S.Q., Thorne, L., Schwartz, A.R., Smith, P.L., O´Donnell, C.P., and Polotsky, V.Y. (2005). Chronic intermittent hypoxia upregulates genes of lipid biosynthesis in obese mice. J. Appl. Physiol. **99,** 1643-1648.

Li-Beisson, Y., Shorrosh, B., Beisson, F., Andersson, M.X., Arondel, V., Bates, P.D., Baud, S.b., Bird, D., DeBono, A., Durrett, T.P., Franke, R.B., Graham, I.A., Katayama, K., Kelly, A.l.A., Larson, T., Markham, J.E., Miquel, M., Molina, I., Nishida, I., Rowland, O., Samuels, L., Schmid, K.M., Wada, H., Welti, R., Xu, C., Zallot, R.m., and Ohlrogge, J. (2010). Acyl-Lipid Metabolism in The *Arabidopsis* Book, (Rockville, MD, USA: American Society of Plant Biologists) doi: 10.1199/tab.0133

Lichtenstein, C., Klee, H., Montoya, A., Garfinkel, D., Fuller, S., Flores, C., Nester, E., and Gordon, M. (1984). Nucleotide sequence and transcript mapping of the tmr gene of the pTiA6NC octopine Ti-plasmid: a bacterial gene involved in plant tumorigenesis. J Mol. Appl. Genet. **2,** 354-362.

Lightner, J., Wu, J., and Browse, J. (1994). A Mutant of *Arabidopsis* with Increased Levels of Stearic Acid. Plant Physiol. **106,** 1443-1451.

Liu, Y., Schiff, M., and Dinesh.Kumar, S. (2002). Virus-induced gene silencing in tomato. Plant J. **31,** 777-786.

Liu, F., Vantoai, T., Moy, L.P., Bock, G., Linford, L.D., and Quackenbush, J. (2005). Global transcription profiling reveals comprehensive insights into hypoxic response in *Arabidopsis*. Plant Physiol. **137,** 1115-1129.

Loreti, E., Poggi, A., Novi, G., Alpi, A., and Perata, P. (2005). A genome-wide analysis of the effects of sucrose on gene expression in *Arabidopsis* seedlings under anoxia. Plant Physiol **137,** 1130-1138.

Los, D.A., and Murata, N. (1998). Structure and expression of fatty acid desaturases. Biochim. Biophys. Acta **1394,** 3-15.

Manoharan, K., Prasad, R., and Guha-Mukherjee, S. (1987). Greening and shoot-differentiation related lipid changes in callus cultures of *Datura innoxia*. Phytochemistry **26,** 407-410.

Matos, A.R., d´Arcy-Lameta, A., Franca, M., Petres, S., Edelman, L., Kader, J., Zuily-Fodil, Y., and Pham-Thi, A.T. (2001). A novel patatin-like gene stimulated by drought stress encodes a galactolipid acyl hydrolase. FEBS Lett. **491,** 188-192.

McConn, M., Hugly, S., Browse, J., and Somerville, C. (1994). A Mutation at the *fad8* Locus of *Arabidopsis* Identifies a Second Chloroplast omega-3 Desaturase. Plant Physiol. **106,** 1609-1614.

Mikami, K., and Murata, N. (2003). Membrane fluidity and the perception of environmental signals in cyanobacteria and plants. Prog. Lipid Res. **42,** 527-543.

Monteiro de Paula, F., Pham-Thi, A., Zuily-Fodil, Y., Ferrari-Iliou, R., Vieira da Silva, J., and Mazliak, P. (1993). Effect of water stress on the biosynthesis and degradation of polyunsaturated lipid molecular species in leaves of *Vigna unguiculata*. Plant Physiol. Biochem. **31,** 707-715.

Mosblech, A., Feussner, I., and Heilmann, I. (2009). Oxylipins: structurally diverse metabolites from fatty acid oxidation. Plant Physiol. Biochem. **47,** 511-517.

Mustroph, A., Zanetti, M.E., Jang, C.J., Holtan, H.E., Repetti, P.P., Galbraith, D.W., Girke, T., and Bailey-Serres, J. (2009). Profiling translatomes of discrete cell populations resolves altered cellular priorities during hypoxia in *Arabidopsis*. Proc. Natl. Acad. Sci. USA **106,** 18843-18848.

Nakagawa, Y., Sugioka, S., Kaneko, Y., and Harashima, S. (2001). O2R, a novel regulatory element mediating Rox1p-independent O_2 and unsaturated fatty acid repression of *OLE1* in *Saccharomyces cerevisiae*. J. Bacteriol. **183,** 745-751.

Nour-Eldin, H.H., Hansen, B.G., Norholm, M.H., Jensen, J.K., and Halkier, B.A. (2006). Advancing uracil-excision based cloning towards an ideal technique for cloning PCR fragments. Nucleic Acids Res. **34,** e122.

Ohlrogge, J., and Browse, J. (1995). Lipid biosynthesis. Plant Cell **7,** 957-970.

Okuley, J., Lightner, J., Feldmann, K., Yadav, N., Lark, E., and Browse, J. (1994). *Arabidopsis FAD2* Gene Encodes the Enzyme That Is Essential for Polyunsaturated Lipid Synthesis. Plant Cell **6,** 147-158.

Olinares, P.D., Ponnala, L., and van Wijk, K.J. (2010). Megadalton complexes in the chloroplast stroma of *Arabidopsis thaliana* characterized by size exclusion chromatography, mass spectrometry, and hierarchical clustering. Mol. Cell. Proteomics **9,** 1594-1615.

op den Camp, R.G., Przybyla, D., Ochsenbein, C., Laloi, C., Kim, C., Danon, A., Wagner, D., Hideg, E., Gobel, C., Feussner, I., Nater, M., and Apel, K. (2003). Rapid induction of distinct stress responses after the release of singlet oxygen in *Arabidopsis*. Plant Cell **15,** 2320-2332.

Pavelic, D., Arpagaus, S., Rawyler, A., and Brandle, R. (2000). Impact of post-anoxia stress on membrane lipids of anoxia-pretreated potato cells. A re-appraisal. Plant Physiol. **124,** 1285-1292.

Pedersen, P.L. (1978). Tumor mitochondria and the bioenergetics of cancer cells. Prog. Exp. Tumor Res. **22,** 190-274.

Peltier, J.B., Cai, Y., Sun, Q., Zabrouskov, V., Giacomelli, L., Rudella, A., Ytterberg, A.J., Rutschow, H., and van Wijk, K.J. (2006). The oligomeric stromal proteome of *Arabidopsis thaliana* chloroplasts. Mol. Cell. Proteomics **5,** 114-133.

Pham-Thi, A.T., Borrel-Flood, B., Justin, A.M., Mazliak, P., and Vieira da Silva, J. (1983). Action de la sécheresse sur l´incorporation du [1-14C]-acétate dans les lipides de feuilles de Cotonnier (Gossypium hirsutum L.). C. R. Acad. Sci. Paris **297,** 613-616.

Pineda, M., Sajnani, C., and Baron, M. (2010). Changes induced by the Pepper mild mottle tobamovirus on the chloroplast proteome of Nicotiana benthamiana. Photosynth. Res. **103,** 31-45.

Pradel, K.S., Ullrich, C.I., Santa Cruz, S., and Oparka, K.J. (1999). Symplastic continuity in *Agrobacterium tumefaciens*-induced tumours J. Exp. Bot. **50,** 183-192.

Rawyler, A., Pavelic, D., Gianinazzi, C., Oberson, J., and Braendle, R. (1999). Membrane Lipid Integrity Relies on a Threshold of ATP Production Rate in Potato Cell Cultures Submitted to Anoxia. Plant Physiol. **120,** 293-300.

Rhoads, D.M., Umbach, A.L., Chalivendra, C.S., and James, N.S. (2006). Mitochondrial Reactive Oxygen Species. Contribution to Oxidative Stress and Interorganellar Signaling. Plant Physiol. **141,** 357-366.

Romeis T., Ludwig AA., Martin, R., and Jones JDG. (2001). Calciumdependent protein kinases play an essential role in a plant defence response. EMBO J. **20,** 5556-5567.

Sanger, F., Nicklen, S., and Coulson, A.R. (1977). DNA sequencing with chain-terminating inhibitors. Proc. Natl. Acad. Sci. USA **74,** 5463-5467.

Santosa, I.E., Ram, P.C., Boamfa, E.I., Laarhoven, L.J.J., Reuss, J., Jackson, M.B., and Harren, F.J.M. (2007). Patterns of peroxidative ethane emission from submerged rice seedlings indicate that damage from reactive oxygen species takes place during submergence and is not necessarily a post-anoxic phenomenon. Planta **226,** 193-202.

Schreiber, L. (2010). Transport barriers made of cutin, suberin and associated waxes. Trends Plant Sci. **15,** 546-553.

Schurr, U., Schuberth, B., Aloni, R., Pradel, K.S., Schmundt, D., Jaehne, B., and Ullrich, C.I. (1996). Structural and functional evidence for xylem-mediated water transport and high transpiration in *Agrobacterium tumefaciens*-induced tumors of *Ricinus communis*. Bot. Acta **109,** 405-411.

Schwab, R., Ossowski, S., Riester, M., Warthmann, N., and Weigel, D. (2006). Highly specific gene silencing by artificial microRNAs in *Arabidopsis*. Plant Cell **18,** 1121-1133.

Shanklin, J., and Somerville, C. (1991). Stearoyl-acyl-carrier-protein desaturase from higher plants is structurally unrelated to the animal and fungal homologs. Proc. Natl. Acad. Sci. USA **88,** 2510-2514.

Shanklin, J., and Cahoon, E.B. (1998). Desaturation and Related Modifications of Fatty Acids. Annu. Rev. Plant Physiol. Plant. Mol. Biol. **49,** 611-641.

Shanklin, J., Guy, J.E., Mishra, G., and Lindqvist, Y. (2009). Desaturases: Emerging Models for Understanding FunctionalDiversification of Diiron-containing Enzymes. J. Biol. Chem. **284,** 18559-18563.

Smith, E.F., and Townsend, C.O. (1907). A Plant-Tumor of Bacterial Origin. Science **25,** 671-673.

Smith, E.F., A., B.N., and C.O., T. (1911). Crown gall of plants: its cause and remedy. US Dept. Agric. Bull. **213,** 1-215.

Strain, H.H., Cope, B.T., Svec, W.A., and Anthony San, P. (1971). [42] Analytical procedures for the isolation, identification, estimation, and investigation of the chlorophylls. In Methods in Enzymology, N.P. Kaplan, N.P. Colorwick, A. San Pietro, eds (San Diego, CA, USA: Academic Press) pp. 452-476.

Szyroki, A., Ivashikina, N., Dietrich, P., Roelfsma, M., Ache, P., Reintanz, B., Deeken, R., Godde, M., Felle, H., and Steinmeyer, R. (2001). KAT1 is not essential for stomatal opening. Proc. Natl. Acad. Sci. USA **98,** 2917-2921.

Thompson, G.A., Scherer, D.E., Foxall-Van Aken, S., Kenny, J.W., Young, H.L., Shintani, D.K., Kridl, J.C., and Knauf, V.C. (1991). Primary structures of the precursor and mature forms of stearoyl-acyl carrier protein desaturase from safflower embryos and requirement of ferredoxin for enzyme activity. Proc. Natl. Acad. Sci. USA **88,** 2578-2582.

Tooker, J.F., and De Moraes, C.M. (2009). A Gall-Inducing Caterpillar Species Increases Essential Fatty Acid Content of Its Host Plant Without Concomitan Increases in Phytohormone Levels. Mol. Plant-Microbe Interact. **22,** 551-559.

Torres-Franklin, M.-L., Repellin, A., Huynh, V.-B., d´Arcy-Lameta, A., Zuily-Fodil, Y., and Pham-Thi, A.-T. (2009). Omega-3 fatty acid desaturase (*FAD3, FAD7, FAD8*) gene expression and linolenic acid content in cowpea leaves submitted to drought and after rehydration. Environ. Exp. Bot. **65,** 162-169.

Triantaphylides, C., Krischke, M., Hoeberichts, F.A., Ksas, B., Gresser, G., Havaux, M., Van Breusegem, F., and Mueller, M.J. (2008). Singlet oxygen is the major reactive oxygen species involved in photooxidative damage to plants. Plant Physiol. **148,** 960-968.

Tzfira, T., and Citovsky, V. (2006). *Agrobacterium*-mediated genetic transformation of plants: biology and biotechnology. Curr. Opin. Biotechnol. **17,** 147-154.

Upchurch, R.G. (2008). Fatty acid unsaturation, mobilization, and regulation in the response of plants to stress. Biotechnol. Lett. **30,** 967-977.

van Kooten, O., and Snel, J. (1990). The use of chlorophyll fluorescence nomenclature in plant stress physiology. Photosynth. Res. **25,** 147-150.

Vasconcelles, M.J., Jiang, Y., McDaid, K., Gilooly, L., Wretzel, S., Porter, D.L., Martin, C.E., and Goldberg, M.A. (2001). Identification and characterization of a low oxygen response element involved in the hypoxic induction of a family of *Saccharomyces cerevisiae* genes. Implications for the conservation of oxygen sensing in eukaryotes. J. Biol. Chem. **276,** 14374-14384.

Vergunst, A.C., van Lier, M.C., den Dulk-Ras, A., and Hooykaas, P.J. (2003). Recognition of the *Agrobacterium tumefaciens* VirE2 translocation signal by the VirB/D4 transport system does not require VirE1. Plant Physiol. **133,** 978-988.

Vergunst, A.C., van Lier, M.C., den Dulk-Ras, A., Stuve, T.A., Ouwehand, A., and Hooykaas, P.J. (2005). Positive charge is an important feature of the C-terminal transport signal of the VirB/D4-translocated proteins of *Agrobacterium*. Proc. Natl. Acad. Sci. USA **102,** 832-837.

Wachter, R., Langhans, M., Aloni, R., Gotz, S., Weilmunster, A., Koops, A., Temguia, L., Mistrik, I., Pavlovkin, J., Rascher, U., Schwalm, K., Koch, K.E., and Ullrich, C.I. (2003). Vascularization, high-volume solution flow, and localized roles for enzymes of sucrose metabolism during tumorigenesis by *Agrobacterium tumefaciens*. Plant Physiol. **133,** 1024-1037.

Warburg, O. (1930). The Metabolism of Tumors. (London: Arnold Constable).

Whittle, E., Cahoon, E.B., Subrahmanyam, S., and Shanklin, J. (2005). A multifunctional acyl-acyl carrier protein desaturase from *Hedera helix* L. (English ivy) can synthesize 16- and 18-carbon monoene and diene products. J. Biol. Chem. **280,** 28169-28176.

Yan, B., Dai, Q., Liu, X., Huang, S., and Wang, Z. (1996). Flooding-induced membrane damage, lipid oxidation and activated oxygen generation in corn leaves. Plant Soil **179,** 261-268.

Yotnda, P., Wu, D., and Swanson, A.M. (2010). Hypoxic tumors and their effect on immune cells and cancer therapy. Methods Mol. Biol. **651,** 1-29.

Zaenen, I., Van Larebeke, N., Van Montagu, M., and Schell, J. (1974). Supercoiled circular DNA in crown-gall inducing *Agrobacterium* strains. J. Mol. Biol. **86,** 109-127.

Zhang, M., Barg, R., Yin, M., Gueta-Dahan, Y., Leikin-Frenkel, A., Salts, Y., Shabtai, S., and Ben-Hayyim, G. (2005). Modulated fatty acid desaturation via overexpression of two distinct omega-3 desaturases differentially alters tolerance to various abiotic stresses in transgenic tobacco cells and plants. Plant J. **44,** 361-371.

Zur, I., Skoczowski, A., Niemczyk, E., and Dubert, F. (2002). Changes in the composition of fatty acids and sterols of membrane lipids during induction and differentation of *Brassica napus* (var. *oleifera* L.) callus. Acta Physiol. Plant. **24,** 3-10.

8. Supplement

8.1 T-DNA insertion lines

A

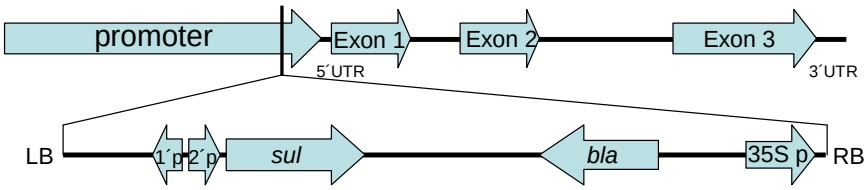

B

gacaaatttaacttttttaaacaaaacccacagaatctcaa~T-DNA~accagttagcacccctttgtttcaccccac
ggtttgtttaacgaacaacagccaaccaccaaattactattataccctcatcaccatttgactatttattagtccacactc
tatagtagttgttacattcaaagaactccaaagtaaattaaagtcttctctacttcaccataaaaaATGCTTGCG
CACAAGTCTCTTCTCTCCTTTACCACCCAATGGGCTACACTAATGCCA
TCTCCGTCTACTTTTCTCGCCTCTCGCCCCCGT

Supplemental figure 1. *Arabidopsis* line (ecotype Col-0) with a T-DNA insertion in the *SAD6* locus (At1g43800). (A) Position and structure of the T-DNA in the *SAD6* promoter region of the GABI-Kat line gk30d04. (B) DNA sequence details next to the position of the T-DNA insertion site in line gk30d04. The transcriptional start site and the translational start site are indicated by "cat" and "ATG", respectively.

A

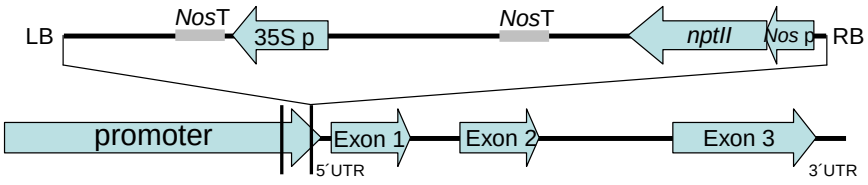

B

gacaaatttaacttttttaaacaaaacccacagaatctcaaaccagttagcacccctttgtttcaccccacggtttgtttaa
cgaacaacagccaaccaccaaattactattataccctcatcaccatttgactatttatt~T-DNA~agtccacactc
tatagtagttgttacattcaaagaactccaaagtaaattaaagtcttctctacttcaccataaaaaATGCTTGCG
ACAAGTCTCTTCTCTCCTTTACCACCCAATGGGCTACACTAATGCCAT
CTCCGTCTACTTTTCTCGCCTCTCGCCCCCG

Supplemental figure 2. *Arabidopsis* line (ecotype Col-0) with a T-DNA insertion in the *SAD6* locus (At1g43800). (A) Position and structure of the T-DNA in the *SAD6* promoter region of the Salk line 70018. (B) DNA sequence details next to the position of the T-DNA insertion site in line Salk70018. The transcriptional start site and the translational start site are indicated by "cat" and "ATG", respectively.

A

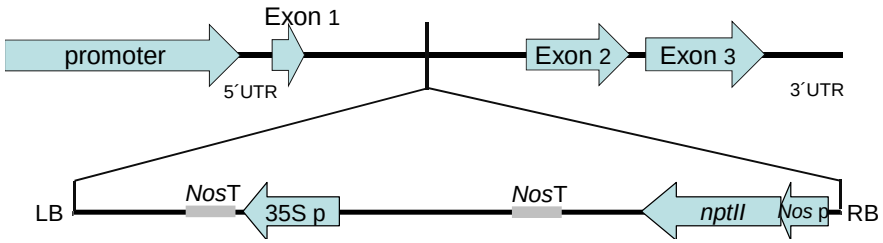

B

cttcttagtcaaagagaaagttttgttttgttttctctggtttagtaatttttaatggtgaaatgtttatccacttgtttcttactc
atttgatgagttttctcttttgtattgacaagagattcttgaacgtatcagtttacgtctgtttatctttcttcaaa~T-DN
A~agacattacgttggatatcacgcttcgtggcctttctctatgcatgcgtacttcgtggcttctctctttagtttgcgtc
caaaattttcacacttttctgtaatttattattcattctttctctgttttgaagacatttggctctttatcttgtctttgtctgatca
gtagtcactacatttgtt

Supplemental figure 3. *Arabidopsis* line (ecotype Col-0) with T-DNA insertion in the *SSI2/FAB2* locus (At2g43710). (A) Position and structure of the T-DNA in the *SSI2/FAB2* locus of the Salk line salk039862. (B) DNA sequence details next to the position of the T-DNA insertion site in line salk039862.

8.2 Sequences and vectors

8.2.1 DNA Sequences

At1g43800 (*SAD6)* CDS

Atgcttgcgcacaagtctcttctctcctttaccacccaatgggctacactaatgccatctccgtctacttttctcgcctctcgcccccgtggaccggccaagatctcggc
cgtggcagcaccagtgaggccggctctaaaacaccaaaacaaaatccacaccatgccaccggagaaaatggagatattcaaatctttagatggatgggccaagga
tcaaatcttgcctcttctcaaacccgttgaccaatgttggcaacccgcttctttcttacccgacccggccttacccttctccgagtttaccgaccaggttcgtgagctgag
ggaaagaacggcctcgctgccagacgaatacttcgtggtgttggttggagatatgataacggaggacgcgttgcctacttaccagacgatgatcaacacccttgatg
gcgtaagggacgagactggtgcgagtgagagcgcgtgggcaagttggacacgagcgtggacggctgaggagaaccgtcatggtgatttgttgcggacttacttgt
acttatccggtcgtgttgatatgcttatggttgaacgcaccgttcagcatctcatcggctcgggcatggatccaggaactgagaacaatccatacttaggtttcgtgtac
acgtcattccaagagcgagccacatttgtgtctcacggcaacacggcaaggctagccaagtccgcaggagatcctgtcctcgctcgcatctgcggaaccattgcag
ctgacgagaagcgccatgaaaacgcttacgtacgcatcgttgagaagctcctcgagatcgaccctaacggtgcagtctcagccgtggccgacatgatgcggaaga
agatcacaatgccggctcatctaatgacagacggtcgagacccgatgctattcgaacatttctccgccgtggctcagcggctagaggtttacacggcggatgattac
gctgacatcttggagtttttggttggacggtggagattggagaagctagaaggattgacgggtgagggccaacgtgcacaggagtttgtgtgtgggttagctcagag
gattagacgccttcaagagcgtgcagacgagagagctaagaagcttaagaagacccatgaggtttgctttagttggatcttcgataagcagattagtgtgta

At1g43800 (*SAD6) CDS*:V5:HIS6

atgcttgcgcacaagtctcttctctcctttaccacccaatgggctacactaatgccatctccgtctacttttctcgcctctcgcccccgtggaccggccaagatctcggcc
gtggcagcaccagtgaggccggctctaaaacaccaaaacaaaatccacaccatgccaccggagaaaatggagatattcaaatctttagatggatgggccaaggat
caaatcttgcctcttctcaaacccgttgaccaatgttggcaacccgcttctttcttacccgacccggccttacccttctccgagtttaccgaccaggttcgtgagctgagg
gaaagaacggcctcgctgccagacgaatacttcgtggtgttggttggagatatgataacggaggacgcgttgcctacttaccagacgatgatcaacacccttgatgg
cgtaagggacgagactggtgcgagtgagagcgcgtgggcaagttggacacgagcgtggacggctgaggagaaccgtcatggtgatttgttgcggacttacttgta
cttatccggtcgtgttgatatgcttatggttgaacgcaccgttcagcatctcatcggctcgggcatggatccaggaactgagaacaatccatacttaggtttcgtgtaca
cgtcattccaagagcgagccacatttgtgtctcacggcaacacggcaaggctagccaagtccgcaggagatcctgtcctcgctcgcatctgcggaaccattgcagc
tgacgagaagcgccatgaaaacgcttacgtacgcatcgttgagaagctcctcgagatcgaccctaacggtgcagtctcagccgtggccgacatgatgcggaagaa
gatcacaatgccggctcatctaatgacagacggtcgagacccgatgctattcgaacatttctccgccgtggctcagcggctagaggtttacacggcggatgattacg
ctgacatcttggagtttttggttggacggtggagattggagaagctagaaggattgacgggtgagggccaacgtgcacaggagtttgtgtgtgggttagctcagagg

attagacgccttcaagagcgtgcagacgagagagctaagaagcttaagaagacccatgaggtttgctttagttggatcttcgataagcagattagtgtgaagggtcaa
gacaattctgcagatatccagcacagtggcggccgctcgagtctagagggcccgcggttcgaaggtaagcctatccctaaccctctcctcggtctcgattctacgcg
taccggtcatcatcaccatcaccat

At1g43800 (*SAD6*) promoter

ttgtgtgtgaatcatttgtttggtgaaataaaaaaaaagcatctgaaatatttatttaaattctttggacaaagatggttcttcaaacttgggttggtgaatggtgatggttttta
tgttctaggagcgaacttttatctctatctctctaagaaaagtaatctttcaaaaaaaactgtagagaaataaaatagatagttgtttttggttaaaacagataatttgtaactg
taactcgataagaatattaattaaaaaaaacatacaatgtcaaatgaaatcatacttaaaattggacatttttctatttgaaaacttggtattggtatactaacacatataccat
gttaatcttctcattatagttctacttaatatttaccaaaacaaaacaaaaaaaacaattatacgtatttaattaacaaaacaaatacattaattctgaagatggagaaaaaaa
ttgtgtcttgataatgctaacttaccaagtctccatacatgataagaaaattacacacacatatatatatatatataaatatgtcatatataagtttatttttgagctaaatctt
caaaaagtttctattgtaatttctaagcttaaacaaaaattgatacattcattgtctaatactgttctggttgaattcaattttatattcaattaaaattaatattttcttaccaaaca
tcacattcatacataaaataaacattggaattatcattctgaaactaatacaacatttaaatattagaaatcctataaaataaaaattcgtcctttctttttctttgtcaaccataa
gatccaatggctcgttgaatacgtagttacgtacaactggcattctcgtgtacaaagtcactaaaacaaaaacaaaatccattatagatattaaaacgactaaatttaatta
tagcaataacaattgaacagcaagatcacaaatttagaattcaagagcttaaaaaattcattaaaagtagaaaaatacaaaaataatacattaaaattcaaagttcatata
attggaagtaaaaagaaatttttttatcactctcaagttttgtcttaaatgggacaaatttaacttttaaacaaaacccacagaatctcaaaccagttagcacccctttgtttc
accccacggtttgtttaacgaacaacagccaaccaccaaattactattataccctcatcaccatttgactatttattagtccacactctatagtagttgttacattcaaagaa
ctccaaagtaaattaaagtcttctctacttcaccataaaaa

AmiRNAi 319 stem and loop

caaacacacgctcggacgcatattacacatgttcatacacttaatactcgctgttttgaattgatgttttaggaatatatatgtagagagagcttccttgagtccattcacag
gtcgtgatatgattcaattagcttccgactcattcatccaaataccgagtcgccaaaattcaaactagactcgttaaatgaatgaatgatgcggtagacaaattggatcat
tgattctctttgattggactgaagggagctccctctctctttttgtattccaattttcttgattaatctttcctgcacaaaaacatgcttgatccactaagtgacatatatgctgcc
ttcgtatatatagttctggtaaaattaacattttgggtttatctttatttaaggcatcgccatg

At1g43800 (*SAD6*) AmiRNAi, overlapping PCR product

Ctgcaaggcgattaagttgggtaacgccagggttttcccagtcacgacgttgtaaaacgacggccagtgaattgtaatacgactcactatagggcgaattgggtacc
gggcccccccctcgaggtcgacggtatcgataagcttgatatcgaattcctgcagccccaaacacacgctcggacgcatattacacatgttcatacacttaatactcgct
gttttgaattgatgttttaggaatatatatgtagagacgatgctattggaacattatcacaggtcgtgatatgattcaattagcttccgactcattcatccaaataccgagtcg
ccaaaattcaaactagactcgttaaatgaatgaatgatgcggtagacaaattggatcattgattctctttgataatgttcgaatagcatcggctctctcttttgtattccaattt
tcttgattaatctttcctgcacaaaaacatgcttgatccactaagtgacatatatgctgccttcgtatatatagttctggtaaaattaacattttgggtttatctttatttaaggca
tcgccatgggggatccactagttctagagcggccgccaccgcggtggagctccagcttttgttcccttagtgagggttaattccgagcttggcgtaatcatggtcat
agctgtttcctgtgtgaaattgttatccgc

Quantitative realtime RT-PCR product At1g43800 (*SAD6*)

atctaatgacagacggtcgagacccgatgctattcgaacatttctccgccgtggctcagcggctagaggtttacacggcggatgattacgctgacatcttggagttttt
ggttggacggtggagattggagaagctagaaggattgacgggtgagggccaacgtgcacaggagtttgtgtgtgggttagctcagaggattagacgccttcaaga
gcgtgcagacgagagagctaagaagcttaagaagacccatgaggtttgctttagttggatcttcgataagca

Quantitative realtime RT-PCR product At2g43710 (*SSI2*)

cagttggatacacgacagagaagtgcagctctaaaaggacaaagacaaaaacaaaaacctatcctcccggttcctcatttcatctgtctgctcttaaaattggtgtaga
ttactatggttttctgataatgttggtgggtctagttacaaagttgagatgcagtgatttagtagctttgtttttcccagtcactatatgtttggtctttggtccgttagcacactt
gtagtagttaaaacagtttaagtatggtctgtactcagtcttcctcttctctgtggagttttgtttaagttcaggttagttttgttttgtctctctgttttttcccctgtttctcgacaa
acaactcatgtggctttttagc

Quantitative realtime RT-PCR product At2g29980 (*FAD3*)

Tcacgacattggaactcacgtgatccatcatctcttcccacaaatccctcactatcacttggtcgacgccacgaaagcagctaaacatgtgttgggaagatactacag
agaaccaaagacgtcaggagcaataccgatccacttggtggagagtttggtcgcaagtattaagaaagatcattacgtcagcgacactggtgatattgtcttctacga
gacagatccagatctctacgtttacgcttctgacaaat

8.2.2 Protein sequences

At2g43710 (SSI2/FAB2)

MALKFNPLVASQPYKFPSSTRPPTPSFRSPKFLCLASSSPALSSGPKEVESLKKPFTPPREVHVQVLHSMP
PQKIEIFKSMENWAEENLLIHLKDVEKSWQPQDFLPDPASDGFEDQVRELRERARELPDDYFVVLVGD
MITEEALPTYQTMLNTLDGVRDETGASPTSWAIWTRAWTAEENRHGDLLNKYLYLSGRVDMRQIEKTI
QYLIGSGMDPRTENNPYLGFIYTSFQERATFISHGNTARQAKEHGDIKLAQICGTIAADEKRHETAYTKI
VEKLFEIDPDGTVMAFADMMRKKISMPAHLMYDGRNDNLFDNFSSVAQRLGVYTAKDYADILEFLVG
RWKIQDLTGLSGEGNKAQDYLCGLAPRIKRLDERAQARAKKGPKIPFSWIHDREVQL

At5g16240 (SAD1)

MVMAMDRIALFSSSSSVYHHGSSHSHGSKSSRVFTIRSDSTAVGRKLYIPPREVHLQVKYSMPPQKLEIF
KSLEGWANDNLLAYLKPVEKSWQPTDFLPEPESEGFYDQVKELRERCKELSDDYLIVLVGDMITEEALP
TYQTMINTLDGVRDETGASPTPWAVWTRAWTAEENRHGDLLNKYLYLSGRVDMRQIEKTIQYLIGSG
MDPKTENNPYLGFIYTSFQERATFISHGNTARLAKDLGDLTLGKICGTIAADERRHEHAYTKIVEKLFEID
PDTTVVGFADMMRKKISMPAHLMYDGRDDNLFDHFSSVAQRLGVYTAKDYADILQHLVERWNVEKL
SDLSSEGNRAQDYLCGLPARIRKLEERAQGRTKEAAKNIPFSWIFGREVRA

At3g02610 (SAD2)

MKMALLLNSTITVAMKQNPLVAVSFPRTTCLGSSFSPPRLLRVSCVATNPSKTSEETDKKKFRPIKEVPN
QVTHTITQEKLEIFKSMENWAQENLLSYLKPVEASWQPQDFLPETNDEDRFYEQVKELRDRTKEIPDDY
FVVLVGDMITEEALPTYQTTLNTLDGVKDETGGSLTPWAVWVRAWTAEENRHGDLLNKYLYLSGRVD
MRHVEKTIQYLIGSGMDSKFENNPYNGFIYTSFQERATFISHGNTAKLATTYGDTTLAKICGTIAADEKR
HETAYTRIVEKLFEIDPDGTVQALASMMRKRITMPAHLMHDGRDDDLFDHYAAVAQRIGVYTATDYA
GILEFLLRRWEVEKLGMGLSGEGRRAQDYLCTLPQRIRRLEERANDRVKLASKSKPSVSFSWIYGREVE
L

At5g16230 (SAD3)

MSMALLLTSPAMKQKPAVITSPRRGSSPSRRLRVSCVTTNPARKKNETCNHFRPIKEVNNQLTHTIPQEK
LEIFKSMENWAEQKLLPYLKPVEDSWQPQDFLPAPENDDEFYDRVKEIRERTKEIPDDYFVVLVGDMIT
EEALPTYQTTLNTLDGVKDETGGSLSPWAVWIRAWTAEENRHGDLLNKYLYLTGRVDMRHVEKTIQY
LIGSGMDSKFENNPYNGFIYTSFQERATFISHGNTARLATTYGDVTLAKICGTIAADEKRHETAYTKIVE
KLFEIDPDGSVQALASMMKKRITMPAHLMHDGRDNDLFDHYAAVAQRIGVYTAADYAGILEFLLRRW
KVESLGLGLSGEGRRAQEYLCTLPQRIKRLEERANDRVKLVSKPSVSFSWVFGRDVKL

At3g02620 (SAD4)

MALLLNSTMTVAMKQNPATAVSFMQTTCLGSSFSPPRHLQVSCVATNPSKTFRPIKEVSNQVTHTITQE
KLEIFKSMENWAQENLLSYLKPVETSWQPQDFLPETKDEDRFYEQVKELRDRTKEIPDDYFVVLVGDMI
TEEALPTYQTVMNTLDGAKDETGVSLTPWAVWLRAWTAEENRHGDLLNKYLYLSGRVDTRHVEKTIQ
YLIGSGMDTKYENNPYNGYIYTSFQERATFISHANTAKLATTYGDTTLAKICGTIAADEKRHEMAYTRI
VEKLFEIDPDGTVQALASMMRKRITMPAQLMHDGRDDNLFDHYAAVAQRIGVYTATDYAGILEFLLRR
WEVEKLGMGLSGEGRRAQDYLCTLPQRIRRLEERADDRVKRASKSKPSVSFSWIYGREVEL

At3g02630 (SAD5)

MAMAMDRIVFSPSSYVYRPCQARGSRSSRVSMASTIRSATTEVTNGRKLYIPPREVHVQVKHSMPPQKL
EIFKSLEGWADETLLTYLKPVEKSWQPTDFLPEPESEGFYDQVKELRERCKELPDDYFVVLVGDMITEE
ALPTYQTMLNTLDGVRDETGASPTPWAIWTRAWTAEENRHGDLLNKYLYLSGRVDMRQIEKTIQYLIG
SGMDPKTENNPYLGFIYTSFQERATFISHGNTARLAKDRGDLKLAQICGTIAADERRHETAYTKIVEKLF
EIDPDGTILGLADMMKKKISMPAHLMYDGQDDNLFEHFSTVAQRLGVYTAKDYADILEFLVERWNVET
LTDLSSEGHRAQDFVCGLPARIRKIEERAQGRAKEAAKNIPFSWIFGRNIRA

At1g43800 (SAD6)

MLAHKSLLSFTTQWATLMPSPSTFLASRPRGPAKISAVAAPVRPALKHQNKIHTMPPEKMEIFKSLDGW
AKDQILPLLKPVDQCWQPASFLPDPALPFSEFTDQVRELRERTASLPDEYFVVLVGDMITEDALPTYQT
MINTLDGVRDETGASESAWASWTRAWTAEENRHGDLLRTYLYLSGRVDMLMVERTVQHLIGSGMDP
GTENNPYLGFVYTSFQERATFVSHGNTARLAKSAGDPVLARICGTIAADEKRHENAYVRIVEKLLEIDPN
GAVSAVADMMRKKITMPAHLMTDGRDPMLFEHFSAVAQRLEVYTADDYADILEFLVGRWRLEKLEG
LTGEGQRAQEFVCGLAQRIRRLQERADERAKKLKKTHEVCFSWIFDKQISV

At3g12120 (FAD2)

MGAGGRMPVPTSSKKSETDTTKRVPCEKPPFSVGDLKKAIPPHCFKRSIPRSFSYLISDIIIASCFYYVATN
YFSLLPQPLSYLAWPLYWACQGCVLTGIWVIAHECGHHAFSDYQWLDDTVGLIFHSFLLVPYFSWKYS
HRRHHSNTGSLERDEVFVPKQKSAIKWYGKYLNNPLGRIMMLTVQFVLGWPLYLAFNVSGRPYDGFA
CHFFPNAPIYNDRERLQIYLSDAGILAVCFGLYRYAAAQGMASMICLYGVPLLIVNAFLVLITYLQHTHP
SLPHYDSSEWDWLRGALATVDRDYGILNKVFHNITDTHVAHHLFSTMPHYNAMEATKAIKPILGDYYQ
FDGTPWYVAMYREAKECIYVEPDREGDKKGVYWYNNKL

At2g29980 (FAD3)

MVVAMDQRTNVNGDPGAGDRKKEERFDPSAQPPFKIGDIRAAIPKHCWVKSPLRSMSYVVRDIIAVAA
LAIAAVYVDSWFLWPLYWAAQGTLFWAIFVLGHDCGHGSFSDIPLLNSVVGHILHSFILVPYHGWRISH
RTHHQNHGHVENDESWVPLPERVYKKLPHSTRMLRYTVPLPMLAYPLYLCYRSPGKEGSHFNPYSSLF
APSERKLIATSTTCWSIMFVSLIALSFVFGPLAVLKVYGVPYIIFVMWLDAVTYLHHHGHDEKLPWYRG
KEWSYLRGGLTTIDRDYGIFNNIHHDIGTHVIHHLFPQIPHYHLVDATKAAKHVLGRYYREPKTSGAIPI
HLVESLVASIKKDHYVSDTGDIVFYETDPDLYVYASDKSKIN

At4g30950 (FAD6)

MASRIADSLFAFTGPQQCLPRVPKLAASSARVSPGVYAVKPIDLLLKGRTHRSRRCVAPVKRRIGCIKAV
AAPVAPPSADSAEDREQLAESYGFRQIGEDLPENVTLKDIMDTLPKEVFEIDDLKALKSVLISVTSYTLGL
FMIAKSPWYLLPLAWAWTGTAITGFFVIGHDCAHKSFSKNKLVEDIVGTLAFLPLVYPYEPWRFKHDRH
HAKTNMLVHDTAWQPVPPEEFESSPVMRKAIIFGYGPIRPWLSIAHWVNWHFNLKKFRASEVNRVKISL
ACVFAFMAVGWPLIVYKVGILGWVKFWLMPWLGYHFWMSTFTMVHHTAPHIPFKPADEWNAAQAQ
LNGTVHCDYPSWIEILCHDINVHIPHHISPRIPSYNLRAAHESIQENWGKYTNLATWNWRLMKTIMTVC
HVYDKEENYIPFDRLAPEESQPITFLKKAMPNYTA

At3g11170 (FAD7)

MANLVLSECGIRPLPRIYTTPRSNFLSNNNKFRPSLSSSSYKTSSSPLSFGLNSRDGFTRNWALNVSTPLTT
PIFEESPLEEDNKQRFDPGAPPPFNLADIRAAIPKHCWVKNPWKSLSYVVRDVAIVFALAAGAAYLNNW
IVWPLYWLAQGTMFWALFVLGHDCGHGSFSNDPKLNSVVGHLLHSSILVPYHGWRISHRTHHQNHGH
VENDESWHPMSEKIYNTLDKPTRFFRFTLPLVMLAYPFYLWARSPGKKGSHYHPDSDLFLPKERKDVLT
STACWTAMAALLVCLNFTIGPIQMLKLYGIPYWINVMWLDFVTYLHHHGHEDKLPWYRGKEWSYLRG
GLTTLDRDYGLINNIHHDIGTHVIHHLFPQIPHYHLVEATEAAKPVLGKYYREPDKSGPLPLHLLEILAKS
IKEDHYVSDEGEVVYYKADPNLYGEVKVRAD

At5g05580 (FAD8)

MASSVLSECGFRPLPRFYPKHTTSFASNPKPTFKFNPPLKPPSSLLNSRYGFYSKTRNWALNVATPLTTL
QSPSEEDTERFDPGAPPPFNLADIRAAIPKHCWVKNPWMSMSYVVRDVAIVFGLAAVAAYFNNWLLWP
LYWFAQGTMFWALFVLGHDCGHGSFSNDPRLNSVAGHLLHSSILVPYHGWRISHRTHHQNHGHVEND
ESWHPLPESIYKNLEKTTQMFRFTLPFPMLAYPFYLWNRSPGKQGSHYHPDSDLFLPKEKKDVLTSTAC
WTAMAALLVCLNFVMGPIQMLKLYGIPYWIFVMWLDFVTYLHHHGHEDKLPWYRGKEWSYLRGGLT
TLDRDYGWINNIHHDIGTHVIHHLFPQIPHYHLVEATEAAKPVLGKYYREPKNSGPLPLHLLGSLIKSMK
QDHFVSDTGDVVYYEADPKLNGQRT

8.2.3 PCR primers

Supplemental table 1. T-DNA screening primers

Gene locus	**T-DNA collection ID**	**Primer name**	**Primer sequence 5´-3´**	**Amplicon size (bp)**	**Annealing temperature (°C)**
At1g43800 (*SAD6*)	Gk30d04	Left border primer	ATATTGACC ATCATACTCA TTGC	With right genomic primer:500-600	With right genomic primer: 55
		Left genomic primer	CCATCCATCT AAAGA		
		Right genomic primer	CTCCATACAT GATAAGAA	With left border primer: 1,020	With left border primer: 55
At1g43800 (*SAD6*)	Salk70018	Left border primer	ATTTTGCCGA TTTCGGAAC	With right genomic primer: 500-600	With right genomic primer: 50
		Left genomic primer	CGCGTCCTCC GTTATCA		
		Right genomic primer	CGTACAACT GGCATTCTCG	With left border primer: 1,040	With left border primer: 50
At2g43710 (*SSI2/FAB2*)	Salk039852	Left border primer	ATTTTGCCGA TTTCGGAAC	With right genomic primer: 500-600	With right genomic primer: 55
		Left genomic primer	GTCGGAAGT GCTTCTTCTG TG		
		Right genomic primer	ATAAGAATG GGCCATCCTC TG	With left border primer: 1,148	With left border primer: 55

Supplemental table 2. Quantitative real time RT PCR primers

Gene locus	**Direction**	**Primer sequence 5´-3´**	**Amplicon size (bp)**	**Annealing temperature (°C)**	**Melting point (°C)**	**Primer mix**
At3g18780 (*ACT2*); At1g49240 (*ACT8*)	sense	ACTGAGC ACAATGT TAC	435	50-60	87	6
	antisense	GGTGATG GTGTGTC T				
At1g43800 (*SAD6*)	sense	ATCTAAT GACAGAC GG	286	57-60	87.8	6
	antisense	TGCTTATC GAAGATC CA				
At2g43710 (*SSI2/FAB2*)	sense	CAGTTGG ATACACG AC	368	55-60	82.6	12
	antisense	GCTAAAA AGCCACA TGA				
FAD3 (At2g29980)	sense	TCACGAC ATTGGAA CT	254	51-60	85	12
	antisense	ATTTGTC AGAAGCG TA				

Supplemental table 3. Primers used for cloning

Cloning step	**Primer name**	**Primer sequence 5´-3´**	**Amplicon size (bp)**	**Annealing temperature (°C)**	**Vector**
At1g43800 (*SAD6*) promoter from *Arabidopsis* (ecotype WS-2) genomic DNA into pCR8/GW-TOPO® (2.8.2)	SAD6 promoter sense	TTGTGTGTGAATCATTTGTTTGGTG	1,303	55	pCR8/GW-TOPO-$SAD6_{PRO}$:GUS
	SAD6 promoter antisense	TTTTATGGTGAAGTAGAGAAGACTTTAATTTAC			
$SAD6_{CDS}$:V5:HIS from pcDNA™3.1-D-V5/His-TOPO-$SAD6_{CDS}$ into pCambia2300 (2.8.5)	SAD6 V5 HIS6 sense	GGCTTAUTCGGATCCAGTAC	1,330	55	pCambia2300-$SAD6_{CDS}$:V5:HIS6
	SAD6 V5 HIS6 antisense	GGTTTAAUTCAATGGTGATGG			
At1g43800 (*SAD6*) CDS without stop codon from *Arabidopsis* (ecotype WS-2) cDNA into pcDNA3.1-D-V5/His-TOPO (2.8.3)	SAD6 CDS oS sense	CACCATGCTTGCGCACAAGTCTCT	1,189	55	pcDNA™3.1-D-V5/His-TOPO-$SAD6_{CDS}$
	SAD6 CDS oS antisense	CACACTAATCTGCTTATCGA			
At1g43800 (*SAD6*) CDS from *Arabidopsis* (ecotype WS-2) cDNA into pCambia3300 (2.8.5)	SAD6 CDS sense	GGCTTAAUATGCTTGCGCACAAGTCTC	1,192	55	pCambia3300-$SAD6_{CDS}$
	SAD6 CDS antisense	GGTTTAAUTTACACACTAATCTGCTTATCGAAGATC			

Supplemental table 4. Primers used for generation of artificial micro RNA

	Primer name	**Primer sequence 5´-3´**	**Amplicon size (bp)**	**Annealing temperature (°C)**
Fragment 1	A sense	CTGCAAGGCGATTAAGTTGGGTAAC	274	55
	microRNA * antisense	GATAATGTTCCAATAGCATCGTCTCTACATATATATTCCT		
Fragment 2	microRNA * sense	GAGACGATGCTATTGGAACATTATCACAGGTCGTGATATG	172	55
	microRNA antisense	GAGCCGATGCTATTCGAACATTATCAAAGAGAATCAATGA		
Fragment 3	microRNA sense	GATAATGTTCGAATAGCATCGGCTCTCTCTTTTGTATTCC	301	55
	B antisense	GCGGATAACAATTTCAC-ACAGGAAACAG		
Overlapping fragment	A1	GGCTTAAUCTGCAAGGC-GATTAAGTTGGGTAAC	701	55
	A2	GGTTTAAUGCGGATAACAATTTCACACAGGAAACAG		

Supplemental table 5. Sequencing primers

Primer name	**Primer sequence 5´-3´**	**Annealing temperature (°C)**
pMDC164 sense	CAGTCACGACGTTGTAAA	55
pMDC164 antisense	CCGGGGATCGATCCTCTA	55
M13 sense	GTAAAACGACGGCCAG	55
M13 antisense	CAGGAAACAGCTATGAC	55
SL sense	AAACACACGCTCGGA	55
SL antisense	CATGGCGATGCCTTAA	55

8.2.4 Vectors

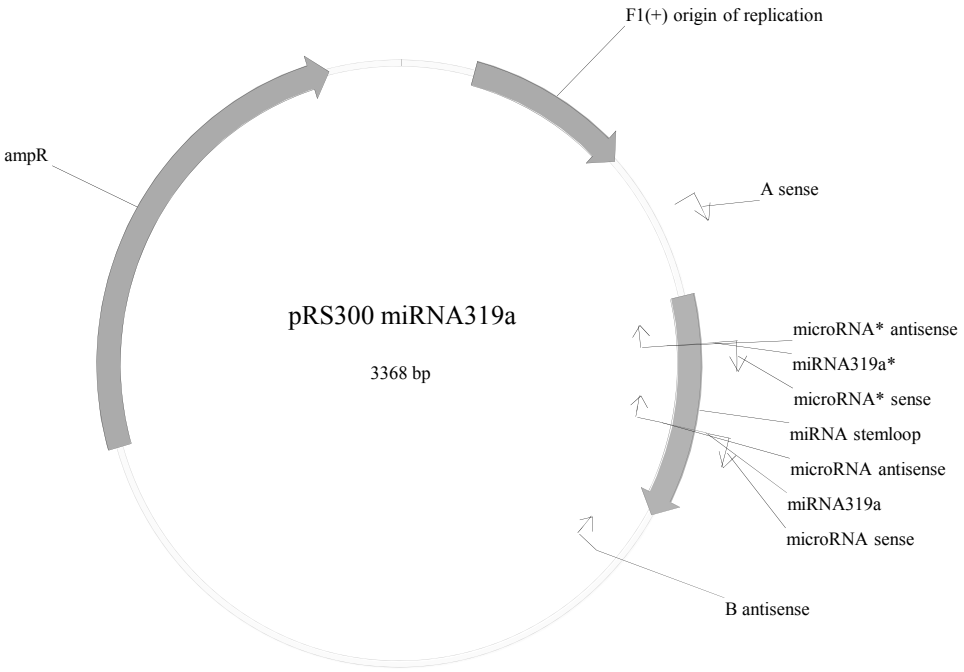

Supplemental figure 4. Vector pRS300 with the stem-loop forming precursor microRNA319a of *Arabidopsis* (pRS300 miRNA319a). The vector was used for generation of a miRNA precursor to knock down *SAD6* gene activity (2.8.1). AmpR, ampicillin resistance gene; A sense, B antisense, microRNA sense, microRNA antisense, microRNA* sense, microRNA* antisense, primers used for generation of artificial micro RNA (8.2.3, supplemental table 4).

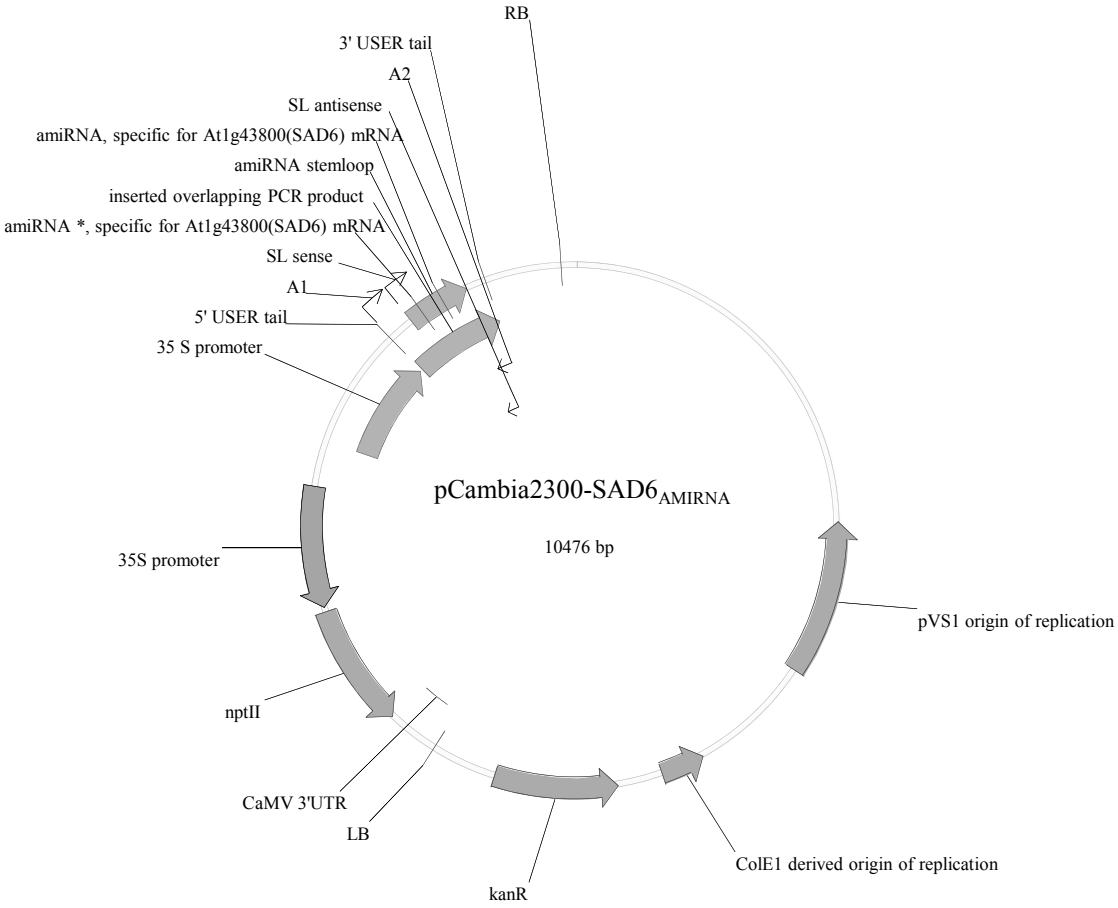

Supplemental figure 5. Binary vector pCambia2300 with the AmiRNA precursor to knock down *SAD6* gene activity (2.8.1 and 2.8.5). A1, A2, primers used for cloning (8.2.3, supplemental table 4); kanR, kanamycin resistance gene; LB, left T-DNA border; nptII, neomycin phosopotransferase; RB, right T-DNA border; SL sense, SL antisense, sequencing primers (8.2.3, supplemental table 5).

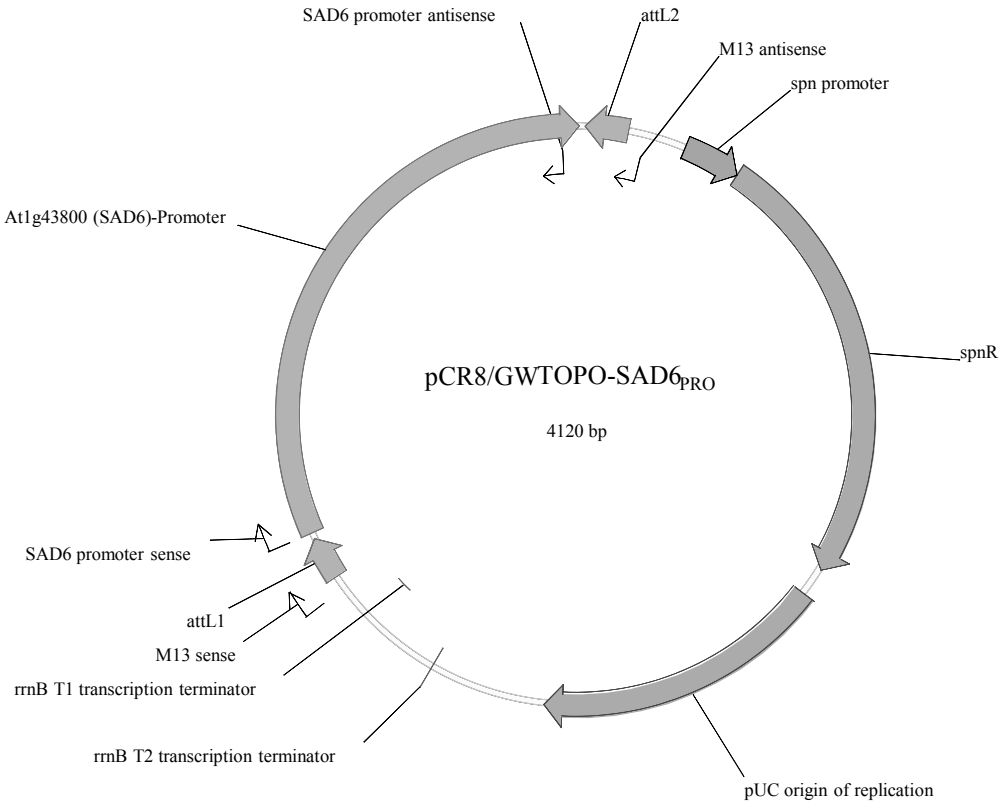

Supplemental figure 6. Entry vector pCR8/GW/TOPO with the At1g43800 (*SAD6*) promoter insertion (pR8/GW-TOPO $SAD6_{PRO}$), used for the Gateway LR reaction (2.8.4). (A)ttL1, attL2, recombination sites; M13 sense, M13 antisense, sequencing primers (8.2.3, supplemental table 5); SAD6 promoter sense, SAD6 promoter antisense, primers used for cloning (8.2.3, supplemental table 4); SpnR, spectinomycin resistance gene.

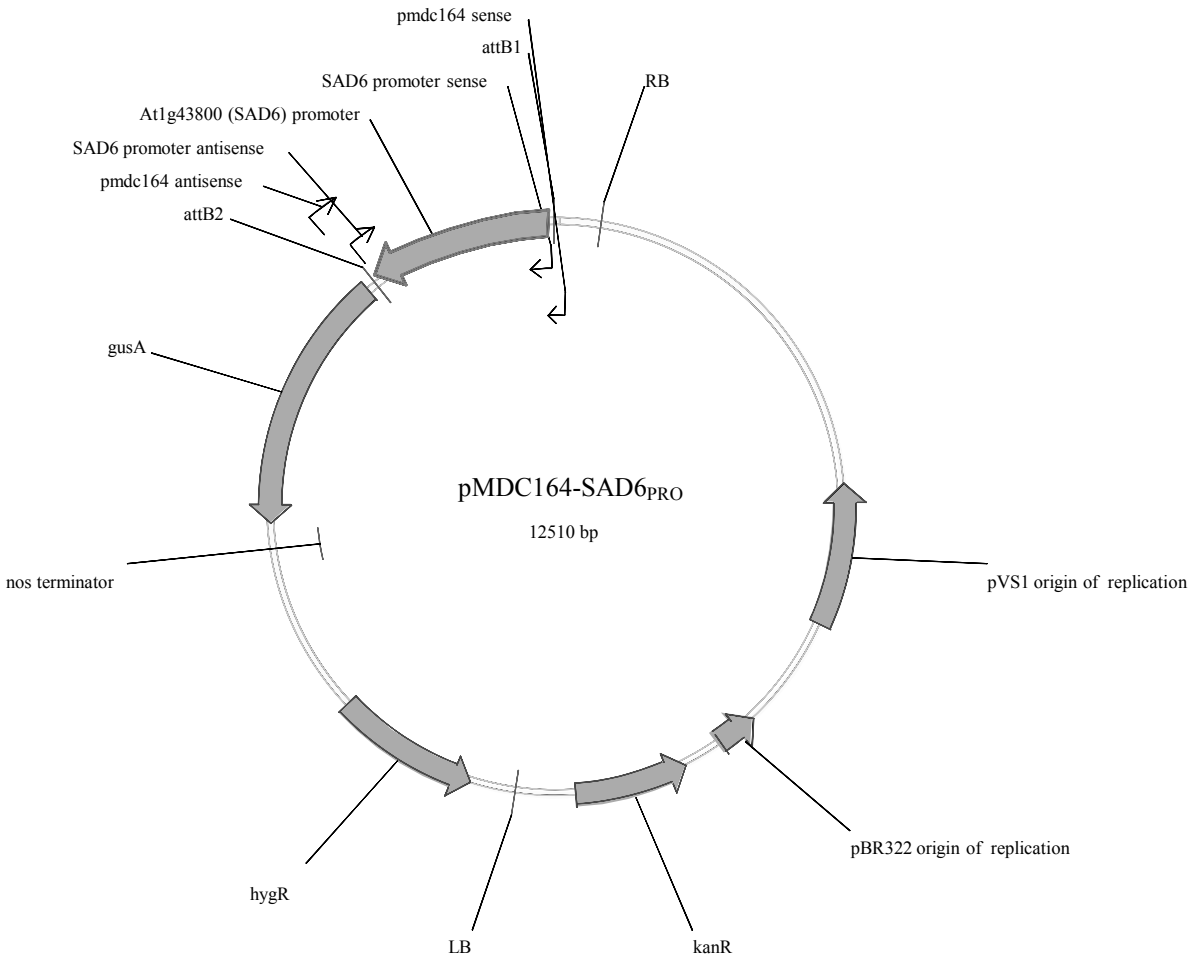

Supplemental figure 7. Recombined destination vector pmd164 with the At1g43800 (*SAD6*) promoter insertion upstream of the beta-glucuronidase gene (gusA; pMDC164-SAD6$_{PRO}$). (A)ttB1, attB2, recombination sites; hygR, hygromycin resistance gene; kanR, kanamycin resistance gene; LB, left T-DNA border, pMDC164 sense, pMDC 164 antisense, sequencing primers (8.2.3, supplemental table 5); RB, right T-DNA border, SAD6 promoter sense, SAD6 promoter antisense, primers used for cloning (8.2.3, supplemental table 4).

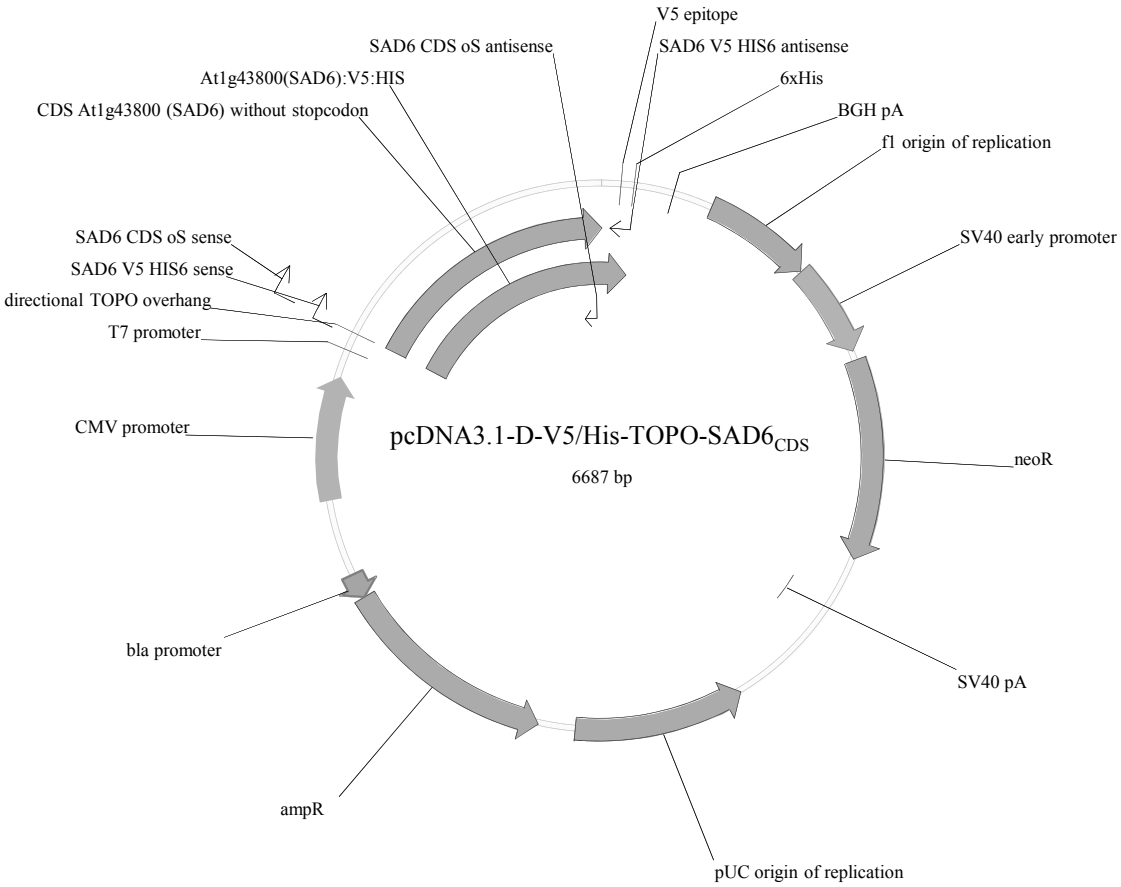

Supplemental figure 8. Vector pcDNA3.1D with the coding sequence (CDS) of At1g43800 (*SAD6*) fused to the V5/HIS6 epitope (pcDNA3.1-D-V/His-TOPO-SAD6$_{CDS}$; 2.8.3). AmpR, ampicillin resistance gene; neoR, neomycin resistance gene; SAD6 CDS os sense, SAD6 CDS os antisense, SAD6 V5 HIS6 sense, SAD6 V5 HIS6, primers used for cloning (8.2.3, supplemental table 4).

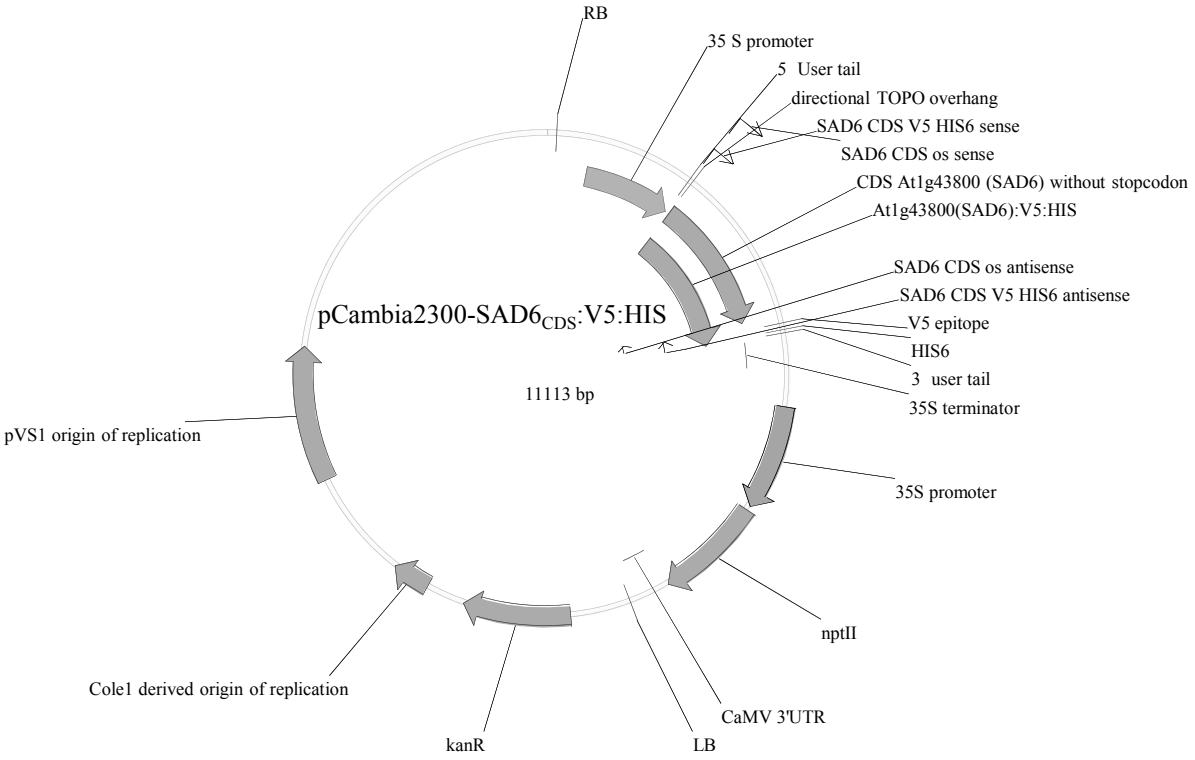

Supplemental figure 9. Binary vector pCambia2300 with the coding sequence (CDS) of At1g43800 (*SAD6*) fused to the V5/HIS6 epitope under 35 S promoter control (pcDNA3.1-D-V/His-TOPO-SAD6$_{CDS}$). AmpR, ampicillin resistance gene; LB, left T-DNA border, nptII, neomycin phosphotransferase 2 gene; RB, right T-DNA border; SAD6 CDS os sense, SAD6 CDS os antisense, SAD6 V5 HIS6 sense, SAD6 V5 HIS6, primers used for cloning (8.2.3, supplemental table 4).

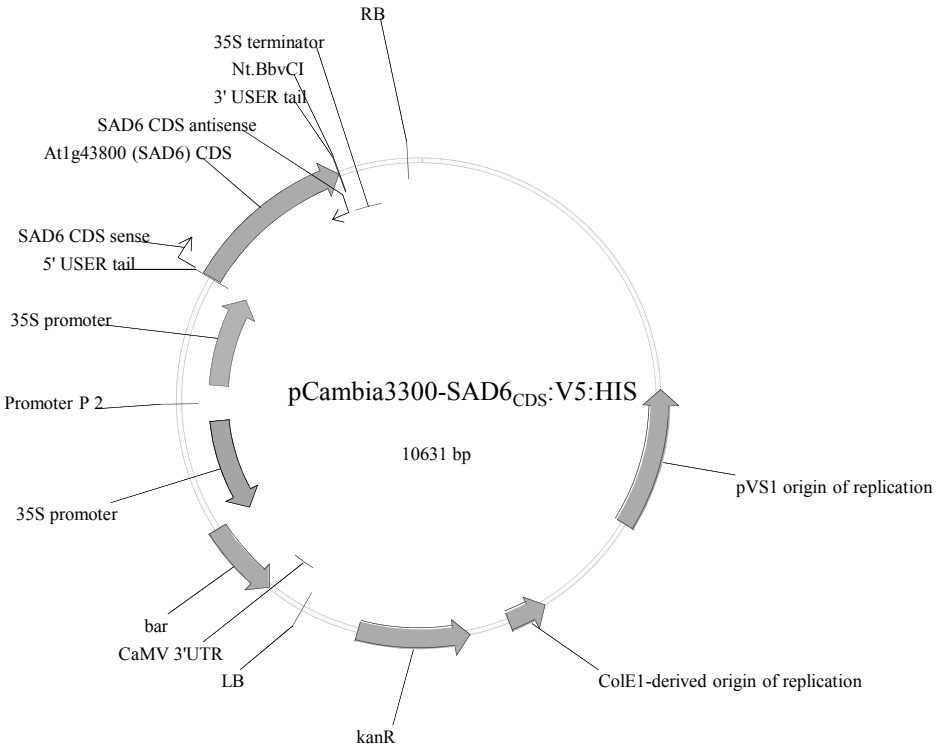

Supplemental figure 10. Binary vector pCambia3300 with the coding sequence (CDS) of At1g43800 (*SAD6*) under 35 S promoter control (pCambia3300-SAD6$_{CDS}$:V5:HIS). AmpR, ampicillin resistance gene; bar, resistance gene against glufosinate (Basta; Bayer, Leverkusen, Germany); LB, left T-DNA border; RB, right T-DNA border; SAD6 CDS sense, SAD6 CDS antisense, primers used for cloning (8.2.3, supplemental table 4).

8.3 Lipids

8.3.1 Multiple Reaction Monitoring (MRM) transitions

Supplemental table 6. MRM transitions for LC-MS/MS of MGDG glycerolipid species.

Glycerolipid species	MRM transition (parent mass > daughter mass)
MGDG-16:3-16:3	717.5 > 249
MGDG-16:3-16:2	719.5 > 249
MGDG-16:3-16:2	719.5 > 251
MGDG-16:3-16:1	721.5 > 249
MGDG-16:2-16:2	721.5 > 251
MGDG-16:3-16:1	721.5 > 253
MGDG-16:3-16:0	723.5 > 249
MGDG-16:2-16:1	723.5 > 251
MGDG-16:2-16:1	723.5 > 253
MGDG-16:3-16:0	723.5 > 255
MGDG-16:2-16:0	725.5 > 251
MGDG-16:1-16:1	725.5 > 253
MGDG-16:2-16:0	725.5 > 255
MGDG-16:1-16:0	727.5 > 253
MGDG-16:1-16:0	727.5 > 255
MGDG-18:3-16:3	745.5 > 249
MGDG-18:3-16:3	745.5 > 277
MGDG-18:3-16:2	747.5 > 251
MGDG-18:3-16:2	747.5 > 277
MGDG-18:3-16:1	749.5 > 253
MGDG-18:3-16:1	749.5 > 277
MGDG-18:1-16:2	751.5 > 251
MGDG-18:3-16:0	751.5 > 255

MGDG-18:3-16:0	751.5 > 277
MGDG-18:1-16:2	751.5 > 281
MGDG-18:0-16:2	753.5 > 251
MGDG-18:1-16:1	753.5 > 253
MGDG-18:1-16:1	753.5 > 281
MGDG-18:0-16:2	753.5 > 283
MGDG-18:0-16:1	755.5 > 253
MGDG-18:1-16:0	755.5 > 255
MGDG-18:1-16:0	755.5 > 281
MGDG-18:0-16:1	755.5 > 283
MGDG-18:0-16:0	757.5 > 255
MGDG-18:0-16:0	757.5 > 283
MGDG-18:3-18:3	773.5 > 277
MGDG-18:3-18:2	775.5 > 277
MGDG-18:3-18:2	775.5 > 279
MGDG-18:3-18:1	777.5 > 277
MGDG-18:2-18:2	777.5 > 279
MGDG-18:3-18:1	777.5 > 281
MGDG-18:3-18:0	779.5 > 277
MGDG-18:2-18:1	779.5 > 279
MGDG-18:2-18:1	779.5 > 281
MGDG-18:3-18:0	779.5 > 283
MGDG-18:2-18:0	781.5 > 279
MGDG-18:1-18:1	781.5 > 281
MGDG-18:2-18:0	781.5 > 283
MGDG-18:1-18:0	783.5 > 281
MGDG-18:1-18:0	783.5 > 283

Supplemental Table 7. MRM transitions for LC-MS/MS of DGDG glycerolipid species.

Lipid species	**MRM transition (parent mass > daughter mass)**
DGDG-16:3-16:3	879.5 > 249
DGDG-16:3-16:2	881.5 > 249
DGDG-16:3-16:2	881.5 > 251
DGDG-16:3-16:1	883.5 > 249
DGDG-16:2-16:2	883.5 > 251
DGDG-16:3-16:1	883.5 > 253
DGDG-16:3-16:0	885.5 > 249
DGDG-16:2-16:1	885.5 > 251
DGDG-16:2-16:1	885.5 > 253
DGDG-16:3-16:0	885.5 > 255
DGDG-16:2-16:0	887.5 > 251
DGDG-16:1-16:1	887.5 > 253
DGDG-16:2-16:0	887.5 > 255
DGDG-16:1-16:0	889.5 > 253
DGDG-16:1-16:0	889.5 > 255
DGDG-18:3-16:3	907.5 > 249
DGDG-18:3-16:3	907.5 > 277
DGDG-18:2-16:3	909.5 > 249
DGDG-18:3-16:2	909.5 > 251
DGDG-18:3-16:2	909.5 > 277
DGDG-18:2-16:3	909.5 > 279
DGDG-18:1-16:3	911.5 > 249
DGDG-18:2-16:2	911.5 > 251
DGDG-18:3-16:1	911.5 > 253
DGDG-18:3-16:1	911.5 > 277
DGDG-18:2-16:2	911.5 > 279
DGDG-18:1-16:3	911.5 > 281
DGDG-18:0-16:3	913.5 > 249
DGDG-18:1-16:2	913.5 > 251
DGDG-18:2-16:1	913.5 > 253
DGDG-18:3-16:0	913.5 > 255
DGDG-18:3-16:0	913.5 > 277
DGDG-18:2-16:1	913.5 > 279
DGDG-18:1-16:2	913.5 > 281
DGDG-18:0-16:3	913.5 > 283
DGDG-18:0-16:2	915.5 > 251
DGDG-18:1-16:1	915.5 > 253
DGDG-18:2-16:0	915.5 > 255
DGDG-18:2-16:0	915.5 > 279
DGDG-18:1-16:1	915.5 > 281

DGDG-18:0-16:2	915.5 > 283
DGDG-18:0-16:1	917.5 > 253
DGDG-18:1-16:0	917.5 > 255
DGDG-18:1-16:0	917.5 > 281
DGDG-18:0-16:1	917.5 > 283
DGDG-18:0-16:0	919.5 > 255
DGDG-18:0-16:0	919.5 > 283
DGDG-18:3-18:3	935.5 > 277
DGDG-18:3-18:2	937.5 > 277
DGDG-18:3-18:2	937.5 > 279
DGDG-18:3-18:1	939.5 > 277
DGDG-18:2-18:2	939.5 > 279
DGDG-18:3-18:1	939.5 > 281
DGDG-18:3-18:0	941.5 > 277
DGDG-18:2-18:1	941.5 > 279
DGDG-18:2-18:1	941.5 > 281
DGDG-18:3-18:0	941.5 > 283
DGDG-18:2-18:0	943.5 > 279
DGDG-18:1-18:1	943.5 > 281
DGDG-18:2-18:0	943.5 > 283
DGDG-18:1-18:0	945.5 > 281
DGDG-18:1-18:0	945.5 > 283

Supplemental Table 8. MRM transitions for LC-MS/MS of PG glycerolipid species.

Lipid species	**MRM transition (parent mass > daughter mass)**
PG-16:1-16:0	719.5 > 253
PG-16:1-16:0	719.5 > 255
PG-16:0-16:0	721.5 > 255
PG-16:1-18:3	741.5 > 253
PG-16:1-18:3	741.5 > 277
PG-16:1-18:2	743.5 > 253
PG-16:0-18:3	743.5 > 255
PG-16:0-18:3	743.5 > 277
PG-16:1-18:2	743.5 > 279
PG-16:1-18:1	745.5 > 253
PG-16:0-18:2	745.5 > 255
PG-16:0-18:2	745.5 > 279
PG-16:1-18:1	745.5 > 281
PG-16:1-18:0	747.5 > 253
PG-16:0-18:1	747.5 > 255
PG-16:0-18:1	747.5 > 281
PG-16:1-18:0	747.5 > 283
PG-16:0-18:0	749.5 > 255
PG-17:0-17:0	749.5 > 269
PG-16:0-18:0	749.5 > 283
PG-18:3-18:3	765.5 > 277
PG-18:3-18:1	769.5 > 277
PG-18:3-18:1	769.5 > 281
PG-18:3-18:0	771.5 > 277
PG-18:2-18:1	771.5 > 279
PG-18:2-18:1	771.5 > 281
PG-18:3-18:0	771.5 > 283
PG-18:2-18:0	773.5 > 279
PG-18:2-18:0	773.5 > 283

Supplemental Table 9. MRM transitions for LC-MS/MS of PC glycerolipid species.

Lipid species	**MRM transition (parent mass > daughter mass)**
PC-16:3-18:3	808.5 > 249
PC-16:3-18:3	808.5 > 277
PC-16:2-18:3	810.5 > 251
PC-16:2-18:3	810.5 > 277
PC-16:1-18:3	812.5 > 253
PC-16:1-18:3	812.5 > 277
PC-16:1-18:2	814.5 > 253
PC-16:0-18:3	814.5 > 255
PC-16:0-18:3	814.5 > 277
PC-16:1-18:2	814.5 > 279

PC-16:0-18:2	816.5 > 255
PC-16:0-18:2	816.5 > 279
PC-16:0-18:1	818.5 > 255
PC-16:0-18:1	818.5 > 281
PC-16:0-18:0	820.5 > 255
PC-17:0-17:0	820.5 > 269
PC-16:0-18:0	820.5 > 283
PC-18:3-18:3	836.5 > 277
PC-18:3-18:2	838.5 > 277
PC-18:3-18:2	838.5 > 279
PC-18:3-18:1	840.5 > 277
PC-18:2-18:2	840.5 > 279
PC-18:3-18:1	840.5 > 281
PC-18:3-18:0	842.5 > 277
PC-18:2-18:1	842.5 > 279
PC-18:2-18:1	842.5 > 281
PC-18:3-18:0	842.5 > 283
PC-18:2-18:0	844.5 > 279
PC-18:2-18:0	844.5 > 283

Supplemental Table 10. MRM transitions for LC-MS/MS of PE glycerolipid species.

Lipid species	**MRM transition (parent mass > daughter mass)**
PE-16:3-18:3	708.5 > 567.5
PE-16:3-18:2	710.5 > 569.5
PE-16:1-18:3	712.5 > 571.5
PE-16:0-18:3	714.5 > 573.5
PE-16:2-18:0	716.5 > 575.5
PE-16:0-18:2	716.5 > 575.5
PE-16:0-18:1	718.5 > 577.5
PE-16:0-18:0	720.5 > 579.5
PE-18:3-18:3	736.5 > 595.5
PE-18:3-18:2	738.5 > 597.5
PE-18:3-18:1	740.5 > 599.5
PE-18:2-18:2	740.5 > 599.5
PE-18:3-18:0	742.5 > 601.5
PE-18:2-18:1	742.5 > 601.5
PE-18:2-18:0	744.5 > 603.5
PE-18:0-18:0	748.5 > 607.5

Supplemental Table 11. MRM transitions for LC-MS/MS of PI glycerolipid species.

Lipid species	**MRM transition (parent mass > daughter mass)**
PI-16:3-18:3	825.5 > 277
PI-16:3-18:3	825.5 > 277
PI-16:3-18:2	827.5 > 249
PI-16:3-18:2	827.5 > 279
PI-16:1-18:3	829.5 > 253
PI-16:1-18:3	829.5 > 277
PI-16:0-18:3	831.5 > 255
PI-16:0-18:3	831.5 > 277
PI-16:0-18:2	833.5 > 255
PI-16:0-18:2	833.5 > 279
PI-16:0-18:1	835.5 > 255
PI-16:0-18:1	835.5 > 281
PI-18:3-18:3	853.5 > 277
PI-18:3-18:2	855.5 > 277
PI-18:3-18:2	855.5 > 279
PI-18:3-18:1	857.5 > 277
PI-18:2-18:2	857.5 > 279
PI-18:3-18:1	857.5 > 281
PI-18:3-18:0	859.5 > 277
PI-18:2-18:1	859.5 > 279
PI-18:2-18:1	859.5 > 281
PI-18:3-18:0	859.5 > 283
PI-18:2-18:0	861.5 > 279
PI-18:2-18:0	861.5 > 283

8.3.2 Lipid analysis of *Arabidopsis* crown galls

Supplemental table 12. Total FA profile in *Arabidopsis* crown gall tumors and mock-inoculated inflorescence stalk tissue (reference).

The relative proportion of a FA species within the total FA pool in mol% was determined by LC-MS/MS in four and five samples each (2.14). Mean values (±SD) were calculated from four and five samples from tumor and the reference, respectively. Ratios were calculated from the mean values of four and five samples from the tumor vs. reference, respectively. Bold numbers mark ratios with an significant difference (P-value≤0.05) between tumors vs. reference. Statistical analysis was performed by using an unpaired two-tailed Student´s t-test.

	Tumor						Reference								
	[mol%]						[mol%]							Tumor vs. Reference	
Fatty acids	Samples				Mean	SD	Samples					Mean	SD	Ratio	P-value
	1	2	3	4			1	2	3	4	5				
16:0	25.08	31.01	22.67	14.67	23.36	6.77	21.01	24.64	17.83	12.19	16.79	18.49	4.67	1.26	0.274
16:1	1.47	1.32	2.57	1.64	1.75	0.56	1.11	1.35	1.64	1.58	2.06	1.55	0.35	1.13	0.559
16:2	0.42	0.31	0.43	0.43	0.40	0.06	0.38	0.40	0.39	0.31	0.27	0.35	0.06	1.13	0.275
16:3	0.85	0.45	0.78	0.86	0.74	0.19	1.84	1.37	1.93	1.27	1.06	1.49	0.37	**-2.03**	**0.007**
18:0	0.00	0.00	0.00	0.00	0.00	0.00	0.00	0.00	0.00	0.33	0.00	0.07	0.15	nc	0.374
18:1	8.51	9.55	11.03	6.50	8.90	1.90	8.71	8.43	9.05	7.17	12.94	9.26	2.18	-1.04	0.798
18:2	12.53	18.80	17.68	25.43	18.61	5.30	34.64	34.61	37.63	41.28	38.42	37.32	2.80	**-2.01**	**0.002**
18:3	51.14	38.55	44.85	50.48	46.25	5.86	32.30	29.20	31.53	35.86	28.46	31.47	2.92	**1.47**	**0.009**

Supplemental table 13. Total amounts of polar glycerolipids in *Arabidopsis* crown gall tumors and mock-inoculated inflorescence stalk tissue (reference).

The amount of individual glycerolipid species was determined by LC-MS/MS using internal lipid standards and summarized (2.14) to calculate the total amount of the respective glycerolipid pool in µg/g fresh weight in three samples each. Mean values (±SD) were calculated from three samples from tumor and reference, respectively. Ratios were calculated from the mean values of three samples from the tumor vs. reference. Bold numbers mark ratios with an significant difference (P-value≤0.05) between tumors vs. reference. Statistical analysis was performed by using an unpaired two-tailed Student´s t-test. MGDG, monogalactosyldiacylglycerol; DGDG, digalactosyldiacylglycerol; PC, phosphatidylcholine; PE, phosphatidylethanolamine; PG, phosphatidylglycerol; PI, phosphatidylinositol.

	Tumor					Reference						
	[µg/g fresh weight]					[µg/g fresh weight]					Tumor vs. Reference	
Lipid class	Samples			Mean	SD	Samples			Mean	SD	Ratio	P-value
	1	2	3			1	2	3				
MGDG	654.96	502.49	439.13	532.19	110.94	794.18	921.08	1084.95	933.40	145.78	**-1.75**	**0.02**
DGDG	291.77	339.96	316.30	316.01	24.10	835.74	581.83	821.76	746.44	142.73	**-2.36**	**0.03**
PG	239.42	270.30	286.23	265.32	23.80	268.11	330.38	370.72	323.07	51.70	-1.22	0.18
PC	519.39	542.00	600.48	553.96	41.84	440.37	260.51	230.19	310.36	113.61	**1.78**	**0.05**
PE	672.56	643.48	611.07	642.37	30.76	648.12	540.14	285.18	491.14	186.37	1.31	0.29
PI	232.51	202.29	243.72	226.17	21.43	100.27	86.19	74.10	86.86	13.10	**2.60**	**0.00**

Supplemental table 14. Lipid profile of the polar glycerolipid class monogalactosyldiacylglycerol (MGDG) in crown gall tumors and mock-inoculated inflorescence stalk tissue (reference) of *Arabidopsis* from three independent samples.

The relative proportion in mol% of each glycerolipid species (upper half) was determined by LC-MS/MS (2.14) in three samples each. The relative proportion in mol% of a fatty acid species (lower half) within the total MGDG pool was calculated (2.14). Mean values (±SD) were calculated from three samples from tumor and reference, respectively. Ratios were calculated from the mean values of three samples from the tumor vs. reference, respectively. Bold numbers mark ratios with an significant difference (P-value≤0.05) between tumors vs. reference. Statistical analysis was performed by using an unpaired two-tailed Student´s t-test.

	Tumor					**Reference**						
	[mol%]					**[mol%]**					**Tumor vs. Reference**	
Glycerolipid species	**Samples**			**Mean**	**SD**	**Samples**			**Mean**	**SD**	**Ratio**	**P-value**
	1	**2**	**3**			**1**	**2**	**3**				
MGDG-16:1-16:0	0.00	0.00	0.00	0.00	0.00	0.00	0.00	0.00	0.00	0.00	nc	nc
MGDG-16:2-16:0	0.00	0.00	0.00	0.00	0.00	0.00	0.00	0.00	0.00	0.00	nc	nc
MGDG-16:1-16:1	0.00	0.00	0.00	0.00	0.00	0.00	0.00	0.00	0.00	0.00	nc	nc
MGDG-16:3-16:0	0.00	0.00	0.00	0.00	0.00	0.00	0.00	0.00	0.00	0.00	nc	nc
MGDG-16:2-16:1	0.00	0.00	0.00	0.00	0.00	0.00	0.00	0.00	0.00	0.00	nc	nc
MGDG-16:3-16:1	0.00	0.00	0.00	0.00	0.00	0.00	0.00	0.00	0.00	0.00	nc	nc
MGDG-16:2-16:2	0.00	0.00	0.00	0.00	0.00	0.00	0.00	0.00	0.00	0.00	nc	nc
MGDG-16:3-16:2	0.00	0.00	0.00	0.00	0.00	0.00	0.00	0.00	0.00	0.00	nc	nc
MGDG-16:3-16:3	0.00	0.00	0.00	0.00	0.00	0.00	0.00	0.00	0.00	0.00	nc	nc
MGDG-18:0-16:0	0.27	0.37	0.41	0.35	0.07	0.37	0.46	0.45	0.43	0.05	-1.22	0.204
MGDG-18:1-16:0	0.00	0.00	0.00	0.00	0.00	0.19	0.20	0.28	0.22	0.05	**nc**	**0.017**
MGDG-18:0-16:1	0.00	0.00	0.00	0.00	0.00	0.00	0.00	0.00	0.00	0.00	nc	nc
MGDG-18:1-16:1	0.00	0.00	0.00	0.00	0.00	0.00	0.18	0.00	0.06	0.10	nc	0.423
MGDG-18:0-16:2	0.00	0.00	0.00	0.00	0.00	0.00	0.00	0.00	0.00	0.00	nc	nc
MGDG-18:3-16:0	0.72	0.77	0.84	0.78	0.06	0.71	0.74	0.68	0.71	0.03	1.10	0.184
MGDG-18:1-16:2	0.00	0.00	0.00	0.00	0.00	0.00	0.00	0.00	0.00	0.00	nc	nc
MGDG-18:3-16:1	0.72	0.88	0.63	0.74	0.13	0.50	0.66	0.64	0.60	0.08	1.24	0.190
MGDG-18:3-16:2	1.21	1.50	1.17	1.30	0.18	1.33	1.24	1.17	1.24	0.08	1.04	0.689
MGDG-18:3-16:3	14.51	19.93	23.68	19.37	4.61	21.33	25.98	24.89	24.07	2.43	-1.24	0.216
MGDG-18:1-18:0	0.00	0.00	0.00	0.00	0.00	0.00	0.00	0.00	0.00	0.00	nc	nc
MGDG-18:2-18:0	0.00	0.00	0.00	0.00	0.00	0.00	0.00	0.00	0.00	0.00	nc	nc
MGDG-18:1-18:1	0.00	0.00	0.00	0.00	0.00	0.00	0.00	0.00	0.00	0.00	nc	nc
MGDG-18:3-18:0	0.00	0.00	0.00	0.00	0.00	0.00	0.00	0.00	0.00	0.00	nc	nc
MGDG-18:2-18:1	0.18	0.20	0.00	0.13	0.11	0.38	0.29	0.34	0.33	0.04	-2.63	0.068
MGDG-18:3-18:1	2.35	2.67	2.29	2.44	0.20	1.97	1.81	1.69	1.82	0.14	**1.34**	**0.016**
MGDG-18:2-18:2	0.45	0.41	0.61	0.49	0.11	1.73	1.04	1.91	1.56	0.46	**-3.19**	**0.049**
MGDG-18:3-18:2	10.36	9.50	9.15	9.67	0.62	14.60	12.18	14.08	13.62	1.28	**-1.41**	**0.018**
MGDG-18:3-18:3	69.21	63.77	61.20	64.73	4.09	56.88	55.23	53.89	55.33	1.50	**1.17**	**0.045**
Fatty acids												
16:0	0.50	0.57	0.63	0.56	0.06	0.64	0.70	0.70	0.68	0.04	-1.20	0.070
16:1	0.36	0.44	0.32	0.37	0.06	0.25	0.42	0.32	0.33	0.08	1.13	0.533
16:2	0.61	0.75	0.59	0.65	0.09	0.66	0.62	0.58	0.62	0.04	1.04	0.689
16:3	7.25	9.97	11.84	9.69	2.31	10.66	12.99	12.44	12.03	1.22	-1.24	0.216
18:0	0.14	0.18	0.21	0.18	0.04	0.19	0.23	0.22	0.21	0.02	-1.22	0.204
18:1	1.27	1.43	1.15	1.28	0.14	1.27	1.23	1.15	1.22	0.06	1.05	0.532
18:2	5.72	5.26	5.19	5.39	0.29	9.22	7.28	9.12	8.54	1.09	**-1.58**	**0.031**
18:3	84.15	81.40	80.09	81.88	2.07	77.10	76.53	75.46	76.36	0.83	**1.07**	**0.031**

Supplemental table 15. Lipid profile of the polar glycerolipid class digalactosyldiacylglycerol (DGDG) in crown gall tumors and mock-inoculated inflorescence stalk tissue (reference) of *Arabidopsis*.

The relative proportion in mol% of each glycerolipid species (upper half) was determined by LC-MS/MS (2.14) in three samples each. The relative proportion in mol% of a fatty acid species (lower half) within the total DGDG pool was calculated (2.14). Mean values (±SD) were calculated from three samples from tumor and reference, respectively. Ratios were calculated from the mean values of three samples from the tumor vs. reference, respectively. Bold numbers mark ratios with an significant difference (P-value≤0.05) between tumors vs. reference. Statistical analysis was performed by using an unpaired two-tailed Student´s t-test.

	Tumor					**Reference**						
	[mol%]					**[mol%]**					**Tumor vs. Reference**	
Glycerolipid species	**Samples**			**Mean**	**SD**	**Samples**			**Mean**	**SD**	**Ratio**	**P-value**
	1	**2**	**3**			**1**	**2**	**3**				
DGDG-16:1-16:0	0.00	0.00	0.00	0.00	0.00	0.00	0.00	0.00	0.00	0.00	nc	nc
DGDG-16:2-16:0	0.00	0.00	0.00	0.00	0.00	0.00	0.00	0.00	0.00	0.00	nc	nc
DGDG-16:1-16:1	0.00	0.00	0.00	0.00	0.00	0.00	0.00	0.00	0.00	0.00	nc	nc
DGDG-16:3-16:0	0.00	0.00	0.00	0.00	0.00	0.00	0.00	0.00	0.00	0.00	nc	nc
DGDG-16:2-16:1	0.00	0.00	0.00	0.00	0.00	0.00	0.00	0.00	0.00	0.00	nc	nc
DGDG-16:3-16:1	0.00	0.00	0.00	0.00	0.00	0.00	0.00	0.00	0.00	0.00	nc	nc
DGDG-16:2-16:2	0.00	0.00	0.00	0.00	0.00	0.00	0.00	0.00	0.00	0.00	nc	nc
DGDG-16:3-16:2	0.00	0.00	0.00	0.00	0.00	0.00	0.00	0.00	0.00	0.00	nc	nc
DGDG-16:3-16:3	0.00	0.00	0.00	0.00	0.00	0.00	0.00	0.00	0.00	0.00	nc	nc
DGDG-18:0-16:0	0.00	0.00	0.00	0.00	0.00	0.00	0.00	0.00	0.00	0.00	nc	nc
DGDG-18:1-16:0	0.00	0.00	0.00	0.00	0.00	0.00	0.00	0.00	0.00	0.00	nc	nc
DGDG-18:0-16:1	0.00	0.00	0.00	0.00	0.00	0.00	0.00	0.00	0.00	0.00	nc	nc
DGDG-18:2-16:0	0.00	0.00	0.00	0.00	0.00	0.00	0.00	0.00	0.00	0.00	nc	nc
DGDG-18:1-16:1	0.00	0.00	0.00	0.00	0.00	0.00	0.00	0.00	0.00	0.00	nc	nc
DGDG-18:0-16:2	0.00	0.00	0.00	0.00	0.00	0.00	0.00	0.00	0.00	0.00	nc	nc
DGDG-18:3-16:0	1.99	2.09	2.53	2.20	0.29	3.15	4.12	3.42	3.56	0.50	**-1.62**	**0.024**
DGDG-18:2-16:1	0.00	0.00	0.00	0.00	0.00	0.00	0.00	0.00	0.00	0.00	nc	nc
DGDG-18:1-16:2	0.00	0.00	0.00	0.00	0.00	0.00	0.00	0.00	0.00	0.00	nc	nc
DGDG-18:0-16:3	0.00	0.00	0.00	0.00	0.00	0.00	0.00	0.00	0.00	0.00	nc	nc
DGDG-18:3-16:1	0.44	0.80	0.51	0.58	0.19	0.54	0.64	0.60	0.59	0.05	-1.01	0.967
DGDG-18:1-16:3	0.00	0.00	0.00	0.00	0.00	0.48	0.49	0.60	0.52	0.07	**nc**	**0.006**
DGDG-18:2-16:2	0.00	0.00	0.00	0.00	0.00	0.00	0.00	0.00	0.00	0.00	nc	nc
DGDG-18:3-16:2	0.52	0.48	0.78	0.59	0.16	0.46	0.67	0.60	0.57	0.11	1.03	0.874
DGDG-18:2-16:3	0.00	0.00	0.00	0.00	0.00	0.00	0.00	0.00	0.00	0.00	nc	nc
DGDG-18:3-16:3	2.42	2.45	2.81	2.56	0.22	2.93	3.19	2.93	3.02	0.15	**-1.18**	**0.048**
DGDG-18:1-18:0	0.00	0.00	0.00	0.00	0.00	0.00	0.00	0.00	0.00	0.00	nc	nc
DGDG-18:2-18:0	0.00	0.00	0.00	0.00	0.00	0.00	0.00	0.00	0.00	0.00	nc	nc
DGDG-18:1-18:1	0.00	0.00	0.00	0.00	0.00	0.00	0.00	0.00	0.00	0.00	nc	nc
DGDG-18:3-18:0	0.00	0.00	0.00	0.00	0.00	0.00	0.00	0.00	0.00	0.00	nc	nc
DGDG-18:2-18:1	0.00	0.00	0.00	0.00	0.00	0.38	0.41	0.44	0.41	0.03	**nc**	**0.002**
DGDG-18:3-18:1	2.54	2.47	2.00	2.33	0.29	2.56	2.35	2.25	2.39	0.16	-1.02	0.798
DGDG-18:2-18:2	0.00	0.00	0.00	0.00	0.00	1.21	0.98	1.30	1.17	0.17	**nc**	**0.007**
DGDG-18:3-18:2	11.85	11.34	11.09	11.43	0.39	13.93	12.73	14.35	13.67	0.84	**-1.20**	**0.028**
DGDG-18:3-18:3	80.24	80.37	80.27	80.29	0.07	74.37	74.42	73.52	74.10	0.51	**1.08**	**0.002**
Fatty acids												
16:0	0.99	1.05	1.27	1.10	0.14	1.58	2.07	1.71	1.79	0.25	**-1.62**	**0.023**
16:1	0.22	0.40	0.26	0.29	0.10	0.27	0.32	0.30	0.30	0.03	-1.01	0.960
16:2	0.26	0.24	0.39	0.30	0.08	0.23	0.33	0.30	0.29	0.05	1.03	0.881
16:3	1.21	1.23	1.41	1.28	0.11	1.71	1.85	1.77	1.77	0.07	**-1.38**	**0.005**
18:0	0.00	0.00	0.00	0.00	0.00	0.00	0.00	0.00	0.00	0.00	nc	nc
18:1	1.27	1.23	1.00	1.17	0.15	1.71	1.63	1.65	1.66	0.04	**-1.42**	**0.021**
18:2	5.93	5.67	5.55	5.72	0.19	8.19	7.36	8.50	8.02	0.59	**-1.40**	**0.014**
18:3	90.12	90.18	90.13	90.15	0.03	86.31	86.44	85.77	86.18	0.35	**1.05**	**0.002**

Supplemental table 16. Lipid profile of the polar glycerolipid class phosphatidylglycerol (PG) in crown gall tumors and mock-inoculated inflorescence stalk tissue (reference) of *Arabidopsis*.

The relative proportion in mol% of each glycerolipid species (upper half) was determined by LC-MS/MS (2.14) in three samples each. The relative proportion in mol% of a fatty acid species (lower half) within the total PG pool was calculated (2.14). Mean values (±SD) were calculated from three samples from tumor and reference, respectively. Ratios were calculated from the mean values of three samples from the tumor vs. reference, respectively. Bold numbers mark ratios with an significant difference (P-value≤0.05) between tumors vs. reference. Statistical analysis was performed by using an unpaired two-tailed Student´s t-test.

	Tumor					Reference						
	[mol%]					[mol%]					Tumor vs. Reference	
Glycerolipid species	Samples			Mean	SD	Samples			Mean	SD	Ratio	P-value
	1	2	3			1	2	3				
PG-16:0-16:0	5.16	5.12	4.83	5.04	0.18	2.81	1.59	1.36	1.92	0.78	**2.62**	**0.016**
PG-16:1-16:0	0.00	0.00	0.00	0.00	0.00	0.00	0.00	0.00	0.00	0.00	nc	nc
PG-18:0-16:0	0.00	0.00	0.00	0.00	0.00	0.00	0.00	0.00	0.00	0.00	nc	nc
PG-18:1-16:0	2.64	3.48	2.66	2.92	0.48	2.52	3.42	5.61	3.85	1.59	-1.32	0.422
PG-18:1-16:1	0.00	0.00	0.00	0.00	0.00	0.00	0.00	0.00	0.00	0.00	nc	nc
PG-18:2-16:0	19.22	18.63	23.74	20.53	2.80	13.57	36.66	41.15	30.46	14.80	-1.48	0.365
PG-18:2-16:1	0.00	0.00	0.00	0.00	0.00	0.70	0.72	0.00	0.47	0.41	nc	0.184
PG-18:3-16:0	64.01	66.83	65.18	65.34	1.41	73.27	51.46	44.64	56.46	14.96	1.16	0.412
PG-18:3-16:1	5.26	1.07	0.00	2.11	2.78	2.95	3.14	3.12	3.07	0.10	-1.45	0.611
PG-18:2-18:0	0.09	0.13	0.09	0.10	0.03	0.15	0.14	0.16	0.15	0.01	-1.41	0.079
PG.18:3-18:0	0.11	0.31	0.33	0.25	0.12	0.22	0.09	0.18	0.17	0.07	1.50	0.382
PG-18:2-18:1	0.37	0.38	0.10	0.28	0.15	0.42	0.24	0.14	0.27	0.14	1.06	0.904
PG-18:3-18:1	1.45	2.00	1.14	1.53	0.43	1.16	0.63	0.54	0.78	0.34	1.97	0.081
PG-18:3-18:3	1.70	2.05	1.93	1.90	0.18	2.24	1.92	3.09	2.42	0.61	-1.28	0.271
Fatty acids												
16:0	46.10	47.90	49.11	47.70	1.52	47.05	47.44	47.83	47.44	0.39	1.01	0.795
16:1	2.82	0.58	0.00	1.13	1.49	1.92	2.00	1.63	1.85	0.19	-1.63	0.493
16:2	0.00	0.00	0.00	0.00	0.00	0.00	0.00	0.00	0.00	0.00	nc	nc
16:3	0.00	0.00	0.00	0.00	0.00	0.00	0.00	0.00	0.00	0.00	nc	nc
18:0	0.11	0.24	0.22	0.19	0.07	0.20	0.12	0.18	0.16	0.04	1.16	0.630
18:1	2.39	3.15	2.09	2.54	0.55	2.16	2.22	3.29	2.56	0.64	-1.00	0.981
18:2	10.56	10.31	12.84	11.24	1.39	7.81	19.56	21.70	16.36	7.48	-1.46	0.357
18:3	38.02	37.82	35.74	37.19	1.26	40.87	28.66	25.37	31.63	8.16	1.18	0.359

Supplemental table 17. Lipid profile of the polar glycerolipid class phosphatidylcholine (PC) in crown gall tumors and mock-inoculated inflorescence stalk tissue (reference) of *Arabidopsis*.

The relative proportion in mol% of each glycerolipid species (upper half) was determined by LC-MS/MS (2.14) in three samples each. The relative proportion in mol% of a fatty acid species (lower half) within the total PC pool was calculated (2.14). Mean values (±SD) were calculated from three samples from tumor and reference, respectively. Ratios were calculated from the mean values of three samples from the tumor vs. reference, respectively. Bold numbers mark ratios with an significant difference (P-value≤0.05) between tumors vs. reference. Statistical analysis was performed by using an unpaired two-tailed Student´s t-test.

	Tumor					Reference						
	[mol%]					[mol%]					Tumor vs. Reference	
Glycerolipid species	Samples			Mean	SD	Samples			Mean	SD	Ratio	P-value
	1	2	3			1	2	3				
PC-18:0-16:0	0.00	0.00	0.00	0.00	0.00	0.00	0.00	0.00	0.00	0.00	nc	nc
PC-18:1-16:0	0.54	1.44	0.57	0.85	0.51	0.63	0.00	0.00	0.21	0.37	4.02	0.158
PC-18:2-16:0	8.64	9.47	8.08	8.73	0.70	14.29	13.68	17.70	15.22	2.17	**-1.74**	**0.026**
PC-18:2-16:1	0.41	0.49	0.51	0.47	0.05	0.00	0.00	0.00	0.00	0.00	**nc**	**0.004**
PC-18:3-16:0	27.10	23.15	23.26	24.50	2.25	18.90	21.67	21.09	20.55	1.46	1.19	0.074
PC-18:3-16:1	1.44	1.43	1.35	1.41	0.05	0.82	0.81	0.00	0.54	0.47	2.58	0.085
PC-18:3-16:2	0.00	0.00	0.00	0.00	0.00	0.00	0.00	0.00	0.00	0.00	nc	nc
PC-18:3-16:3	0.00	0.00	0.00	0.00	0.00	0.00	0.00	0.00	0.00	0.00	nc	nc
PC-18:2-18:0	0.00	0.41	0.00	0.14	0.24	0.00	0.00	0.00	0.00	0.00	nc	0.423
PC-18:3-18:0	1.20	1.38	0.87	1.15	0.26	0.58	0.72	1.02	0.78	0.22	1.48	0.136
PC-18:2-18:1	2.89	3.78	3.05	3.24	0.47	4.54	4.57	5.64	4.92	0.63	**-1.52**	**0.024**
PC-18:3-18:1	11.39	13.02	11.36	11.92	0.95	7.98	8.64	8.57	8.40	0.36	**1.42**	**0.014**
PC-18:2-18:2	3.51	5.22	4.30	4.34	0.86	10.54	9.19	10.37	10.03	0.73	**-2.31**	**0.001**
PC-18:3-18:2	15.49	15.77	18.31	16.53	1.55	23.68	21.33	19.53	21.51	2.08	**-1.30**	**0.033**
PC-18:3-18:3	27.39	24.44	28.34	26.72	2.03	18.03	19.39	16.09	17.84	1.66	**1.50**	**0.005**

Fatty acids												
16:0	18.14	17.03	15.95	17.04	1.09	16.91	17.68	19.39	17.99	1.27	-1.06	0.381
16:1	0.93	0.96	0.93	0.94	0.02	0.41	0.41	0.00	0.27	0.24	**3.45**	**0.038**
16:2	0.00	0.00	0.00	0.00	0.00	0.00	0.00	0.00	0.00	0.00	nc	nc
16:3	0.00	0.00	0.00	0.00	0.00	0.00	0.00	0.00	0.00	0.00	nc	nc
18:0	0.60	0.90	0.43	0.64	0.23	0.29	0.36	0.51	0.39	0.11	1.66	0.192
18:1	7.41	9.12	7.49	8.01	0.96	6.58	6.61	7.10	6.76	0.30	1.18	0.145
18:2	17.23	20.18	19.27	18.90	1.51	31.79	28.98	31.80	30.86	1.63	**-1.63**	**0.001**
18:3	55.69	51.81	55.91	54.47	2.31	44.01	45.97	41.19	43.73	2.41	**1.25**	**0.005**

Supplemental table 18. Lipid profile of the polar glycerolipid class phosphatidylethanolamine (PE) in crown gall tumors and mock-inoculated inflorescence stalk tissue (reference) of *Arabidopsis*.

The relative proportion in mol% of each glycerolipid species (upper half) was determined by LC-MS/MS (2.14) in three samples each. The relative proportion in mol% of a fatty acid species (lower half) within the total PE pool was calculated (2.14). Mean values (±SD) were calculated from three samples from tumor and reference, respectively. Ratios were calculated from the mean values of three samples from the tumor vs. reference, respectively. Bold numbers mark ratios with an significant difference (P-value≤0.05) between tumors vs. reference. Statistical analysis was performed by using an unpaired two-tailed Student´s t-test.

	Tumor					**Reference**						
	[mol%]					**[mol%]**					**Tumor vs. Reference**	
Glycerolipid species	**Samples**			**Mean**	**SD**	**Samples**			**Mean**	**SD**	**Ratio**	**P-value**
	1	**2**	**3**			**1**	**2**	**3**				
PE-16:0-16:0	0.00	0.00	0.00	0.00	0.00	0.00	0.00	0.00	0.00	0.00	nc	nc
PE-16:1-16:0	0.00	0.00	0.00	0.00	0.00	0.00	0.00	0.00	0.00	0.00	nc	nc
PE-16:2-16:0	0.00	0.00	0.00	0.00	0.00	0.00	0.00	0.00	0.00	0.00	nc	nc
PE-16:3-16:0	0.00	0.00	0.00	0.00	0.00	0.00	0.00	0.00	0.00	0.00	nc	nc
PE-18:0-16:0	0.03	0.04	0.03	0.03	0.01	0.03	0.04	0.04	0.04	0.00	-1.22	0.178
PE-18:1-16:0	0.29	0.39	0.25	0.31	0.07	0.38	0.38	0.44	0.40	0.03	-1.28	0.146
PE-18:0-16:2	0.00	0.00	0.00	0.00	0.00	0.00	0.00	0.00	0.00	0.00	nc	nc
PE-18:2-16:0	9.98	11.76	9.27	10.34	1.28	15.25	16.74	18.63	16.87	1.69	**-1.63**	**0.007**
PE-18:3-16:0	17.63	17.69	15.68	17.00	1.14	13.16	15.35	14.03	14.18	1.11	**1.20**	**0.037**
PE-18:3-16:1	1.92	1.66	1.63	1.74	0.16	1.01	0.95	0.80	0.92	0.11	**1.89**	**0.003**
PE-18:2-16:3	0.22	0.21	0.23	0.22	0.01	0.14	0.10	0.08	0.11	0.03	**1.98**	**0.020**
PE-18:3-16:3	0.18	0.16	0.22	0.18	0.03	0.21	0.15	0.13	0.16	0.04	1.14	0.492
PE-18:1-18:0	0.00	0.00	0.00	0.00	0.00	0.00	0.00	0.00	0.00	0.00	nc	nc
PE-18:2-18:0	0.59	0.67	0.51	0.59	0.08	1.00	0.92	1.14	1.02	0.11	**-1.73**	**0.007**
PE-18:3-18:0	1.43	1.30	0.99	1.24	0.22	0.94	1.04	1.26	1.08	0.17	1.15	0.390
PE-18:2-18:1	5.41	5.84	4.10	5.12	0.91	5.37	5.82	6.94	6.04	0.81	-1.18	0.259
PE-18:3-18:1	0.00	0.00	0.00	0.00	0.00	0.00	0.00	0.00	0.00	0.00	nc	nc
PE-18:2-18:2	15.81	16.49	15.27	15.86	0.61	18.35	18.93	20.69	19.33	1.22	**-1.22**	**0.022**
PE-18:3-18:2	22.11	21.15	23.31	22.19	1.08	24.15	22.26	20.79	22.40	1.68	**-1.01**	0.870
PE-18:3-18:3	24.40	22.65	28.50	25.18	3.00	20.02	17.32	15.04	17.46	2.49	**1.44**	**0.028**
Fatty acids												
16:0	13.96	14.94	12.62	13.84	1.17	14.41	16.25	16.56	15.74	1.16	-1.14	0.116
16:1	0.96	0.83	0.82	0.87	0.08	0.50	0.48	0.40	0.46	0.05	**1.89**	**0.003**
16:2	0.00	0.00	0.00	0.00	0.00	0.00	0.00	0.00	0.00	0.00	nc	nc
16:3	0.20	0.18	0.22	0.20	0.02	0.17	0.13	0.11	0.14	0.04	1.48	0.065
18:0	1.02	1.00	0.76	0.93	0.14	0.98	1.00	1.22	1.07	0.13	-1.15	0.282
18:1	2.85	3.11	2.18	2.72	0.48	2.88	3.10	3.69	3.22	0.42	-1.19	0.245
18:2	34.97	36.30	33.98	35.09	1.16	41.31	41.85	44.48	42.55	1.70	**-1.21**	**0.005**
18:3	46.03	43.63	49.42	46.36	2.91	39.74	37.20	33.54	36.83	3.12	**1.26**	**0.018**

Supplemental table 19. Lipid profile of the polar glycerolipid class phosphatidylinositol (PI) in crown gall tumors and mock-inoculated inflorescence stalk tissue (reference) of *Arabidopsis*.

The relative proportion in mol% of each glycerolipid species (upper half) was determined by LC-MS/MS (2.14) in three samples each. The relative proportion in mol% of a fatty acid species (lower half) within the total PI pool was calculated (2.14). Mean values (±SD) were calculated from three samples from tumor and reference, respectively. Ratios were calculated from the mean values of three samples from the tumor vs. reference, respectively. Bold numbers mark ratios with an significant difference (P-value≤0.05) between tumors vs. reference. Statistical analysis was performed by using an unpaired two-tailed Student´s t-test.

	Tumor					Reference						
	[mol%]					[mol%]					Tumor vs. Reference	
Glycerolipid species	Samples			Mean	SD	Samples			Mean	SD	Ratio	P-value
	1	2	3			1	2	3				
PI-18:1-16:0	0.21	0.37	0.33	0.30	0.07	0.00	0.00	0.00	0.00	0.00	**nc**	**0.025**
PI-18:2-16:0	13.52	15.55	12.96	14.01	1.11	20.12	21.18	23.09	21.46	1.23	**-1.53**	**0.003**
PI-18:3-16:0	68.73	65.42	68.51	67.56	1.51	59.75	56.30	55.89	57.31	1.73	**1.18**	**0.003**
PI-18:3-16:1	0.60	1.33	0.59	0.84	0.34	0.69	0.00	0.00	0.23	0.32	3.66	0.143
PI-18:2-16:3	0.00	0.00	0.00	0.00	0.00	0.00	0.00	0.00	0.00	0.00	nc	nc
PI-18:3-16:3	0.00	0.00	0.00	0.00	0.00	0.00	0.00	0.00	0.00	0.00	nc	nc
PI-18:2-18:0	0.00	0.00	0.17	0.06	0.08	0.00	0.63	0.75	0.46	0.33	-8.00	0.222
PI-18:3-18:0	0.59	0.62	0.69	0.63	0.04	0.00	0.97	0.65	0.54	0.41	1.17	0.777
PI-18:2-18:1	0.46	0.50	0.37	0.44	0.05	0.00	1.04	0.89	0.64	0.46	-1.46	0.597
PI-18:2-18:2	0.52	0.61	0.62	0.58	0.04	1.46	2.00	2.11	1.86	0.28	**-3.18**	**0.022**
PI-18:3-18:1	1.65	1.80	2.08	1.84	0.18	1.16	2.17	1.61	1.65	0.41	1.12	0.584
PI-18:3-18:2	4.78	4.88	5.05	4.91	0.11	7.48	8.35	8.71	8.18	0.52	**-1.67**	**0.010**
PI-18:3-18:3	8.93	8.92	8.62	8.82	0.15	9.34	7.37	6.29	7.67	1.26	1.15	0.324
Fatty acids												
16:0	41.23	40.67	40.90	40.94	0.23	39.94	38.74	39.49	39.39	0.49	**1.04**	**0.031**
16:1	0.30	0.66	0.29	0.42	0.17	0.34	0.00	0.00	0.11	0.16	3.66	0.143
16:2	0.00	0.00	0.00	0.00	0.00	0.00	0.00	0.00	0.00	0.00	nc	nc
16:3	0.00	0.00	0.00	0.00	0.00	0.00	0.00	0.00	0.00	0.00	nc	nc
18:0	0.30	0.31	0.43	0.35	0.06	0.00	0.80	0.70	0.50	0.36	-1.45	0.603
18:1	1.16	1.33	1.39	1.29	0.10	0.58	1.60	1.25	1.15	0.42	1.13	0.674
18:2	9.90	11.08	9.90	10.29	0.55	15.26	17.60	18.83	17.23	1.48	**-1.67**	**0.013**
18:3	47.11	45.95	47.08	46.71	0.54	43.88	41.26	39.73	41.62	1.71	**1.12**	**0.042**

8.3.3 Lipid analysis of *Arabidopsis* overexpressing SAD6 (SAD6-OE)

Supplemental table 20. Amounts of the different arabidopside types in *Arabidopsis* overexpressing the *SAD6* gene (SAD6-OE).

Amounts (nmol/g fresh weight±SD) of the arabidopside types A-G were determined in young leaf tissue of SAD6-OE and Col-0 (WT) plants by LC-MS/MS (2.14) from three independent samples. Mean values (±SD) were calculated from three samples from SAD6-OE and WT, respectively. Ratios were calculated from the mean values of three samples from the SAD6-OE vs. WT, respectively. Statistical analysis was performed by using an unpaired two-tailed Student´s t-test.

	SAD6-OE					WT						
	[nmol/g fresh weight]					[nmol/g fresh weight]					SAD6-OEvs. WT	
Arabidopside type	Samples			Mean	SD	Samples			Mean	SD	Ratio	P-value
	1	2	3			1	2	3				
Arabidopside A	54.56	52.28	151.72	86.18	56.76	19.54	15.08	7.60	14.07	6.03	6.12	0.157
Arabidopside B	39.14	40.95	96.75	58.95	32.75	17.96	13.34	6.83	12.71	5.59	4.64	0.131
Arabidopside C	1.73	1.67	5.11	2.84	1.97	0.62	0.40	0.33	0.45	0.15	6.31	0.169
Arabidopside D	14.70	14.16	45.08	24.65	17.70	11.56	6.46	5.02	7.68	3.44	3.21	0.236
Arabidopside E	0.13	0.29	0.51	0.31	0.19	0.24	0.20	0.32	0.25	0.06	1.22	0.668
Arabidopside G	0.17	0.38	0.48	0.35	0.16	0.08	0.03	0.10	0.07	0.04	5.11	0.085

Supplemental table 21. Lipid profile of the polar glycerolipid class monogalactosyldiacylglycerol (MGDG) from *Arabidopsis* overexpressing the *SAD6* gene (SAD6-OE) and wildtype Col-0.

The relative proportion in mol% of each glycerolipid species (upper half) was determined by LC-MS/MS (2.14) in three samples each. The relative proportion in mol% of a fatty acid species (lower half) within the total MGDG pool was calculated (2.14). Mean values (±SD) were calculated from three samples from SAD6-OE and WT, respectively. Ratios were calculated from the mean values of three samples from SAD6-OE and WT, respectively. Bold numbers mark ratios with an significant difference (P-value≤0.05) between SAD6-OE vs. WT. Statistical analysis was performed by using an unpaired two-tailed Student´s t-test. "Nc" means "not calculable".

	SAD6-OE					**WT**						
	[mol%]					**[mol%]**					**SAD6-OE vs. WT**	
Glycerolipid species	**Samples**			**Mean**	**SD**	**Samples**			**Mean**	**SD**	**Ratio**	**P-value**
	1	**2**	**3**			**1**	**2**	**3**				
MGDG-18:1-16:0	0.74	0.79	0.73	0.75	0.03	0.87	3.82	1.55	2.08	1.55	-0.36	0.275
MGDG-18:2-16:0	0.43	0.44	0.40	0.42	0.02	1.80	5.17	1.79	2.92	1.95	-0.14	0.157
MGDG-18:1-16:1	0.67	0.66	0.69	0.67	0.02	0.72	2.70	0.64	1.35	1.17	-0.50	0.418
MGDG-18:3-16:0	0.71	0.71	0.67	0.70	0.03	2.79	1.47	2.79	2.35	0.76	-0.30	0.064
MGDG-18:2-16:1	0.87	0.80	0.77	0.82	0.05	1.04	4.85	1.03	2.31	2.21	-0.35	0.363
MGDG-18:1-16:2	0.25	0.23	0.22	0.23	0.01	0.22	1.04	0.21	0.49	0.48	-0.47	0.447
MGDG-18:3-16:1	1.60	1.33	1.44	1.46	0.14	1.63	1.91	1.80	1.78	0.14	**-0.82**	**0.049**
MGDG-18:2-16:2	1.21	1.08	0.89	1.06	0.16	1.19	6.89	1.35	3.14	3.25	-0.34	0.382
MGDG-18:1-16:3	0.64	0.55	0.48	0.55	0.08	0.44	1.94	0.46	0.95	0.86	-0.59	0.515
MGDG-18:3-16:2	4.91	4.15	4.63	4.57	0.39	7.60	6.67	7.40	7.22	0.49	**-0.63**	**0.002**
MGDG-18:2-16:3	2.53	1.90	2.45	2.29	0.34	2.48	11.61	2.39	5.49	5.30	-0.42	0.405
MGDG-18:3-16:3	41.69	41.13	45.71	42.84	2.50	39.26	24.65	37.92	33.94	8.08	1.26	0.189
MGDG-18:3-18:0	0.00	0.00	0.00	0.00	0.00	0.00	0.00	0.00	0.00	0.00	2.09	0.319
MGDG-18:2-18:1	0.17	0.18	0.16	0.17	0.01	0.21	0.90	0.23	0.44	0.39	-0.37	0.342
MGDG-18:3-18:1	0.00	0.00	0.00	0.00	0.00	0.00	0.00	0.00	0.00	0.00	nc	nc
MGDG-18:2-18:2	0.32	0.33	0.29	0.31	0.02	0.65	2.35	0.65	1.22	0.98	-0.26	0.250
MGDG-18:3-18:2	4.69	5.21	4.38	4.76	0.42	6.43	3.92	6.86	5.73	1.59	-0.83	0.401
MGDG-18:3-18:3	38.59	40.52	36.10	38.40	2.22	32.68	20.11	32.95	28.58	7.34	1.34	0.137
Fatty acids												
16:0	0.94	0.97	0.90	0.94	0.03	2.73	5.23	3.06	3.68	1.36	-0.25	0.073
16:1	1.57	1.39	1.45	1.47	0.09	1.69	4.73	1.73	2.72	1.74	-0.54	0.341
16:2	3.19	2.73	2.87	2.93	0.23	4.50	7.30	4.48	5.43	1.62	-0.54	0.114
16:3	22.43	21.79	24.31	22.84	1.31	21.09	19.10	20.38	20.19	1.01	1.13	0.054
18:0	0.00	0.00	0.00	0.00	0.00	0.00	0.00	0.00	0.00	0.00	2.09	0.319
18:1	1.23	1.20	1.14	1.19	0.05	1.23	5.20	1.54	2.66	2.21	-0.45	0.368
18:2	5.26	5.13	4.81	5.07	0.23	7.22	19.02	7.47	11.24	6.74	-0.45	0.254
18:3	65.39	66.79	64.51	65.56	1.15	61.53	39.42	61.33	54.09	12.71	1.21	0.258

Supplemental table 22. Lipid profile of the polar glycerolipid class digalactosyldiacylglycerol (DGDG) from *Arabidopsis* overexpressing the *SAD6* gene (SAD6-OE) and wildtype Col-0.

The relative proportion in mol% of each glycerolipid species (upper half) was determined by LC-MS/MS (2.14) in three samples each. The relative proportion in mol% of a fatty acid species (lower half) within the total DGDG pool was calculated (2.14). Mean values (±SD) were calculated from three samples from SAD6-OE and WT, respectively. Ratios were calculated from the mean values of three samples SAD6-OE and WT, respectively. Bold numbers mark ratios with a significant difference (P-value≤0.05) between SAD6-OE vs. WT. Statistical analysis was performed by using an unpaired two-tailed Student´s t-test.

	SAD6-OE					WT						
	[mol%]					[mol%]					SAD6-OE vs. WT	
	Samples					Samples						
Glycerolipid species	**1**	**2**	**3**	**Mean**	**SD**	**1**	**2**	**3**	**Mean**	**SD**	**Ratio**	**P-value**
DGDG-18:3-16:0	7.91	8.65	8.04	8.20	0.40	16.64	15.91	17.49	16.68	0.79	**-2.03**	**0.001**
DGDG-18:3-16:1	0.64	0.60	0.64	0.62	0.02	0.94	0.81	0.78	0.84	0.09	**-1.35**	**0.039**
DGDG-18:3-16:2	1.44	1.19	1.55	1.39	0.19	1.65	1.95	1.60	1.73	0.19	-1.24	0.092
DGDG-18:3-16:3	4.01	3.59	4.32	3.97	0.37	4.70	6.36	4.23	5.10	1.12	-1.28	0.217
DGDG-18:3-18:0	0.25	0.27	0.28	0.27	0.01	1.75	1.26	1.53	1.51	0.24	**-5.65**	**0.012**
DGDG-18:3-18:1	1.84	1.99	2.01	1.94	0.09	2.12	1.68	2.03	1.94	0.23	-1.00	1.000
DGDG-18:3-18:2	18.60	19.13	18.19	18.64	0.47	17.22	17.23	17.20	17.22	0.02	**1.08**	**0.034**
DGDG-18:3-18:3	65.31	64.58	64.97	64.95	0.36	54.99	54.79	55.14	54.97	0.18	**1.18**	**0.000**
Fatty acids												
16:0	3.96	4.33	4.02	4.10	0.20	8.32	7.96	8.74	8.34	0.39	**-2.03**	**0.001**
16:1	0.32	0.30	0.32	0.31	0.01	0.47	0.40	0.39	0.42	0.04	**-1.35**	**0.039**
16:2	0.72	0.59	0.78	0.70	0.09	0.82	0.98	0.80	0.87	0.10	-1.24	0.092
16:3	2.01	1.79	2.16	1.99	0.18	2.35	3.18	2.12	2.55	0.56	-1.28	0.217
18:0	0.13	0.14	0.14	0.13	0.01	0.87	0.63	0.76	0.76	0.12	**-5.65**	**0.012**
18:1	0.92	0.99	1.00	0.97	0.05	1.06	0.84	1.02	0.97	0.12	-1.00	1.000
18:2	9.30	9.57	9.10	9.32	0.23	8.61	8.62	8.60	8.61	0.01	**1.08**	**0.034**
18:3	82.65	82.29	82.48	82.48	0.18	77.49	77.40	77.57	77.49	0.09	**1.06**	**0.000**

Supplemental table 23. Lipid profile of the polar glycerolipid class phosphatidylglycerol (PG) from *Arabidopsis* overexpressing the *SAD6* gene (SAD6-OE) and wildtype Col-0.

The relative proportion in mol% of each glycerolipid species (upper half) was determined by LC-MS/MS (2.14) in three samples each. The relative proportion in mol% of a fatty acid species (lower half) within the total PG pool was calculated (2.14). Mean values (±SD) were calculated from three samples SAD6-OE and WT, respectively. Ratios were calculated from the mean values of three samples from the SAD6-OE and WT, respectively. Statistical analysis was performed by using an unpaired two-tailed Student´s t-test. "Nm" means not measured.

	SAD6-OE					WT						
	[mol%]					[mol%]					SAD6-OE vs. WT	
Glycerolipid species	Samples					Samples						
	1	**2**	**3**	**Mean**	**SD**	**1**	**2**	**3**	**Mean**	**SD**	**Ratio**	**P-value**
PG-16:0-16:0	0.35	0.00	0.79	0.38	0.39	1.17	2.14	0.63	1.31	0.76	-3.46	0.158
PG-16:1-16:0	0.30	0.42	0.29	0.34	0.07	0.32	0.42	0.36	0.36	0.05	-1.08	0.641
PG-18:0-16:0	0.00	0.00	0.12	0.04	0.07	0.20	0.20	0.00	0.13	0.11	-3.38	0.306
PG-18:1-16:0	3.51	3.46	0.51	2.49	1.72	4.57	5.36	4.47	4.80	0.49	-1.93	0.137
PG-18:1-16:1	0.75	0.60	0.07	0.47	0.35	0.34	0.37	0.81	0.50	0.27	-1.06	0.913
PG-18:2-16:0	16.09	23.83	11.01	16.98	6.45	16.28	21.95	10.33	16.19	5.81	1.05	0.883
PG-18:2-16:1	2.87	2.37	0.53	1.92	1.24	0.93	1.53	2.83	1.76	0.97	1.09	0.868
PG-18:2-18:0	0.00	0.07	0.00	0.02	0.04	0.06	0.05	0.00	0.04	0.03	-1.62	0.656
PG-18:2-18:1	0.17	0.23	0.00	0.13	0.12	0.08	0.08	0.21	0.12	0.07	1.06	0.929
PG-18:3-16:0	40.08	34.71	70.04	48.27	19.04	62.30	49.52	43.99	51.94	9.39	-1.08	0.785
PG-18:3-16:1	33.19	33.21	14.22	26.87	10.96	11.87	16.06	32.95	20.30	11.16	1.32	0.507
PG-18:3-18:0	0.07	0.19	0.16	0.14	0.06	0.18	0.24	0.00	0.14	0.13	1.00	0.999
PG-18:3-18:1	0.27	0.58	0.19	0.34	0.20	0.29	0.26	0.53	0.36	0.15	-1.04	0.927
PG-18:3-18:3	2.36	0.33	2.07	1.59	1.10	1.42	1.83	2.88	2.04	0.75	-1.29	0.589
Fatty acids												
16:0	30.33	31.21	41.77	34.44	6.37	43.00	40.86	30.21	38.02	6.85	-1.10	0.544
16:1	18.56	18.30	7.55	14.80	6.28	6.73	9.19	18.48	11.46	6.20	1.29	0.548
16:2	nm	nm	nm	nm	nm	nm	nm	nm	nm	nm	nm	nm
16:3	nm	nm	nm	nm	nm	nm	nm	nm	nm	nm	nm	nm
18:0	0.00	0.03	0.06	0.03	0.03	0.13	0.12	0.00	0.08	0.07	-2.74	0.334

18:1	2.38	2.53	0.47	1.79	1.15	2.73	3.15	3.01	2.97	0.21	-1.65	0.217
18:2	9.57	13.25	5.77	9.53	3.74	8.67	11.81	6.69	9.06	2.58	1.05	0.867
18:3	39.16	34.68	44.37	39.40	4.85	38.74	34.87	41.62	38.41	3.39	1.03	0.787

Supplemental table 24. Lipid profile of the polar glycerolipid class phosphatidylcholine (PC) from *Arabidopsis* overexpressing the *SAD6* gene (SAD6-OE) and wildtype Col-0.

The relative proportion in mol% of each glycerolipid species (upper half) was determined by LC-MS/MS (2.14) in three samples each. The relative proportion in mol% of a fatty acid species (lower half) within the total PC pool was calculated (2.14). Mean values (±SD) were calculated from four samples from SAD6-OE and WT, respectively. Ratios were calculated from the mean values of four samples SAD6-OE and WT, respectively. Bold numbers mark ratios with an significant difference (P-value≤0.05) between SAD6-OE vs. WT. Statistical analysis was performed by using an unpaired two-tailed Student´s t-test.

	SAD6-OE						**WT**							
	[mol%]						**[mol%]**						**SAD6-OE vs. WT**	
Glycerolipid species	**Samples**				**Mean**	**SD**	**Samples**				**Mean**	**SD**	**Ratio**	**P-value**
	1	**2**	**3**	**4**			**1**	**2**	**3**	**4**				
PC-18:1-16:0	8.19	7.75	11.38	7.16	8.62	1.89	8.85	13.05	12.32	13.84	12.02	2.20	-1.39	0.059
PC-18:2-16:0	16.95	15.29	15.74	16.43	16.10	0.74	22.28	20.75	19.56	18.51	20.27	1.62	**-1.26**	**0.008**
PC-18:3-16:0	12.88	12.48	12.13	12.81	12.58	0.34	16.30	14.74	13.70	12.00	14.19	1.81	-1.13	0.172
PC-18:2-16:1	1.21	1.39	1.58	1.30	1.37	0.16	0.94	1.00	1.05	1.18	1.04	0.10	**1.31**	**0.017**
PC-18:0-16:3	0.00	0.00	0.01	0.01	0.01	0.00	0.02	0.02	0.03	0.02	0.02	0.01	**-3.89**	**0.007**
PC-18:3-16:1	1.11	1.25	1.42	1.27	1.26	0.12	1.14	1.14	1.13	1.40	1.20	0.13	1.05	0.522
PC-18:2-16:2	0.16	0.21	0.16	0.18	0.18	0.02	0.16	0.15	0.15	0.15	0.15	0.01	1.14	0.168
PC-18:1-16:3	0.07	0.09	0.12	0.10	0.09	0.02	0.07	0.06	0.06	0.08	0.07	0.01	1.44	0.067
PC-18:3-16:2	0.24	0.27	0.21	0.20	0.23	0.03	0.21	0.22	0.23	0.24	0.23	0.01	1.02	0.838
PC-18:2-16:3	0.19	0.26	0.33	0.27	0.26	0.06	0.23	0.22	0.26	0.27	0.25	0.02	1.06	0.683
PC-18:3-16:3	0.93	1.11	1.12	1.04	1.05	0.09	1.29	1.20	1.27	1.11	1.22	0.08	**-1.16**	**0.031**
PC-18:1-18:0	0.40	0.46	0.36	0.31	0.38	0.06	0.48	0.89	0.98	1.32	0.92	0.34	**-2.42**	**0.050**
PC-18:2-18:0	1.54	1.61	1.51	1.32	1.50	0.12	3.58	3.86	3.94	3.95	3.83	0.17	**-2.56**	**0.000**
PC-18:1-18:1	3.45	3.71	4.22	3.48	3.72	0.36	0.86	1.74	1.92	2.12	1.66	0.56	**2.23**	**0.001**
PC-18:3-18:0	1.92	1.94	2.10	1.53	1.87	0.24	6.82	5.97	7.21	8.60	7.15	1.10	**-3.82**	**0.002**
PC-18:2-18:1	13.79	14.28	15.20	14.16	14.36	0.60	7.21	9.34	9.96	10.51	9.26	1.44	**1.55**	**0.003**
PC-18:3-18:2	18.92	18.87	17.32	20.35	18.86	1.24	15.06	13.09	12.83	12.08	13.27	1.27	**1.42**	**0.001**
PC-18:3-18:3	18.06	19.02	15.10	18.08	17.56	1.70	14.46	12.54	13.40	12.62	13.26	0.89	**1.32**	**0.008**
Fatty acids														
16:0	19.01	17.76	19.63	18.20	18.65	0.83	23.72	24.27	22.79	22.18	23.24	0.94	**-1.25**	**0.000**
16:1	1.16	1.32	1.50	1.29	1.32	0.14	1.04	1.07	1.09	1.29	1.12	0.11	1.17	0.074
16:2	0.20	0.24	0.18	0.19	0.20	0.03	0.19	0.18	0.19	0.20	0.19	0.01	1.07	0.406
16:3	0.59	0.73	0.79	0.71	0.70	0.08	0.81	0.75	0.81	0.74	0.77	0.04	-1.10	0.191
18:0	1.93	2.01	1.99	1.58	1.88	0.20	5.45	5.37	6.08	6.95	5.96	0.73	**-3.17**	**0.001**
18:1	14.68	15.00	17.75	14.34	15.44	1.56	9.17	13.41	13.59	15.00	12.79	2.52	1.21	0.133
18:2	26.38	25.95	25.92	27.01	26.31	0.51	24.74	24.21	23.87	23.32	24.04	0.59	**1.09**	**0.001**
18:3	36.05	36.98	32.25	36.68	35.49	2.19	34.88	30.73	31.58	30.33	31.88	2.07	1.11	0.054

Supplemental table 25. Lipid profile of the polar glycerolipid class phosphatidylethanolamine (PE) from *Arabidopsis* overexpressing the *SAD6* gene (SAD6-OE) and wildtype Col-0.

The relative proportion in mol% of each glycerolipid species (upper half) was determined by LC-MS/MS (2.14) in three samples each. The relative proportion in mol% of a fatty acid species (lower half) within the total PE pool was calculated (2.14). Mean values (±SD) were calculated from three samples from SAD6-OE and WT, respectively. Ratios were calculated from the mean values of three samples SAD6-OE and WT, respectively. Bold numbers mark ratios with an significant difference (P-value≤0.05) between SAD6-OE vs. WT. Statistical analysis was performed by using an unpaired two-tailed Student´s t-test.

	SAD6-OE					**WT**						
	[mol%]					**[mol%]**					**SAD6-OE vs. WT**	
Glycerolipid species	**Samples**			**Mean**	**SD**	**Samples**			**Mean**	**SD**	**Ratio**	**P-value**
	1	**2**	**3**			**1**	**2**	**3**				
PE-16:0-16:0	0.01	0.02	0.01	0.02	0.00	0.01	0.01	0.02	0.02	0.00	-1.06	0.793
PE-16:1-16:0	0.59	1.00	0.81	0.80	0.20	0.51	0.35	0.47	0.44	0.08	1.80	0.081
PE-16:2-16:0	0.25	0.37	0.29	0.31	0.06	0.15	0.17	0.15	0.16	0.01	**1.96**	**0.048**
PE-16:3-16:0	0.25	0.25	0.29	0.26	0.02	0.31	0.27	0.28	0.29	0.02	-1.08	0.226
PE-18:1-16:0	1.25	1.26	1.28	1.26	0.02	1.13	1.97	1.63	1.57	0.42	-1.25	0.330
PE-18:2-16:0	20.12	19.82	19.84	19.93	0.17	25.74	23.28	25.13	24.72	1.28	**-1.24**	**0.021**

PE-18:3-16:0	10.45	10.74	10.99	10.72	0.27	14.18	12.33	13.72	13.41	0.96	**-1.25**	**0.033**
PE-18:3-16:1	1.08	0.85	0.95	0.96	0.11	0.57	0.60	0.63	0.60	0.03	**1.60**	**0.027**
PE-18:2-16:3	0.29	0.24	0.29	0.27	0.03	0.18	0.15	0.16	0.17	0.01	**1.65**	**0.013**
PE-18:3-16:3	0.29	0.20	0.29	0.26	0.05	0.14	0.10	0.11	0.12	0.02	**2.20**	**0.023**
PE-18:1-18:0	0.14	0.49	0.33	0.32	0.18	0.20	0.31	0.20	0.24	0.06	1.35	0.511
PE-18:2-18:0	3.47	4.42	3.95	3.95	0.47	6.13	8.15	5.04	6.44	1.57	-1.63	0.101
PE-18:3-18:0	1.12	1.08	1.28	1.16	0.11	1.12	2.11	2.62	1.95	0.76	-1.68	0.213
PE-18:2-18:1	6.80	6.95	7.38	7.05	0.30	5.85	6.88	6.10	6.27	0.54	1.12	0.114
PE-18:2-18:2	17.77	16.23	17.10	17.03	0.77	16.18	15.33	15.31	15.61	0.50	1.09	0.065
PE-18:3-18:2	21.59	21.48	20.84	21.31	0.41	14.71	15.09	15.89	15.23	0.60	**1.40**	**0.000**
PE-18:3-18:3	14.52	14.59	14.09	14.40	0.27	12.89	12.90	12.53	12.77	0.21	**1.13**	**0.002**
Fatty acids												
16:0	16.47	16.74	16.76	16.66	0.16	21.02	19.20	20.71	20.31	0.97	**-1.22**	**0.020**
16:1	0.83	0.92	0.88	0.88	0.05	0.54	0.48	0.55	0.52	0.04	**1.68**	**0.001**
16:2	0.13	0.19	0.15	0.15	0.03	0.08	0.08	0.07	0.08	0.01	**1.96**	**0.048**
16:3	0.42	0.35	0.43	0.40	0.04	0.32	0.26	0.28	0.29	0.03	**1.40**	**0.027**
18:0	2.36	3.00	2.78	2.71	0.32	3.72	5.28	3.93	4.31	0.85	-1.59	0.068
18:1	4.09	4.35	4.50	4.31	0.20	3.59	4.58	3.96	4.04	0.50	1.07	0.455
18:2	43.92	42.68	43.25	43.28	0.62	42.48	42.10	41.47	42.02	0.51	**1.03**	**0.054**
18:3	31.78	31.76	31.26	31.60	0.30	28.25	28.01	29.02	28.43	0.53	**1.11**	**0.002**

Supplemental table 26. Lipid profile of the polar glycerolipid class phosphatidylinositol (PI) from *Arabidopsis* overexpressing the *SAD6* gene (SAD6-OE) and wildtype Col-0.

The relative proportion in mol% of each glycerolipid species (upper half) was determined by LC-MS/MS (2.14) in three samples each. The relative proportion in mol% of a fatty acid species (lower half) within the total PI pool was calculated (2.14). Mean values (±SD) were calculated from three samples from SAD6-OE and WT, respectively. Ratios were calculated from the mean values of three samples SAD6-OE and WT, respectively. Bold numbers mark ratios with an significant difference (P-value≤0.05) between SAD6-OE vs. WT. Statistical analysis was performed by using an unpaired two-tailed Student´s t-test. "Nc" means "not calculable".

	SAD6-OE					**WT**						
	[mol%]					**[mol%]**					**SAD6-OE vs. WT**	
Glycerolipid	**Samples**					**Samples**						
species	**1**	**2**	**3**	**Mean**	**SD**	**1**	**2**	**3**	**Mean**	**SD**	**Ratio**	**P-value**
PI-18:1-16:0	0.00	0.00	0.00	0.00	0.00	0.00	0.00	0.41	0.14	0.24	nc	0.423
PI-18:2-16:0	15.78	14.48	7.55	12.60	4.42	29.26	26.40	28.03	27.90	1.43	**-2.21**	**0.019**
PI-18:2-16:3	0.00	0.00	0.36	0.12	0.21	0.00	0.00	0.00	0.00	0.00	nc	0.423
PI-18:2-18:0	0.00	0.00	0.00	0.00	0.00	0.00	0.00	0.35	0.12	0.20	nc	0.423
PI-18:2-18:1	0.62	0.57	0.81	0.67	0.12	0.49	0.58	0.38	0.48	0.10	1.39	0.117
PI-18:2-18:2	2.19	1.71	3.37	2.43	0.85	1.15	1.54	0.84	1.18	0.35	2.06	0.112
PI-18:3-16:0	53.22	49.83	32.18	45.08	11.30	52.38	55.04	59.23	55.55	3.45	-1.23	0.245
PI-18:3-16:1	0.84	0.66	0.96	0.82	0.15	1.94	0.74	0.44	1.04	0.80	-1.27	0.680
PI-18:3-16:3	0.00	0.78	1.67	0.82	0.84	0.00	0.60	0.00	0.20	0.34	4.11	0.331
PI-18:3-18:0	0.52	0.00	0.41	0.31	0.27	0.87	0.90	0.94	0.90	0.04	-2.94	0.060
PI-18:3-18:1	1.91	1.64	2.25	1.93	0.31	0.95	1.25	0.83	1.01	0.22	**1.91**	**0.016**
PI-18:3-18:2	9.64	10.49	19.58	13.23	5.51	5.38	6.79	3.74	5.30	1.53	2.50	0.121
PI-18:3-18:3	15.27	19.85	30.86	22.00	8.01	7.59	6.15	4.81	6.18	1.39	3.56	0.072
Fatty acids												
16:0	34.50	32.15	19.86	28.84	7.86	40.82	40.72	43.84	41.79	1.77	-1.45	0.097
16:1	0.42	0.33	0.48	0.41	0.08	0.97	0.37	0.22	0.52	0.40	-1.27	0.680
16:2	0.00	0.00	0.00	0.00	0.00	0.00	0.00	0.00	0.00	0.00	nc	nc
16:3	0.00	0.39	1.02	0.47	0.51	0.00	0.30	0.00	0.10	0.17	4.72	0.339
18:0	0.26	0.00	0.20	0.15	0.14	0.43	0.45	0.65	0.51	0.12	**-3.32**	**0.027**
18:1	1.27	1.10	1.53	1.30	0.21	0.72	0.92	0.81	0.81	0.10	**1.60**	**0.041**
18:2	15.21	14.48	17.52	15.74	1.59	18.71	18.43	17.08	18.07	0.87	-1.15	0.109
18:3	48.34	51.55	59.39	53.09	5.68	38.35	38.81	37.40	38.19	0.72	**1.39**	**0.043**

8.3.4 Lipid analysis of *Arabidopsis* SAD6-OE-RNAi

Supplemental table 27. Lipid profile of the polar glycerolipid class monogalactosyldiacylglyerol (MGDG) from SAD6-OE-RNAi and wildtype Col-0.

The relative proportion in mol% of each glycerolipid species (upper half) was determined by LC-MS/MS (2.14) in three samples each. The relative proportion in mol% of a fatty acid species (lower half) within the total MGDG pool was calculated (2.14). Mean values (±SD) were calculated from three samples from SAD6-OE-RNAi and WT, respectively. Ratios were calculated from the mean values of three samples SAD6-OE-RNAi and WT, respectively. Statistical analysis was performed by using an unpaired two-tailed Student´s t-test. "Nc" means "not calculable".

	SAD6-OE-RNAi					WT						
	[mol%]					[mol%]					SAD6-OE-RNAi vs. WT	
Glycerolipid species	Samples			Mean	SD	Samples			Mean	SD	Ratio	P-value
	1	2	3			1	2	3				
MGDG-16:1-16:0	0.00	0.00	0.04	0.01	0.02	0.00	0.00	0.00	0.00	0.00	nc	0.42
MGDG-16:2-16:0	0.00	0.00	0.00	0.00	0.00	0.00	0.00	0.00	0.00	0.00	nc	nc
MGDG-16:1-16:1	0.00	0.00	0.00	0.00	0.00	0.00	0.00	0.00	0.00	0.00	nc	nc
MGDG-16:3-16:0	0.10	0.00	0.15	0.08	0.08	0.00	0.00	0.00	0.00	0.00	nc	0.20
MGDG-16:2-16:1	0.00	0.00	0.00	0.00	0.00	0.00	0.00	0.00	0.00	0.00	nc	nc
MGDG-16:3-16:1	0.00	0.00	0.05	0.02	0.03	0.00	0.00	0.00	0.00	0.00	nc	0.42
MGDG-16:2-16:2	0.00	0.00	0.00	0.00	0.00	0.00	0.00	0.00	0.00	0.00	nc	nc
MGDG-16:3-16:2	0.00	0.00	0.04	0.01	0.02	0.03	0.00	0.00	0.01	0.02	1.38	0.84
MGDG-16:3-16:3	0.00	0.00	0.00	0.00	0.00	0.05	0.00	0.00	0.02	0.03	nc	0.42
MGDG-18:0-16:0	0.02	2.09	1.18	1.10	1.04	0.03	0.24	0.21	0.16	0.11	6.80	0.26
MGDG-18:1-16:0	0.26	11.67	3.25	5.06	5.92	0.33	1.97	1.56	1.29	0.85	3.93	0.38
MGDG-18:0-16:1	0.02	0.75	0.17	0.31	0.38	0.00	0.14	0.11	0.08	0.07	3.81	0.41
MGDG-18:1-16:1	0.25	9.28	4.21	4.58	4.53	0.43	2.26	1.30	1.33	0.92	3.44	0.34
MGDG-18:0-16:2	0.00	0.00	0.04	0.01	0.02	0.00	0.00	0.00	0.00	0.00	nc	0.42
MGDG-18:3-16:0	0.89	1.16	1.54	1.20	0.33	0.34	0.84	0.84	0.67	0.29	1.78	0.11
MGDG-18:1-16:2	0.14	4.19	0.57	1.63	2.22	0.32	1.05	0.56	0.64	0.37	2.54	0.52
MGDG-18:3-16:1	0.84	1.17	1.94	1.32	0.56	0.59	0.89	0.81	0.76	0.16	1.73	0.22
MGDG-18:3-16:2	3.16	2.20	4.29	3.22	1.05	3.38	3.95	3.17	3.50	0.40	-1.09	0.70
MGDG-18:3-16:3	58.89	39.24	39.29	45.81	11.33	56.48	45.76	45.94	49.39	6.14	-1.08	0.66
MGDG-18:1-18:0	0.00	0.00	0.52	0.17	0.30	0.00	0.00	0.00	0.00	0.00	nc	0.42
MGDG-18:2-18:0	0.00	0.00	0.09	0.03	0.05	0.00	0.00	0.00	0.00	0.00	nc	0.42
MGDG-18:1-18:1	0.00	0.00	0.08	0.03	0.05	0.00	0.00	0.00	0.00	0.00	nc	0.42
MGDG-18:3-18:0	0.09	0.00	0.36	0.15	0.19	0.03	0.10	0.09	0.07	0.04	2.04	0.56
MGDG-18:2-18:1	0.08	0.00	0.37	0.15	0.19	0.02	0.11	0.00	0.05	0.06	3.33	0.45
MGDG-18:3-18:1	0.38	0.49	1.04	0.63	0.35	0.19	0.57	0.44	0.40	0.19	1.60	0.38
MGDG-18:2-18:2	0.26	0.37	0.58	0.40	0.16	0.11	0.40	0.32	0.27	0.15	1.46	0.38
MGDG-18:3-18:2	4.46	4.44	3.17	4.02	0.74	4.25	4.94	5.06	4.75	0.44	-1.18	0.23
MGDG-18:3-18:3	30.16	22.96	36.66	29.93	6.85	33.41	36.80	39.59	36.60	3.09	-1.22	0.23
Fatty acids												
16:0	0.64	7.46	3.08	3.73	3.46	0.36	1.52	1.31	1.06	0.62	3.51	0.31
16:1	0.55	5.60	3.20	3.12	2.52	0.51	1.64	1.11	1.09	0.57	2.87	0.30
16:2	1.65	3.19	2.47	2.44	0.77	1.87	2.50	1.86	2.08	0.36	1.17	0.52
16:3	29.50	19.62	19.96	23.03	5.60	28.31	22.88	22.97	24.72	3.11	-1.07	0.68
18:0	0.07	1.42	1.18	0.89	0.72	0.03	0.24	0.21	0.16	0.11	5.60	0.22
18:1	0.55	12.81	5.25	6.21	6.19	0.65	2.98	1.93	1.85	1.17	3.35	0.35
18:2	2.53	2.59	2.39	2.50	0.10	2.25	2.93	2.85	2.67	0.37	-1.07	0.51
18:3	64.52	47.31	62.47	58.10	9.40	66.04	65.32	67.76	66.37	1.25	-1.14	0.27

Supplemental table 28. Lipid profile of the polar glycerolipid class digalactosyldiacyglycerol DGDG from SAD6-OE-RNAi and wildtype Col-0.

The relative proportion in mol% of each glycerolipid species (upper half) was determined by LC-MS/MS (2.14) in three samples each. The relative proportion in mol% of a fatty acid species (lower half) within the total DGDG pool was calculated (2.14). Mean values (±SD) were calculated from three samples from SAD6-OE-RNAi and WT, respectively. Ratios were calculated from the mean values of three samples SAD6-OE-RNAi and WT, respectively. Statistical analysis was performed by using an unpaired two-tailed Student´s t-test. "Nc" means "not calculable".

	SAD6-OE-RNAi					WT						
											SAD6-OE-RNAi vs. WT	
Glycerolipid species	Samples			Mean	SD	Samples			Mean	SD	Ratio	P-value
	1	2	3			1	2	3				
DGDG-16:1-16:0	0.00	0.00	0.00	0.00	0.00	0.00	0.00	0.00	0.00	0.00	nc	nc
DGDG-16:2-16:0	0.00	0.00	0.00	0.00	0.00	0.00	0.00	0.00	0.00	0.00	nc	nc
DGDG-16:1-16:1	0.00	0.00	0.00	0.00	0.00	0.00	0.00	0.00	0.00	0.00	nc	nc
DGDG-16:3-16:0	0.00	0.00	0.00	0.00	0.00	0.00	0.00	0.00	0.00	0.00	nc	nc
DGDG-16:2-16:1	0.00	0.00	0.00	0.00	0.00	0.00	0.00	0.00	0.00	0.00	nc	nc
DGDG-16:3-16:1	0.00	0.00	0.00	0.00	0.00	0.00	0.00	0.00	0.00	0.00	nc	nc
DGDG-16:2-16:2	0.00	0.00	0.00	0.00	0.00	0.00	0.00	0.00	0.00	0.00	nc	nc
DGDG-16:3-16:2	0.00	0.00	0.00	0.00	0.00	0.00	0.00	0.00	0.00	0.00	nc	nc
DGDG-16:3-16:3	0.17	0.00	0.00	0.06	0.10	0.22	0.00	0.16	0.13	0.11	-2.24	0.46
DGDG-18:0-16:0	0.00	0.00	0.53	0.18	0.31	0.00	0.00	0.00	0.00	0.00	nc	0.42
DGDG-18:1-16:0	0.18	0.73	2.44	1.12	1.18	0.00	0.51	0.27	0.26	0.25	4.33	0.33
DGDG-18:0-16:1	0.00	0.00	0.00	0.00	0.00	0.00	0.00	0.00	0.00	0.00	nc	nc
DGDG-18:2-16:0	1.03	3.16	5.91	3.37	2.44	0.65	3.18	1.92	1.92	1.27	1.75	0.43
DGDG-18:1-16:1	0.00	0.00	0.00	0.00	0.00	0.00	0.00	0.00	0.00	0.00	nc	nc
DGDG-18:0-16:2	0.00	0.00	0.00	0.00	0.00	0.00	0.00	0.00	0.00	0.00	nc	nc
DGDG-18:3-16:0	8.27	0.60	16.04	8.31	7.72	4.48	9.65	8.76	7.63	2.77	1.09	0.90
DGDG-18:2-16:1	0.00	0.00	0.20	0.07	0.12	0.00	0.00	0.00	0.00	0.00	nc	0.42
DGDG-18:1-16:2	0.00	0.00	0.00	0.00	0.00	0.00	0.00	0.00	0.00	0.00	nc	nc
DGDG-18:0-16:3	0.00	0.00	0.00	0.00	0.00	0.00	0.00	0.00	0.00	0.00	nc	nc
DGDG-18:3-16:1	0.38	0.68	0.54	0.53	0.15	0.25	0.37	0.37	0.33	0.07	1.62	0.13
DGDG-18:2-16:2	0.06	0.00	0.20	0.09	0.10	0.00	0.15	0.00	0.05	0.09	1.73	0.66
DGDG-18:1-16:3	0.00	0.00	0.00	0.00	0.00	0.00	0.00	0.00	0.00	0.00	nc	nc
DGDG-18:3-16:2	1.55	0.71	0.77	1.01	0.47	1.76	1.53	1.20	1.50	0.28	-1.48	0.21
DGDG-18:2-16:3	0.09	0.00	0.20	0.10	0.10	0.12	0.19	0.14	0.15	0.04	-1.59	0.43
DGDG-18:3-16:3	5.91	1.46	3.98	3.79	2.23	8.76	6.70	7.33	7.60	1.05	-2.01	0.08
DGDG-18:1-18:0	0.00	0.00	0.00	0.00	0.00	0.00	0.00	0.00	0.00	0.00	nc	nc
DGDG-18:2-18:0	0.00	0.00	0.18	0.06	0.10	0.00	0.00	0.00	0.00	0.00	nc	0.42
DGDG-18:1-18:1	0.00	0.00	0.00	0.00	0.00	0.00	0.00	0.00	0.00	0.00	nc	nc
DGDG-18:3-18:0	0.46	8.21	1.39	3.35	4.23	0.27	0.45	0.38	0.37	0.09	9.16	0.35
DGDG-18:2-18:1	0.00	0.00	0.07	0.02	0.04	0.00	0.00	0.00	0.00	0.00	nc	0.42
DGDG-18:3-18:1	0.34	9.54	0.69	3.52	5.21	0.17	0.43	0.40	0.33	0.14	10.67	0.40
DGDG-18:2-18:2	0.40	0.32	0.24	0.32	0.08	0.06	0.36	0.31	0.24	0.16	1.31	0.51
DGDG-18:3-18:2	10.63	9.94	3.47	8.01	3.95	9.72	10.06	9.22	9.67	0.42	-1.21	0.54
DGDG-18:3-18:3	70.52	64.65	63.15	66.11	3.90	73.54	66.41	69.54	69.83	3.58	-1.06	0.29
Fatty acids												
16:0	4.74	2.25	12.46	6.48	5.32	2.57	6.67	5.47	4.90	2.11	1.32	0.67
16:1	0.19	0.34	0.37	0.30	0.10	0.12	0.18	0.18	0.16	0.04	1.82	0.12
16:2	0.81	0.36	0.48	0.55	0.23	0.88	0.84	0.60	0.77	0.15	-1.41	0.24
16:3	3.17	0.73	2.09	2.00	1.22	4.66	3.45	3.90	4.00	0.61	-2.00	0.09
18:0	0.23	4.10	1.05	1.79	2.04	0.13	0.23	0.19	0.18	0.05	9.80	0.31
18:1	0.26	5.13	1.60	2.33	2.52	0.08	0.47	0.33	0.29	0.19	7.93	0.30
18:2	6.31	6.87	5.35	6.18	0.77	5.31	7.15	5.95	6.14	0.93	1.01	0.96
18:3	84.29	80.22	76.59	80.37	3.85	86.24	81.01	83.37	83.54	2.62	-1.04	0.31

Supplemental table 29. Lipid profile of the polar glycerolipid class phosphatidylglycerol(PG) from SAD6-OE-RNAi and wildtype Col-0.

The relative proportion in mol% of each glycerolipid species (upper half) was determined by LC-MS/MS (2.14) in three samples each. The relative proportion in mol% of a fatty acid species (lower half) within the total PG pool was calculated (2.14). Mean values (±SD) were calculated from three samples from SAD6-OE-RNAiand WT, respectively. Ratios were calculated from the mean values of three samples SAD6-OE-RNAi and WT, respectively. Statistical analysis was performed by using an unpaired two-tailed Student´s t-test. "Nc" means "not calculable".

	SAD6-OE-RNAi					WT						
	[mol%]					[mol%]					SAD6-OE-RNAi vs. WT	
Glycerolipid species	Samples 1	2	3	Mean	SD	Samples 1	2	3	Mean	SD	Ratio	P-value
PG-16:0-16:0	1.03	1.41	4.89	2.41	2.15	1.17	2.14	0.63	1.31	0.76	1.84	0.48
PG-16:1-16:0	0.66	0.40	2.05	1.02	0.90	0.32	0.42	0.36	0.36	0.05	2.82	0.33
PG-18:0-16:0	0.00	0.28	0.82	0.36	0.42	0.20	0.20	0.00	0.13	0.11	2.71	0.45
PG-18:1-16:0	3.72	6.47	16.28	8.67	6.71	4.57	5.36	4.47	4.80	0.49	1.81	0.42
PG-18:2-16:0	18.18	25.57	20.88	20.90	3.13	16.28	21.95	10.33	16.19	5.81	1.29	0.30
PG-18:1-16:1	0.64	0.00	1.85	0.83	0.94	0.34	0.37	0.81	0.50	0.27	1.64	0.62
PG-18:3-16:0	34.43	40.78	32.24	34.76	3.19	62.30	49.52	43.99	51.94	9.39	-1.49	0.07
PG-18:2-16:1	4.88	1.81	4.03	3.50	1.61	0.93	1.53	2.83	1.76	0.97	1.99	0.20
PG-18:3-16:1	36.31	23.05	16.22	24.47	9.96	11.87	16.06	32.95	20.30	11.16	1.21	0.65
PG-18:2-18:0	0.00	0.12	0.08	0.06	0.06	0.06	0.05	0.00	0.04	0.03	1.76	0.51
PG-18:3-18:0	0.00	0.00	0.16	0.17	0.18	0.18	0.24	0.00	0.14	0.13	1.23	0.81
PG-18:2-18:1	0.15	0.12	0.04	0.10	0.05	0.08	0.08	0.21	0.12	0.07	-1.26	0.64
PG-18:3-18:1	0.00	0.00	0.07	0.24	0.17	0.29	0.26	0.53	0.36	0.15	-1.50	0.42
PG-18:3-18:3	0.00	0.00	0.38	2.50	2.47	1.42	1.83	2.88	2.04	0.75	1.23	0.78
Fatty acids												
16:0	29.53	38.16	41.03	35.27	6.09	43.00	40.86	30.21	38.02	6.85	-1.08	0.63
16:1	21.25	12.62	12.08	14.91	5.09	6.73	9.19	18.48	11.46	6.20	1.30	0.50
16:2	0.00	0.00	0.00	0.00	0.00	0.00	0.00	0.00	0.00	0.00	nc	nc
16:3	0.00	0.00	0.00	0.00	0.00	0.00	0.00	0.00	0.00	0.00	nc	nc
18:0	0.00	0.20	0.45	0.21	0.23	0.13	0.12	0.00	0.08	0.07	2.51	0.44
18:1	2.25	3.30	9.20	5.00	3.68	2.73	3.15	3.01	2.97	0.21	1.69	0.44
18:2	11.60	13.81	12.52	12.28	0.84	8.67	11.81	6.69	9.06	2.58	1.36	0.15
18:3	35.37	31.92	24.72	32.32	6.61	38.74	34.87	41.62	38.41	3.39	-1.19	0.25

Supplemental table 30. Lipid profile of the polar glycerolipid class phosphatidylcholine (PC) from SAD6-OE-RNAi and wildtype Col-0.

The relative proportion in mol% of each glycerolipid species (upper half) was determined by LC-MS/MS (2.14) in three samples each. The relative proportion in mol% of a fatty acid species (lower half) within the total PC pool was calculated (2.14). Mean values (±SD) were calculated from three samples from SAD6-OE-RNAi and WT, respectively. Ratios were calculated from the mean values of three samples SAD6-OE-RNAi and WT, respectively. Statistical analysis was performed by using an unpaired two-tailed Student´s t-test. "Nc" means "not calculable".

	SAD6-OE-RNAi					WT						
											SAD6-OE RNAi vs. WT	
Glycerolipid species	Samples 1	2	3	Mean	SD	Samples 1	2	3	Mean	SD	Ratio	P-value
PC-18:0-16:0	0.00	0.00	0.00	0.00	0.00	0.00	0.00	0.00	0.00	0.00	nc	nc
PC-18:1-16:0	0.96	1.22	7.53	3.24	3.72	1.22	0.00	2.85	1.36	1.43	2.39	0.48
PC-18:2-16:0	11.49	10.71	26.48	16.23	8.89	10.71	12.26	18.10	13.69	3.90	1.19	0.68
PC-18:3-16:0	14.02	13.04	16.95	14.67	2.04	13.04	18.82	18.12	16.66	3.16	-1.14	0.42
PC-18:2-16:1	0.00	0.00	3.99	1.33	2.30	0.00	0.00	0.00	0.00	0.00	nc	0.42
PC-18:3-16:1	0.00	0.64	2.12	0.92	1.09	0.64	0.00	0.00	0.21	0.37	4.33	0.38
PC-18:3-16:2	3.49	1.80	1.06	2.12	1.25	1.80	3.28	1.62	2.23	0.91	-1.05	0.90
PC-18:3-16:3	0.00	0.48	2.31	0.93	1.22	0.48	0.00	0.00	0.16	0.28	5.81	0.39
PC-18:2-18:0	0.00	0.78	3.08	1.29	1.60	0.78	0.00	1.26	0.68	0.64	1.89	0.59
PC-18:3-18:0	0.75	1.57	3.87	2.06	1.62	1.57	0.00	1.33	0.97	0.84	2.14	0.37
PC-18:2-18:1	1.89	2.35	5.97	3.40	2.24	2.35	1.73	2.92	2.33	0.59	1.46	0.50

PC-18:3-18:1	4.41	4.05	3.19	3.89	0.63	4.05	4.71	4.34	4.37	0.33	-1.12	0.32
PC-18:2-18:2	7.70	6.85	6.70	7.09	0.54	6.85	9.25	7.69	7.93	1.22	-1.12	0.36
PC-18:3-18:2	24.37	27.43	10.14	20.65	9.23	27.43	24.72	21.32	24.49	3.06	-1.19	0.55
PC-18:3-18:3	30.92	29.09	6.60	22.20	13.54	29.09	25.24	20.45	24.93	4.32	-1.12	0.77
Fatty acids												
16:0	13.24	12.48	25.48	17.07	7.30	12.48	15.54	19.54	15.85	3.54	1.08	0.81
16:1	0.00	0.32	3.05	1.12	1.68	0.32	0.00	0.00	0.11	0.18	10.59	0.40
16:2	1.74	0.90	0.53	1.06	0.62	0.90	1.64	0.81	1.12	0.46	-1.05	0.90
16:3	0.00	0.24	1.16	0.47	0.61	0.24	0.00	0.00	0.08	0.14	5.81	0.39
18:0	0.37	1.17	3.48	1.67	1.61	1.17	0.00	1.30	0.82	0.72	2.04	0.47
18:1	3.63	3.81	8.35	5.26	2.67	3.81	3.22	5.05	4.03	0.93	1.31	0.52
18:2	26.58	27.49	31.53	28.53	2.64	27.49	28.60	29.49	28.53	1.01	1.00	1.00
18:3	54.44	53.59	26.42	44.82	15.93	53.59	51.00	43.81	49.47	5.06	-1.10	0.67

Supplemental table 31. Lipid profile of the polar glycerolipid class phosphatidyethanolamine (PE) from SAD6-OE-RNAi and wildtype Col-0.

The relative proportion in mol% of each glycerolipid species (upper half) was determined by LC-MS/MS (2.14) in three samples each. The relative proportion in mol% of a fatty acid species (lower half) within the total PE pool was calculated (2.14). Mean values (±SD) were calculated from three samples from SAD6-OE-RNAi and WT, respectively. Ratios were calculated from the mean values of three samples SAD6-OE-RNAi and WT, respectively. Statistical analysis was performed by using an unpaired two-tailed Student´s t-test. "Nc" means "not calculable".

	SAD6-OE-RNAi					**WT**						
	[mol%]					**[mol%]**					**SAD6-OE RNAi vs. WT**	
	Samples					**Samples**						
Glycerolipid species	**1**	**2**	**3**	**Mean**	**SD**	**1**	**2**	**3**	**Mean**	**SD**	**Ratio**	**P-value**
PE-16:0-16:0	0.00	0.00	0.00	0.00	0.00	0.00	0.00	0.00	0.00	0.00	nc	nc
PE-16:1-16:0	0.00	0.00	0.00	0.00	0.00	0.00	0.00	0.00	0.00	0.00	nc	nc
PE-16:2-16:0	0.00	0.00	0.00	0.00	0.00	0.00	0.00	0.00	0.00	0.00	nc	nc
PE-16:3-16:0	0.00	0.00	0.00	0.00	0.00	0.00	0.00	0.00	0.00	0.00	nc	nc
PE-18:0-16:0	0.03	0.07	0.00	0.04	0.04	0.04	0.04	0.04	0.04	0.00	-1.15	0.82
PE-18:1-16:0	0.42	1.06	1.57	1.02	0.58	0.59	0.43	0.59	0.54	0.09	1.89	0.29
PE-18:2-16:0	20.79	28.10	39.34	29.41	9.34	21.76	21.35	23.86	22.32	1.35	1.32	0.32
PE-18:0-16:2	0.00	0.00	0.00	0.00	0.00	0.00	0.00	0.00	0.00	0.00	nc	nc
PE-18:3-16:0	15.33	20.23	19.29	18.28	2.60	14.26	16.96	16.48	15.90	1.44	1.15	0.26
PE-18:3-16:1	0.92	0.57	0.20	0.56	0.36	0.82	0.85	0.66	0.78	0.10	-1.38	0.41
PE-18:2-16:3	0.13	0.09	0.04	0.09	0.04	0.12	0.14	0.09	0.12	0.03	-1.38	0.34
PE-18:3-16:3	0.36	0.13	0.00	0.16	0.18	0.33	0.24	0.17	0.24	0.08	-1.50	0.53
PE-18:0-18:0	0.00	0.13	0.00	0.04	0.07	0.00	0.00	0.00	0.00	0.00	nc	0.42
PE-18:1-18:0	0.00	0.00	0.00	0.00	0.00	0.00	0.00	0.00	0.00	0.00	nc	nc
PE-18:2-18:0	0.97	1.93	1.73	1.55	0.51	1.47	0.90	1.12	1.16	0.29	1.33	0.33
PE-18:3-18:0	1.62	1.21	4.37	2.40	1.72	2.20	0.67	1.19	1.35	0.78	1.78	0.41
PE-18:2-18:1	2.75	3.37	2.08	2.73	0.64	3.66	3.07	3.41	3.38	0.30	-1.24	0.22
PE-18:3-18:1	0.00	0.00	0.00	0.00	0.00	0.00	0.00	0.00	0.00	0.00	nc	nc
PE-18:2-18:2	12.56	14.26	10.55	12.46	1.85	11.03	11.23	11.24	11.17	0.12	1.12	0.35
PE-18:3-18:2	23.68	18.19	15.30	19.06	4.26	24.43	23.52	24.06	24.00	0.46	-1.26	0.18
PE-18:3-18:3	20.43	10.68	5.51	12.21	7.58	19.30	20.59	17.09	18.99	1.77	-1.56	0.26
Fatty acids												
16:0	18.29	24.73	30.10	24.37	5.92	18.33	19.39	20.49	19.40	1.08	1.26	0.28
16:1	0.46	0.28	0.10	0.28	0.18	0.41	0.43	0.33	0.39	0.05	-1.38	0.41
16:2	0.00	0.00	0.00	0.00	0.00	0.00	0.00	0.00	0.00	0.00	nc	nc
16:3	0.24	0.11	0.02	0.12	0.11	0.22	0.19	0.13	0.18	0.05	-1.46	0.48
18:0	1.32	1.73	3.05	2.03	0.91	1.86	0.81	1.17	1.28	0.53	1.59	0.30
18:1	1.58	2.21	1.83	1.88	0.32	2.12	1.75	2.00	1.96	0.19	-1.04	0.72
18:2	36.73	40.09	39.80	38.87	1.86	36.74	35.72	37.51	36.66	0.90	1.06	0.16
18:3	41.38	30.84	25.09	32.44	8.26	40.31	41.71	38.37	40.13	1.68	-1.24	0.25

Supplemental table 32. Lipid profile of the polar glycerolipid class phosphatidylinositol (PI) from SAD6-OE-RNAi and wildtype Col-0.

The relative proportion in mol% of each glycerolipid species (upper half) was determined by LC-MS/MS (2.14) in three samples each. The relative proportion in mol% of a fatty acid species (lower half) within the total PI pool was calculated (2.14). Mean values (±SD) were calculated from three samples from SAD6-OE-RNAi and WT, respectively. Ratios were calculated from the mean values of three samples SAD6-OE-RNAi and WT, respectively. Statistical analysis was performed by using an unpaired two-tailed Student´s t-test. "Nc" means "not calculabe"; "nm" means "not measured".

	SAD6-OE-RNAi					WT						
	[mol%]					[mol%]					SAD6-OE RNAi vs. WT	
Glycerolipid species	Samples			Mean	SD	Samples			Mean	SD	Ratio	P-value
	1	2	3			1	2	3				
PI-18:3-18:3	0.00	7.95	3.61	3.85	3.98	7.59	6.15	4.81	6.18	1.39	-1.60	0.42
PI-18:3-18:2	9.27	5.61	2.99	5.96	3.16	5.38	6.79	3.74	5.30	1.53	1.12	0.77
PI-18:3-18:1	0.00	0.00	0.74	0.25	0.42	0.95	1.25	0.83	1.01	0.22	-4.13	0.07
PI-18:3-18:0	0.00	1.20	1.84	1.01	0.93	0.87	0.90	0.94	0.90	0.04	1.12	0.86
PI-18:3-16:3	1.59	0.00	0.00	0.53	0.92	0.00	0.60	0.00	0.20	0.34	2.67	0.61
PI-18:3-16:1	3.38	0.00	0.62	1.33	1.80	1.94	0.74	0.44	1.04	0.80	1.28	0.82
PI-18:3-16:0	65.21	59.94	50.62	58.59	7.39	52.38	55.04	59.23	55.55	3.45	1.05	0.57
PI-18:2-18:2	1.66	0.00	0.84	0.83	0.83	1.15	1.54	0.84	1.18	0.35	-1.41	0.56
PI-18:2-18:1	0.00	0.00	0.00	0.00	0.00	0.49	0.58	0.38	0.48	0.10	nc	0.01
PI-18:2-18:0	0.00	0.00	1.50	0.50	0.86	0.00	0.00	0.35	0.12	0.20	4.30	0.53
PI-18:2-16:3	0.00	0.00	0.00	0.00	0.00	0.00	0.00	0.00	0.00	0.00	nc	nc
PI-18:2-16:0	18.89	24.16	35.22	26.09	8.33	29.26	26.40	28.03	27.90	1.43	-1.07	0.74
PI-18:1-16:0	0.00	1.14	2.04	1.06	1.02	0.00	0.00	0.41	0.14	0.24	7.79	0.25
Fatty acids												
16:0	42.05	42.62	44.08	42.91	1.05	40.82	40.72	43.84	41.79	1.77	1.03	0.41
16:1	1.69	0.00	0.00	0.56	0.98	0.97	0.37	0.22	0.52	0.40	1.08	0.95
16:2	nm	nm	nm	nm	nm	nm	nm	nm	nm	nm	nm	nm
16:3	0.80	0.00	0.00	0.27	0.46	0.00	0.30	0.00	0.10	0.17	2.67	0.61
18:0	0.00	0.60	1.67	0.76	0.85	0.43	0.45	0.65	0.51	0.12	1.48	0.67
18:1	0.00	0.57	1.39	0.65	0.70	0.72	0.92	0.81	0.81	0.10	-1.24	0.73
18:2	15.74	14.88	20.75	17.12	3.17	18.71	18.43	17.08	18.07	0.87	-1.06	0.66
18:3	39.73	41.33	32.11	37.72	4.93	38.35	38.81	37.40	38.19	0.72	-1.01	0.88

9. Abbreviations

A	adenylate
Acetyl Coa	acetyl-coenzyme a
ACP	acyl carrier protein
atg	attogramm
bp	base pair
BSA	bovine serum albumin
°C	degree Celsius
cDNA	copy DNA
CID	collision-induced dissociation
CDP	cytidine diphosphate
CDS	coding sequence
CE	collision energy
DAG	diacylglycerin
dai	days after inoculation
d	days
DGDG	digalactosyldiacylglycerol
DNA	desoxyribonucleic acid
dNTP	desoxynucleoside triphosphate
dT	desoxy thymidilate
dTTP	desoxythymidylate triphosphate
DTT	dithiothreitol
EDTA	ethylenediaminetetraaceticacid
ER	endoplasmic reticulum
ev	electron volt
FA	fatty acid
FAD	fatty acid desaturase
FAS	fatty acid synthase
fg	femtogram
g	gram
G3P	glycerol-3-phosphate
gDNA	genomic DNA

GUS	glucuronidase
HEPES	4-(2-hydroxyethyl)-1-piperazineethanesulfonic acid
h	hour
HO·	hydroxyl radical
HPLC	high performance liquid chromatography
hz	hertz
id	identity
KAS II	ketoacyl-ACP synthase II
kb	kilobase
kDA	kilodalton
l	litre
µ-	micro-
m-	milli-
MES	2-(N-morpholino) ethanesulfonic acid
MGDG	monogalactosyldiacylglycerol
miRNA	micro RNA
min	minute
mRNA	messenger RNA
MS	Murashige und Skoog
MS	Mass spectrometry
MUFA	mono unsaturated fatty acid
MW	molecular weight
NADPH	nicotinamide adenine dinucleotide phosphate
n-	nano-
nc	not calculable
nm	not measured
OD	optical density
OPDA	12-Oxo phytodienoic acid
ox	oxidized
PA	phosphatidic acid
PC	phosphatidylcholine
PCR	polymerase chain reaction
PE	phosphatidylethanolamine

PG	phosphatidylglycerol
PI	phosphatidylinositol
PR	pathogenesis related
PRO	promoter
PS	photosystem
PUFA	poly unsaturated fatty acid
P value	probability value
rcf	relative centrifugal force
red	reduced
RNA	ribonucleic acid
RNAi	RNA inteference
ROS	reactive oxygen species
rpm	rounds per minute
SAD	stearoyl-acyl carrier protein delta-9-desaturase
SD	standard deviation
SE	standard error
SDS	sodium dodecyl sulfate
SOD	superoxide dismutase
SQDG	sulphoquinovosyldiacylglycerol
T-DNA	transfer DNA
Ti Plasmid	Tumor inducing plasmid
UDP	uridine diphosphate
v	volt
vir genes	virulence genes
vs.	versus